

*Microwave Electronics*

**Substrate Integrated Waveguide Filters for  
Narrow and Wideband Applications**

*A thesis submitted by*

**ANJU P MATHEWS**

*in partial fulfillment of the requirements*

*for the award of the degree of*

**DOCTOR OF PHILOSOPHY**

*Under the guidance of*

**Prof. C. K. AANANDAN**



**DEPARTMENT OF ELECTRONICS  
FACULTY OF TECHNOLOGY  
COCHIN UNIVERSITY OF SCIENCE AND TECHNOLOGY  
KOCHI-22, INDIA**

**August 2019**

# **Substrate Integrated Waveguide Filters for Narrow and Wideband Applications**

***Ph.D. Thesis under the Faculty of Technology***

*Author*

**Anju P Mathews**

Department of Electronics

Cochin University of Science and Technology

Kochi - 682022

Email: anjupmathews@gmail.com

*Supervising Guide*

**Dr. C. K. Aanandan**

Emeritus Professor

Department of Electronics

Cochin University of Science and Technology

Kochi - 682022

Email: aanandan@gmail.com

Department of Electronics

Cochin University of Science and Technology

Kochi - 682022

August 2019

*Dedicated to the Almighty*





**DEPARTMENT OF ELECTRONICS  
COCHIN UNIVERSITY OF SCIENCE AND TECHNOLOGY  
KOCHI - 682 022**

---

**Dr. C. K. Aanandan**  
Emeritus Professor

Email:aanandan@gmail.com  
Ph: 0484 2576418

---

## *Certificate*

This is to certify that this thesis entitled “**Substrate Integrated Waveguide Filters for Narrow and Wideband Applications**” is a bonafide record of the research work carried out by Ms. Anju P Mathews under my supervision in the Department of Electronics, Cochin University of Science and Technology. The results embodied in this thesis or parts of it have not been presented for the award of any other degree.

I further certify that the corrections and modifications suggested by the audience during the pre-synopsis seminar and recommendations by the Doctoral Committee of the candidate are incorporated in the thesis.

Kochi-22  
August 2019

*Dr. C. K. Aanandan*  
(Supervising Guide)



## *Declaration*

I, **Anju P Mathews**, hereby declare that this thesis entitled, **“Substrate Integrated Waveguide Filters for Narrow and Wideband Applications”** is based on the original research work carried out by me under the supervision and guidance of Prof. C. K. Anandan, Emeritus Professor, Department of Electronics, Cochin University of Science and Technology, Kochi-682022 and has not been included in any other thesis submitted previously for the award of any degree.

Kochi-22  
August 2019

**Anju P. Mathews**





## *Words of Gratitude...*

---

*I remember with utmost gratefulness ...*

*My supervising guide, Dr. C. K. Aanandan, Emeritus Professor, Department of Electronics, Cochin University of Science and Technology, for his valuable guidance and advice extended to me during my research period. His constant encouragement, innovative ideas and immense patience made me capable to complete this research work,*

*Prof. James Kurian, Head of the Department for the support I received from him during my research period.*

*Prof. P. R. S. Pillai, Prof. K. Vasudevan, Prof. Supriya M. H, former Heads of the Department, Department of Electronics for the help rendered to me in pursuing the research.*

*Prof. P. Mohanan and Prof. Tesamma Thomas for the suggestions and support I received from them during my research.*

*My great teachers over the years, from the first grade of elementary school to the university who carved me to this level.*

*All faculty members of the Department of Electronics for sharing their pearls of wisdom with me during the course of research. I thank all the technical, administrative and non-teaching staff of the department for the warm and cordial relations shared and invaluable helps.*

*Rev. Fr. Sebastian Elanjickal CMI, Provincial, CMI St. Joseph's Province Kottayam and Rev. Dr. Jose Nedumpara, Manager, St. Joseph's College, Moolamattom for giving me all support to successfully complete the research work,*

*Rev. Dr. Gilson John CMI, Dr. George V Thomas, former principals St. Joseph's College Moolamattom, Dr. Saju M Sebastian, Principal St. Joseph's College Moolamattom for the boundless help given to me for completing the research.*

*Rev. Fr. Jobin Thayyil CMI, Rev. Fr. Libin Valiyaparambil CMI for the support offered by them during my research period.*

*Prof. Jacob Sebastian former HOD Department of Physics St. Joseph's College Moolamattom, Dr. Roy Sebastian, Head of the department, Dept. of Physics, St. Joseph's College Moolamattom, Dr. Praveen Joseph, Ms. Doniamol Sebastian, Ms. Aleena Sabu, Mr. Lijin Scaria and Ms. Preetha Vasu faculty members of St. Joseph's College Moolamattom for their very valuable help.*

*The non-teaching staff, St. Joseph's College Moolamattom for their support during my research.*

*The University Grants Commission for granting FDP and for the financial support.*

*My friends and colleagues at St. Joseph's College Moolamattom for their constant encouragement.*

*My senior researchers Dr. Gopikrishna. M, Dr. Deepti Das Krishna, Dr. Ashkar Ali, Dr. Shameena V.A for their help and support.*

*My friend researchers Dr. Sreenath S, Dr. Sarin V. P, Dr. Sujith. R, Dr. Dinesh R, Dr. Nishamol M. S, Dr. Deepak, U, Ms. Roshna T.K, Dr. Sarah Jacob, Dr. Laila Das, Dr. Sreejith. M, Dr. Nijas C.M, Mr. Prakash K, C, Dr. Sumitha Mathew, Dr. Sajith V. R, Dr. Sherin B. M, Dr. Aju John and Ms. Anila P.V for the memorable times we spent together.*

*My friends Ms. Libimol V. A and Ms. Sreekala P. S for their timely help and suggestions.*

*Tony Sir and Cyriac Sir for their care and support.*

*Mr. Manoj. M and Ms. Remsha. M for their patient help and encouragement.*

*My research colleagues Ms. Sruthi Dinesh, Ms. Indu K, Ms. Dibin Mary George, Mr. Anil Kumar, Mr. Prasanth M. N, Mr. Paulbert Thomas, Mr. Nerraj K Pushkaran, Mr. Abhilash A. P and Mr. Nelson K, J.*

*All research scholars of the department especially, Mr. Suraj Kamal, Mr. Satheesh Chandran, Mr. Aji George, Mr. Midhun M.S, Mr. Athul Thomas, Mr. Prasanth P. P, Mr. Vinesh P. V, Mr. Vivek V. Kurup, Ms. Navya Mohan, Ms. Ann Varghese, Ms. Vinisha C. V, Ms. Sangeetha P. V, Ms. Deepthi, Ms. Suja, Ms. Bindhya, Mr. Akhil, Ms. Deepa, Ms. Gisha, Ms. Revathi.*

*My dear friends Ms. Raji S Nair, Ms. Divya S, Ms. Renju Thomas, Ms. Shijina Karim, Ms. Nithya. C and Ms. Anuritha Sukumaran for their moral support.*

*My husband, Mr. Lindo Ouseph for his love, support and care.*

*My son, Benjamin for making me blissful with his presence.*

*My family and my husband's family for the care and patience bestowed on me.*

*Finally, I would like to thank everybody who was important to the successful realization of the thesis, as well as expressing my apology that I could not mention personally one by one.*

*Above all there is that supreme power whose blessings and kindness without which one single step would not have been possible.*

*Anju P Mathews*



## Abstract

Rectangular waveguides are the preferred transmission lines at microwave and millimeter wave systems because of their high performance in terms of quality factor and power handling capability. Substrate integrated waveguide (SIW) is a new class of transmission line which can be thought of as a transition between microstrip line and waveguide. This technology provides an attractive solution to the integration of planar and nonplanar circuits by using a planar circuit fabrication process and as result, the use of SIW components has been increased dramatically over the last decade. With the rapid development of microwave and millimeter wave systems, the performance requirements for filters, which is an essential part in these systems, are becoming stringent. The SIW technology has gained wide acceptance for the realization of efficient, cost effective and miniaturized bandpass filters. This thesis focuses on the development of narrow and wide bandpass filters using substrate integrated waveguide (SIW) and half mode substrate integrated waveguide (HMSIW).



# Contents

Abstract .....	i
List of Tables.....	vii
List of Figures .....	ix
Abbreviations and Symbols .....	xv

## *Chapter 1*

<b>INTRODUCTION .....</b>	<b>01 - 36</b>
1.1 Microwave Communication System .....	02
1.1.1 Microwave frequency bands .....	03
1.2 Filters .....	04
1.2.1 Role of filters in microwave communication .....	04
1.2.2 Evolution of Filters.....	05
1.2.3 Applications of filters .....	07
1.2.3.1 Radar systems .....	07
1.2.3.2 Mobile and cellular systems.....	08
1.2.3.3 Satellite systems.....	09
1.2.4 Filter Classification .....	09
1.2.4.1 Classification of filters based on passband types .....	09
1.2.4.2 Classification of filters based on fractional bandwidth.....	11
1.2.4.3 Classification of filter by transmission media.....	11
1.3 Substrate Integrated Waveguide (SIW) and its Derivatives.....	12
1.3.1 Half Mode Substrate Integrated Waveguide (HMSIW) .....	15
1.3.2 Substrate Integrated Folded Waveguide (SIFW) .....	17
1.3.3 Substrate Integrated Slab Waveguide (SISW) .....	18
1.3.4 Substrate Integrated Ridge Waveguide (SIRW) .....	18
1.3.5 Quarter-Mode Substrate Integrated Waveguide (QMSIW) .....	19
1.4 Overview of SIW Filters .....	20
1.5 Split Ring Resonator (SRR)/ Complementary Split Ring Resonator (CSRR) .....	21
1.6 Important filter specifications and parameters .....	23
1.6.1 Filter Specifications.....	23
1.6.1.1 Frequency Specifications.....	23
1.6.1.2 Power handling capability .....	24
1.6.1.3 Mechanical Specifications .....	24
1.6.2 Filter Parameters .....	24
1.6.2.1 Frequency domain parameters.....	25
1.6.2.1.1 S parameters .....	25

1.6.2.1.2 Group delay .....	25
1.6.2.2 Performance parameters in frequency domain .....	27
1.7 Motivation behind the current research .....	28
1.8 Thesis Organization .....	31
1.8.1 Chapter 1 Introduction .....	31
1.8.2 Chapter 2 Literature Review .....	31
1.8.3 Chapter 3 Methodology.....	31
1.8.4 Chapter 4 HMSIW narrow bandstop and bandpass filters .....	32
1.8.5 Chapter 5 SIW wide bandpass filters .....	32
1.8.6 Chapter 6 Conclusions .....	32
References .....	33
<b><i>Chapter 2</i></b>	
<b>LITERATURE REVIEW.....</b>	<b>37 - 89</b>
2.1 Microwave filters .....	38
2.2 Microstrip filters employing split ring resonators (SRRs)/complementary split ring resonators (CSRRs) .....	39
2.3 Substrate integrated waveguide bandstop, narrow and wide bandpass filters.....	43
2.4 SRR and CSRR loaded SIW and HMSIW filters.....	64
References .....	75
<b><i>Chapter 3</i></b>	
<b>METHODOLOGY .....</b>	<b>91 - 101</b>
3.1 Simulation and Optimization.....	92
3.1.1 Frequency Domain Solver.....	95
3.2 Filter Fabrication .....	96
3.2.1 Photolithography .....	98
3.3 Filter Measurement .....	99
3.4 Summary of the chapter .....	101
References .....	101
<b><i>Chapter 4</i></b>	
<b>HMSIW NARROW BANDSTOP AND BANDPASS FILTERS.....</b>	<b>103 - 136</b>
4.1 Bandstop Filter using HMSIW and SRR.....	104
4.1.1 Geometry.....	104
4.1.2 Design Evolution.....	106
4.1.3 Simulation and Analysis.....	111
4.1.4 Fabrication and Measurement .....	112



4.2	HMSIW bandpass filter with SRRs.....	113
4.2.1	Geometry.....	113
4.2.2	Design evolution .....	114
4.2.3	Simulation and Analysis.....	122
4.2.3.1	Lumped element model .....	125
4.2.4	Fabrication and Measurement .....	126
4.3	HMSIW bandpass filter with SRR and CSRRs .....	127
4.3.1	Geometry.....	127
4.3.2	Design Evolution.....	128
4.3.3	Simulation and Analysis.....	130
4.3.3.1	Lumped element model .....	133
4.3.4	Measurement results.....	134
4.4	Summary of the chapter .....	135
	References .....	135

## ***Chapter 5***

### **SIW AND HMSIW COMPACT BANDPASS FILTERS ..... 137 - 168**

5.1	SIW bandpass filter with cross slot and CSRRs .....	138
5.1.1	Geometry.....	138
5.1.2	Design Evolution.....	140
5.1.3	Simulation and Analysis.....	142
5.1.4	Fabrication and Measurement .....	146
5.2	SIW and HMSIW bandpass filter with embedded vertical loops .....	148
5.2.1	Geometry.....	149
5.2.1.1	Geometry of SIW Filter.....	149
5.2.1.2	Geometry of HMSIW Filter.....	150
5.2.2	Design Evolution.....	152
5.2.2.1	SIW Filter .....	152
5.2.2.2	HMSIW Filter Design .....	154
5.2.3	Simulation and Analysis.....	154
5.2.3.1	SIW Filter .....	154
5.2.3.2	HMSIW Filter .....	156
5.2.4	Fabrication and Measurement .....	158
5.2.4.1	SIW Filter .....	158
5.2.4.2	HMSIW Filter .....	160
5.3	HMSIW bandstop filter with coupled vertical loops .....	161
5.3.1	Geometry.....	161
5.3.2	Design Evolution.....	163
5.3.3	Simulation and Analysis.....	165

5.3.4 Fabrication and Measurement .....	167
5.4 Summary of the chapter .....	168
References .....	168
 <i>Chapter 6</i>	
<b>CONCLUSIONS .....</b>	<b>169 - 174</b>
6.1 Thesis highlights .....	170
6.2 HMSIW narrow bandstop and bandpass filters .....	170
6.3 SIW and HMSIW compact bandpass filters.....	171
6.4 Suggestions for future work .....	174
 <b>LIST OF PUBLICATIONS .....</b>	 <b>175 - 176</b>
<b>RESUME OF AUTHOR .....</b>	<b>177 - 178</b>

## List of Tables

Table 1.1	Frequency Band Allocation.....	03
Table 4.1	Filter Parameters.....	105
Table 4.2	SRR Dimensions.....	105
Table 4.3	Filter Parameters.....	114
Table 4.4	SRR Dimensions.....	114
Table 4.5	Filter Parameters.....	128
Table 4.6	SRR Dimensions.....	128
Table 4.7	Comparison of the Designed filter with Reported Filters ...	135
Table 5.1	Filter Parameters.....	139
Table 5.2	SRR Dimensions .....	139
Table 5.3	Filter Parameters.....	150
Table 5.4	Loop Parameters.....	150
Table 5.5	Filter Parameters.....	151
Table 5.6	Loop Parameters.....	151
Table 5.7	Filter Parameters.....	162
Table 5.8	Loop Parameters.....	163
Table 6.1	Comparison of salient features of various filters developed.....	173



## List of Figures

Figure 1.1	Frequency Responses of (a) Lowpass, (b) Highpass, (c) Bandpass (d) Bandstop filter .....	10
Figure 1.2	(a) Air filled waveguide, (b) dielectric filled waveguide, (c) substrate integrated waveguide .....	13
Figure 1.3	Rectangular Waveguide and its SIW Equivalent.....	13
Figure 1.4	Dimensions of rectangular waveguide .....	14
Figure 1.5	SIW and HMSIW Field Distributions .....	16
Figure 1.6	SIW to HMSIW conversion.....	16
Figure 1.7	Layout of SIFW.....	17
Figure 1.8	Layout of SISW.....	18
Figure 1.9	Layout of SIRW .....	19
Figure 1.10	SIW to QMSIW Conversion.....	19
Figure 1.11	Comparison of Q-factor of SIW with respect to that of 50 $\Omega$ microstrip line and standard waveguide at Ka-band. ....	20
Figure 1.12	(a) Circular SRR and CSRR (b) Rectangular CSRR and SRR (c) CSRR and equivalent LC circuit.....	22
Figure 1.13	Important Filter Parameters .....	24
Figure 2.1	Microstrip line coupled SRR/CSRR Filter [9] (a) Fabricated Filter structure (SRR) (b) S-Parameters (c) Fabricated Filter structure (CSRR) (d) S-Parameters.....	41
Figure 2.2	CSRR Embedded SIW Filters [84] (a) Top loaded CSRR (b) Bottom loaded CSRR (c) S-Parameters.....	65
Figure 2.3	Ultra- Wideband HMSIW-CSRR filter [85] (a) Filter Structure (b) S-Parameters.....	66
Figure 2.4	Square SRR loaded SIW Bandpass Filter [86] (a)-(d) Different types of SRR orientations and corresponding S-Parameters (e) Four SRR loaded narrow bandpass filter.....	67

Figure 2.5	Electrically Tunable CSRR loaded SIW Filter [92] (a) Filter Structure (b) S-Parameters .....	70
Figure 3.1	Classification of popular EM solvers .....	92
Figure 3.2	Modelled Structure in CST MW Studio Window .....	93
Figure 3.3	S-Parameter Plots of Simulated Structure.....	94
Figure 3.4	Surface current distribution of the SRR in simulated structure.....	96
Figure 3.5	Various steps involved in the photolithography process .....	97
Figure 3.6	Experimental setup.....	100
Figure 3.7	Network Analyser- Generalized Internal Block Diagram .....	100
Figure 4.1	Filter Layout (a) Top View (b) Bottom View .....	105
Figure 4.2	SRR Schematic.....	105
Figure 4.3	(a) SIW (6 GHz cutoff frequency)(b) S-Parameters.....	106
Figure 4.4	(a) HSIW (6 GHz cutoff frequency) (b) S-Parameters .....	107
Figure 4.5	(a) Microstrip Line with SRR (b) S-Parameters .....	107
Figure 4.6	(a) HSIW with SRR (b) S-Parameters (Outer Ring Slit Orientation 1) .....	108
Figure 4.7	(a) HSIW with SRR (b) S-Parameters (Outer Ring Slit Orientation 2) .....	108
Figure 4.8	Surface Current Distributions Corresponding to (a) Figure 4.6 (b) Figure 4.7 .....	109
Figure 4.9	(a) HSIW with SRR (b) S-Parameters (Outer Ring Slit Orientation 3) .....	109
Figure 4.10	(a) HSIW with SRR (b) S-Parameters (Outer Ring Slit Orientation 4) .....	110
Figure 4.11	(a) HSIW with two SRRs (b) S-Parameters .....	110
Figure 4.12	Parametric Simulation of SRR Dimensions .....	111
Figure 4.13	(a) Photograph of Fabricated Bandstop Filter (b) Insertion and Return Loss Characteristics .....	112
Figure 4.14	Filter Layout (a) Top View (b) Bottom View .....	113

Figure 4.15	SRR Schematic.....	114
Figure 4.16	(a) HSIW (6 GHz cutoff frequency) (b) S-Parameters .....	116
Figure 4.17	(a) HSIW with a well-defined (b) S-Parameters Discontinuity.....	116
Figure 4.18	Parametric Simulations for various HMSIW discontinuity widths (Wcut) (a) $S_{11}$ (b) $S_{21}$ .....	117
Figure 4.19	(a) HMSIW with SRR at center (b) S-Parameters (Outer Ring Slit Orientation 1) .....	117
Figure 4.20	(a) HMSIW with SRR at center (b) S- Parameters (Outer Ring Slit Orientation 2) .....	118
Figure 4.21	Surface Current Distributions of SRR Orientations of (a) Figure 4.19 (b) Figure 4.20 at $f= 9.2476$ GHz (c) Figure 4.20 at $f = 17.216$ GHz.....	118
Figure 4.22	(a) HMSIW with SRR at center (b) S- Parameters (Outer Ring Slit Orientation 3) .....	119
Figure 4.23	(a) HMSIW with SRR at center (b) S- Parameters (Outer Ring Slit Orientation 4) .....	119
Figure 4.24	(a) HMSIW with SRR at center (b) S- Parameters (Outer Ring Slit Orientation 5) .....	120
Figure 4.25	(a) HMSIW with SRR at center (b) S- Parameters (Outer Ring Slit Orientation 6) .....	120
Figure 4.26	(a) HMSIW with SRR at center (b) S- Parameters (Selected for filter design) .....	121
Figure 4.27	(a) Filter Structure (b) S- Parameters .....	121
Figure 4.28	(a) Filter Structure (b) S- Parameters (with covering in HMSIW discontinuity) .....	122
Figure 4.29	Surface Current distributions (a) at 9.19 GHz (b) 8.93 GHz (c) at 9.44 GHz .....	123
Figure 4.30	Electric field distribution at 9.19GHz .....	124
Figure 4.31	Parametric Simulations (a) All SRR dimensions at 0.2 mm, 0.3 mm, 0.4mm (b) $X_{off}$ (c) $Y_{off}$ .....	124
Figure 4.32	LC equivalent circuit model .....	125

Figure 4.33	(a) Photograph of Fabricated Filter (b) Insertion and Return Loss Characteristics .....	126
Figure 4.34	Filter Layout (a) Top View (b) Bottom View .....	127
Figure 4.35	(a) HSIW (4 GHz cutoff frequency) (b) S-Parameters .....	129
Figure 4.36	(a) HSIW with a well-defined Discontinuity (b) S-Parameters .....	129
Figure 4.37	(a) HMSIW with SRR at center (b) S-Parameters .....	130
Figure 4.38	(a) Filter Structure (b) S-Parameters .....	130
Figure 4.39	Electric Field Distributions (a) 4.76 GHz (b) at 5.33 GHz.....	131
Figure 4.40	Surface Current Distribution at 5.15 GHz .....	132
Figure 4.41	Parametric Simulations (a) $S_{11}$ - $Y_{off}$ (b) $S_{21}$ - $Y_{off}$ (c) $S_{11}$ - $X_{off}$ and (d) .....	132
Figure 4.43	(a) Photograph of Fabricated Filter (b) Insertion and Return Loss Characteristics .....	134
Figure 5.1	Filter Layout (a) Top View (b) Bottom View .....	139
Figure 5.2	(a) SIW (6 GHz cutoff frequency) (b) S-Parameters.....	140
Figure 5.3	(a) SIW with Cross slot (b) S-Parameters.....	141
Figure 5.4	(a) Filter Structure (b) S-Parameters .....	141
Figure 5.5	Surface Current Distribution (around the cross slot at the passband center frequency - 8.4 GHz) .....	142
Figure 5.6	Electric Field Distribution at SRR Resonant Frequency (a) at 7.38 GHz (b) at 9.71 GHz.....	143
Figure 5.7	Parametric Simulations of (a) Cross slot length ( $L_c$ )- $S_{11}$ (b) Cross slot length ( $L_c$ )- $S_{21}$ (c) Cross slot width ( $W_c$ )- $S_{11}$ (d) Cross slot width ( $W_c$ )- $S_{21}$ (e) Cross slot $X_{off}$ - $S_{11}$ (f) Cross slot $X_{off}$ - $S_{21}$ (g) Cross slot $Y_{off}$ - $S_{11}$ (h) Cross slot $Y_{off}$ - $S_{21}$ .....	144
Figure 5.8	Parametric Simulations of (a) CSRR-Large- $X_{off}$ - $S_{11}$ (b) CSRR-Large- $X_{off}$ - $S_{21}$ (c) CSRR-Large- $Y_{off}$ - $S_{11}$ (d) CSRR-Large- $Y_{off}$ - $S_{21}$ (e) CSRR-Small- $X_{off}$ - $S_{11}$ (f) CSRR-Small- $X_{off}$ - $S_{21}$ (g) CSRR-Small- $Y_{off}$ - $S_{11}$ (h) CSRR-Small- $Y_{off}$ - $S_{21}$ .....	145



Figure 5.9	Photograph of Fabricated Filter (a) Top (b) Bottom .....	147
Figure 5.10	(a) Insertion and Return Loss Characteristics (b) Group Delay Characteristics.....	147
Figure 5.11	(a) SIW Bandpass Filter with Vertical Loops (top) (b) SIW Bandpass Filter with Vertical Loops (bottom) (c) Enlarged View of Vertical Loop.....	149
Figure 5.12	(a) HSIW Bandpass Filter with Vertical Loops (top) (b) HSIW Bandpass Filter with Vertical Loops (bottom) (c) Enlarged View of Vertical Loop .....	151
Figure 5.13	(a) Loop Orientation 1 (b) S-Parameters.....	152
Figure 5.14	(a) Loop Orientation 2(b) S-Parameters.....	153
Figure 5.15	(a) Filter Structure (b) S-Parameters .....	153
Figure 5.16	(a) Filter Structure (b) S-Parameters .....	154
Figure 5.17	Parametric Simulations of (a) Loop width (W) – $S_{11}$ (b) Loop width (W) – $S_{21}$ (c) Loop length changes (11, 12, 13,14) – $S_{11}$ (d) Loop length changes (11, 12, 13,14) – $S_{21}$ (e) Gap change (c)- $S_{11}$ (f) Gap change (c)- $S_{21}$ (g) Yoff- $S_{11}$ (h) Yoff- $S_{21}$ .....	155
Figure 5.18	Electric Field Distribution of the Vertical Loops at 12.86 GHz (passband center frequency) .....	156
Figure 5.19	Parametric Simulations of (a) Gap change (C1)- $S_{11}$ (b) Gap change (C1)- $S_{21}$ (c) Loop length changes (11, 12, 13) – $S_{11}$ (d) Loop length changes (11, 12, 13) - $S_{21}$ (e) Yoff- $S_{11}$ (h) Yoff- $S_{21}$ .....	157
Figure 5.20	Electric Field Distribution of the Vertical Loops at 8.7 GHz (passband center frequency) .....	158
Figure 5.21	SIW Bandpass Filter with Vertical Loops (a) Top (b) Bottom.....	159
Figure 5.22	(a) Insertion and Return Loss Characteristics (b) Group Delay Characteristics.....	159
Figure 5.23	HMSIW Bandpass Filter with Vertical Loops (a) Top (b) Bottom.....	160

Figure 5.24	(a) Insertion and Return Loss Characteristics (b) Group Delay Characteristics.....	160
Figure 5.24	(a) HSIW Bandstop Filter with Vertical Loop with slit (top) (b) HSIW Bandstop Filter with Vertical Loop with slit (bottom) (c) Enlarged View of Vertical Loop with slit.....	162
Figure 5.25	(a) Loop Orientation (b) S-Parameters.....	163
Figure 5.26	(a) Loop with slit at the bottom plane (b) S-Parameters.....	164
Figure 5.27	(a) HMSIW with two loops (b) S-Parameters.....	164
Figure 5.28	Parametric Simulations of (a) Loop Length (Ls) –S <sub>11</sub> (b) Loop Length (Ls) –S <sub>21</sub> (c) Loop width (Ws)- S <sub>11</sub> (d) Loop width (Ws)- S <sub>21</sub> .....	165
Figure 5.28	Parametric Simulations of (e) Gap (C2)-S <sub>11</sub> (f) Gap (C2)-S <sub>21</sub> (g) Xoff- S <sub>11</sub> (h) Xoff- S <sub>21</sub> (i) Slit Width (G1)-S <sub>11</sub> (j) Slit Width (G1)-S <sub>21</sub> .....	166
Figure 5.29	Photograph of Fabricated Filter (a) Top (b) Bottom .....	167
Figure 5.30	Insertion and Return Loss Characteristics .....	167

## ||| List of Abbreviations and Symbols |||

CST	Computer Simulation Technology
SIW	Substrate Integrated Waveguide
HMSIW	Half Mode Substrate Integrated Waveguide
QMSIW	Quarter Mode Substrate Integrated Waveguide
SRR	Split Ring Resonator
CSRR	Complementary split Ring Resonator
TE	Transverse Electric
EM	Electro Magnetic
FIT	Finite Integration Technique
RF	Radio Frequency
EBG	Electronic Band gap
DGS	Defected Ground Structure
NRN	Non-Resonating Node
TZ	Transmission Zero
LPF	Low Pass Filter
HPF	High Pass filter
BPF	Band Pass filter
BSF	Band Stop Filter
FBW	Full Bandwidth

.....❧.....



# Chapter 1

## INTRODUCTION

### Contents

- 1.1 *Microwave Communication System*
- 1.2 *Filters*
- 1.3 *Substrate Integrated Waveguide (SIW) and Its Derivatives*
- 1.4 *Overview of SIW Filters*
- 1.5 *Split Ring Resonator (SRR)/ Complementary Split Ring Resonator (CSRR)*
- 1.6 *Important Filter Specifications and Parameters*
- 1.7 *Motivation behind the Current Research*
- 1.8 *Thesis Organization*

*This chapter discusses microwave communication system with an emphasis on substrate integrated waveguide (SIW) technology. The chapter highlights the role of filters and filter technologies. An overview of SIW filters with applications of split ring resonators (SRRs) and complementary split ring resonators (CSRRs) on it are also described. The important filter specifications and parameters are also detailed in this chapter. The chapter concludes with the motivation behind the current research and the thesis organization.*

Filters are essential components in any communication system. They are used to select or reject the RF/ microwave signals within the assigned spectral limits so as to share the limited electromagnetic spectrum. Emerging applications in wireless communication demand RF/ microwave filter with even more cutting edge requirements such as smaller size, lighter weight, and lower cost with better performance. Depending on the requirements and specification, RF/ microwave filters may be designed and realized in various transmission line structures such as waveguides, coaxial lines or microstrip lines. The substrate integrated waveguide (SIW) - planar equivalent of the conventional rectangular waveguide- is a fast developing technology in the component design industry. Development of compact narrow and wideband filters based on substrate integrated waveguide (SIW) technology is discussed in this thesis.

## **1.1 Microwave Communication System**

Microwave is a line-of-sight wireless communication technology that uses high frequency beams from several hundred MHz to few GHz to provide high speed wireless connections that can send and receive voice, video and data.

The IEEE standard frequency allocation for various applications is illustrated in Table 1. 1.

### 1.1.1 Microwave frequency bands

**Table 1.1 Frequency Band Allocation**

<b>Band Designation</b>	<b>Frequency Range</b>	<b>Applications</b>
VLF	3- 30 KHz	Long distance telegraphy and navigation
LF	30- 300KHz	Aeronautical navigation services, Radio broadcasting, Long distance communication
MF	300- 3000 KHz	Regional broadcasting, AM radio
HF	3- 30 MHz	Communications, Broadcasting, Surveillance, C B radio
VHF	30- 300 MHz	Surveillance, F M radio, T V broadcasting
UHF	300- 1000 MHz	Cellular communications
L	1-2 GHz	Long range surveillance , Remote sensing
S	2-4 GHz	Weather detection, Long- range tracking
C	4- 8 GHz	Weather detection, Long-range tracking
X	8- 12 GHz	Satellite communications, Missile guidance, Mapping
Ku	12- 18 GHz	Satellite communications, Altimetry, High resolution mapping
K	18- 27 GHz	Very high-resolution mapping
Ka	27- 40 GHz	Airport surveillance

## 1.2 Filters

Filters are two port networks used to control the frequency response at certain point in the electromagnetic spectrum by providing low loss transmission at frequencies for the desired band and high attenuation in the rest of the frequencies. Filters find applications virtually in any type of communication, radars to test and measurement systems.

### 1.2.1 Role of filters in microwave communication

The electromagnetic (EM) spectrum is the distribution of various wireless signal frequencies in connection with communication and sensing devices. Technically advanced radio-frequency (RF), microwave, and millimeter-wave filters are required for the selection and/or rejection of specific frequency bands. This will be suitable for the future wireless systems, such as the fifth-generation communication systems for the realization of high performance, smaller size, light weight and low cost devices. The most popular type of filters are band pass filters and are most difficult to design and develop compared to the other bandnotch and lowpass filters. RF/microwave filters may be designed as lumped element or distributed element circuits depending on the requirements and specifications. Filters are used in communication and radar applications and can be realized on various transmission line structures, such as waveguides, coaxial lines and microstrip lines. Filters are also the integral part of multiplexers which are of major demand in the broadband wireless communication systems [1].



### **1.2.2 Evolution of Filters**

Filters in electronic circuits have played an important role since early stages of telecommunication and have progressed steadily in accordance with the advancement of communication technology. The introduction of telephony which drastically reformed the technological landscape surrounding telecommunication system required the development of new technology to extract and detect signals contained within a specific frequency band. This technological advancement further accelerated the research and development of filter technology.

The foundation of modern filter theory and practice took place during the period of World War II and the years immediately following, especially by such pioneers like P. L. Richards [2]. Work on microwave filters commenced prior to the war, a particularly significant paper being published by Mason and Sykes [3]. They used ABCD parameters, although not in matrix format, to derive the image impedance and image phase and attenuation functions of a rather large variety of useful filter sections. Network theory was probably the most advanced topic in engineering at that time, Darlington published his famous cascade synthesis theory as far back as 1939 [4].

The direct coupled cavity filter theory was one of the first great contributions from the group formed at Stanford Research Institute, among whose workers were Leo Young. The direct coupled cavity filters have excessive length in coaxial or stripline form. The dimension was reduced by a factor of two with the introduction of parallel coupled lines [5, 6]. Parallel coupling is much stronger than end coupling, so that

realizable bandwidths could be much greater. The prime mover here was George Matthaei, who published the theory and practical realizations of interdigital filters [8] and the combline filters in the following year.

Turning to other types of filters, waveguide bandstop filters were described by Fano and Lawson [9]. A very good account of early developments are given in the classic volume of Matthaei, Young and Jones [10].

Most of the research was carried out in the early 1960's is summarized in [11]. These filters consist of a number of coupled dielectric disks mounted in a waveguide beyond cut off. In order to give important size reduction, a high dielectric constant must be used, but originally such dielectrics possessed excessive temperature sensitivity. Now this drawback has been overcome with the development of high- Q ceramics with good temperature coefficients of expansion. One of the first dielectrics having improved frequency stability was reported by workers at Raytheon [12]. Considerable improvements carried out at Bell Telephone Laboratories and Murata Manufacturing Company of Japan were reported at the Workshop on Filter Technology during the 1979 MTT- S International Microwave Symposium. Bell used a barium titanate ceramic having a relative permittivity of 40 to achieve resonator Q's between 5000 and 10000 in the 2- 7 GHz frequency range [13, 14]. Filters may be constructed in all the common transmission media ranging from waveguides to microstrip, and the techniques is, therefore, quite versatile.

Emerging applications continue to challenge RF/microwave filters with even more stringent requirements. The recent advances in novel

materials and fabrication technologies, including thick film, thin film technology, low-temperature co-fired ceramics (LTCC), monolithic microwave integrated circuits (MMIC), micro-electro mechanic systems (MEMS), system on substrate (SOS), and micromachining technology have stimulated the rapid development of new SIW and other filters for RF/microwave applications. In the meantime, advances in computer-aided design (CAD) tools such as full-wave electromagnetic (EM) simulators have revolutionized filter design.

### **1.2.3 Applications of filters**

#### **1.2.3.1 Radar systems**

World War II and the invention of radar led to significant developments in filters at various laboratories in the U. S, where the work mainly concentrated on narrowband waveguide filters. Advances on broadband TEM filters for electronic support measures (ESM) systems and tunable narrowband filters for search receivers were made.

Military applications required wideband and tunable devices for ESM receivers, which led to the development of highly selective waveguide filters, coaxial resonator, suspended substrate multiplexers and electronically tunable filters. One of the critical parts of any military system is the electronic counter measure (ECM) system and its associated ESM system. The ESM system detects and classifies incoming radar signals by amplitude, frequency, pulse width etc. and the ECM system can then take appropriate countermeasures, such as jamming. One method of classifying signals by frequency is to split the complete microwave band of interest into smaller sub-bands. This can be done using a

multiplexer, which consists of separate bandpass filters whose passbands crossover at their 3 dB frequencies. The outputs of the individual channels can be detected, giving coarse frequency information while retaining unity probability of interest [15].

### 1.2.3.2 Mobile and cellular systems

Cellular communications base stations demand low loss high power handling selective filters with small physical size, capable of being manufactured in tens of thousands at a reasonable cost. This demands led to advances in coaxial resonator, dielectric resonator, and also methods of cost reduction, including computer aided alignment. Cellular radio handsets have required the manufacture of hundreds of millions of extremely small very low cost filters, still with reasonably low loss and high selectivity. The filters used in cellular radio handsets have completely different requirements. The original analog handsets in 1980's were large, bulky and manufactured in relatively small volumes. However, these phones used frequency division multiple access (FDMA) scheme; thus, they were transmitting and receiving simultaneously. Handsets for second generation time division multiple access (TDMA) systems, such as GSM, transmit and receive in different time slots. This has driven significant advances in integrated ceramic, surface and bulk acoustic wave active and passive filters using MEMS. Cellular radio has provided a significant driver for filter technology since the analog systems were launched in the early 1980s. This resulted in various innovations in filter technology for both base stations and handsets, which have depended upon the frequency planning of the various systems standards. The first analog systems

required filters with percentage bandwidths in the region of 2 % and with reasonable guard bands between channels. These specifications may be met with asymmetric generalized chebyshev bandpass filters, typically with six resonators with a Q of 3000 and one or possibly two transmission zeros located on the passband [16].

### **1.2.3.3 Satellite Systems**

The satellite communications industry created demand for low-mass narrowband low loss filters with severe specifications on amplitude selectivity and phase linearity. These requirements resulted in the development of dual-mode waveguide and dielectric resonator filters, and advances in the design of multiplexers. High performance waveguide filters were used to avoid problems caused by the devices used when channelized architecture was first implemented in Intelsat IV series launched in 1971 [17]. The first major electrical innovation was the use of dual mode filters, where size reduction is obtained by exciting two orthogonal degenerate modes in the same physical cavity. Surface acoustic wave (SAW) also has application in satellite industry.

### **1.2.4 Filter Classification**

#### **1.2.4.1 Classification of filters based on passband types**

Filters are used in all frequency ranges and are categorized into four different groups:

- Low pass filter (LPF) that transmits all signals from DC to a cut-off value,  $\omega_c$  and attenuates all signals with frequencies above  $\omega_c$ .

- High pass filter (HPF) that passes all signals with frequencies above the cutoff value  $\omega_c$  and rejects all signals below  $\omega_c$ .
- Bandpass filter (BPF) that passes signals with frequencies in the range of  $\omega_1$  to  $\omega_2$  and rejects frequencies outside this range.
- The complement to BPF is the bandstop filter (BSF).

Fig. 1.1 shows the characteristics of the four filter categories.

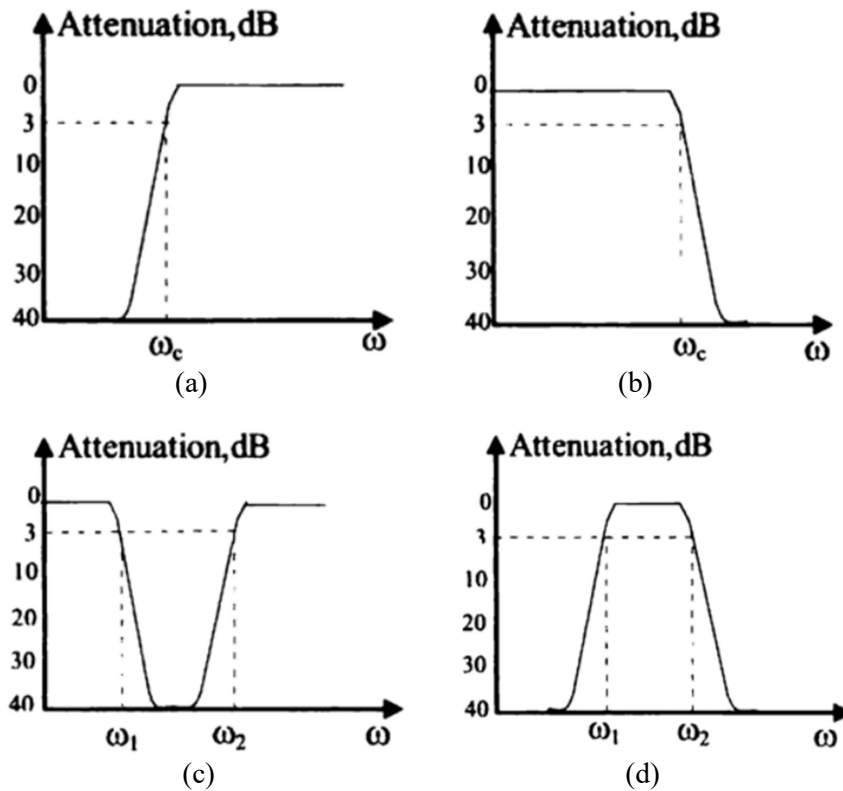


Fig. 1.1. Frequency Responses of (a) Lowpass, (b) Highpass, (c) Bandpass (d) Bandstop filter

The characteristics of a passive filter can be described using the transfer function approach or attenuation function approach. In low frequency circuit the transfer function ( $H(\omega)$ ) description is used while at microwave frequencies the attenuation function description is preferred.

#### **1.2.4.2 Classification of filters based on fractional bandwidth**

Fractional bandwidth or percentage bandwidth is a simple calculation, and gives a normalized measure of how much frequency variation a system or component can handle. If we know the center frequency and the bandwidth, the percentage bandwidth is

$$BW \% = BW/f_c * 100$$

Here BW is the absolute bandwidth and  $f_c$ , the center frequency.

- Narrowband filters: BW below 5%
- Moderately wide bandwidth: BW between 5% to 25%
- Wideband filters: BW greater than 25%.

#### **1.2.4.3 Classification of filter by transmission media**

The transmission media are classified into two: lumped elements and distributed elements. When the behavior of a resistor, capacitor, or inductor can be fully described by a simple linear equation, microwave engineers refer it to as a lumped element media where the operation is restricted to lower frequencies where they are physically smaller than a quarter-wavelength. At microwave frequencies, other factors must also be considered. To accurately calculate the behavior of the same 50  $\Omega$  resistor, we need to consider its length, width, and thickness of metal (due

to the skin effect), and its proximity to the ground plane. This is when we must consider it as a distributed element. The transmission media at microwave frequencies include the following:

- Coaxial cables
- Strip lines
- Slot lines
- Coplanar lines
- Rectangular waveguides (Its planar realization, SIW).

### **1.3 Substrate Integrated Waveguide (SIW) and its Derivatives**

The RF printed circuit industry has been rapidly grown by the inventions of several controlled impedance transmission lines and waveguides in the printed form. The stripline family, microstrip line and coplanar waveguide family of guiding structures are very common in the modern wireless communication scenario. A new class of printed guiding structures are introduced to the microwave and the millimeterwave range by the invention of the substrate integrated waveguide (SIW) technology. The SIW can be realized by electrically connecting two parallel metal plates by means of two rows of conducting cylinders or slot trenches in a dielectric substrate. By using this technique, the conventional rectangular waveguide can be modeled in the planar form, suitable for fabricating in the already existing printed circuit board (PCB) or miniaturization enabled technique such as low temperature co-fired ceramic (LTCC). The evolution of SIW from air filled waveguide is shown in Fig. 1.2. The three dimensional view of SIW along with its important parameters are shown in Fig. 1.3.



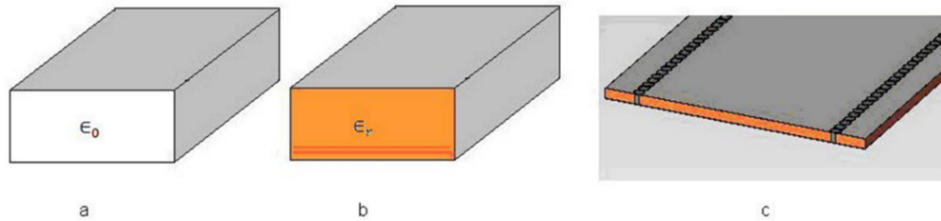


**Fig. 1.2. (a) Air filled waveguide, (b) dielectric filled waveguide, (c) substrate integrated waveguide**

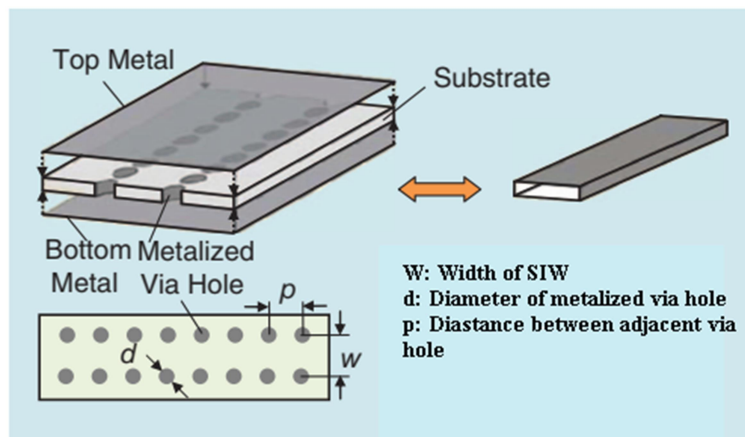


**Fig. 1.3. Rectangular Waveguide and its SIW Equivalent**

The electrical characteristics such as field pattern and dispersion characteristics of the rectangular waveguide are exhibited by the SIW. High quality factor, better power handling capability and good electrical shielding are the important qualities that are retained by the SIW structure when compared with the bulk rectangular waveguides. The passive as well as active components and other printed components like antennas, filters, diplexers etc. can be integrated on the same substrate with the development of SIW technology. This realizes the system- on- substrate

(SoS) concept which is an excellent method for developing performance oriented, fabrication friendly and cost-effective systems [19]. The dimensions of a rectangular waveguide is shown in Fig. 1.4.

The SIW Design Procedure is as follows

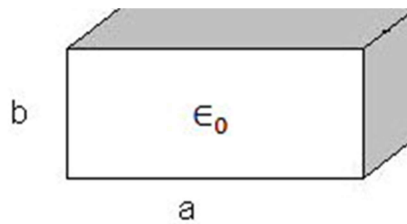


**Fig. 1.4. Dimensions of rectangular waveguide**

The equation for cut off frequency of a rectangular waveguide is given by

$$f_{c(m,n)} = \frac{1}{2\pi\sqrt{\mu\epsilon}} \sqrt{\frac{(m\pi)^2}{a^2} + \frac{(n\pi)^2}{b^2}} \dots\dots\dots(1)$$

Where m, n are mode numbers and a, b are the dimensions of the rectangular waveguide.

For TE<sub>1,0</sub> mode

$$f_c = \frac{c}{2a} \dots\dots\dots(2)$$

For Dielectric filled waveguide (DFW) with the same cut off frequency, dimension a<sub>d</sub> is given by

$$a_d = \frac{a}{\sqrt{\epsilon_r}} \dots\dots\dots(3)$$

Having determined the dimension "a" for the DFW, we can now pass to the design equations for SIW.

$$a_s = a_d + \frac{d^2}{0.95p} \dots\dots\dots (4)$$

Where d is the diameter of the vias, p is the via pitch (centre to centre distance),  $a_s$  is the SIW width.

For the selection of via diameter and pitch to get the desired waveguide cut off frequency the relations given in equations 5 and 6 can be used.

$$p \leq 2d \dots\dots\dots (5)$$

$$d < 0.2\lambda_g \dots\dots\dots (6)$$

Where  $\lambda_g = \frac{2\pi}{\sqrt{\frac{\epsilon_R(2\pi f)^2}{c^2} - \left(\frac{\pi}{a}\right)^2}} \dots\dots\dots (7)$

### 1.3.1 Half Mode Substrate Integrated Waveguide (HMSIW)

This waveguide structure is obtained by cutting the SIW such that the symmetric plane along the transmission direction is equivalent to a magnetic wall. If the cutting plane is a magnetic wall, the half of the SIW will keep the half field distribution unchanged. The SIW, HMSIW field distributions and the SIW to HMSIW conversion steps are shown in Fig.1.5, Fig.1.6 respectively.

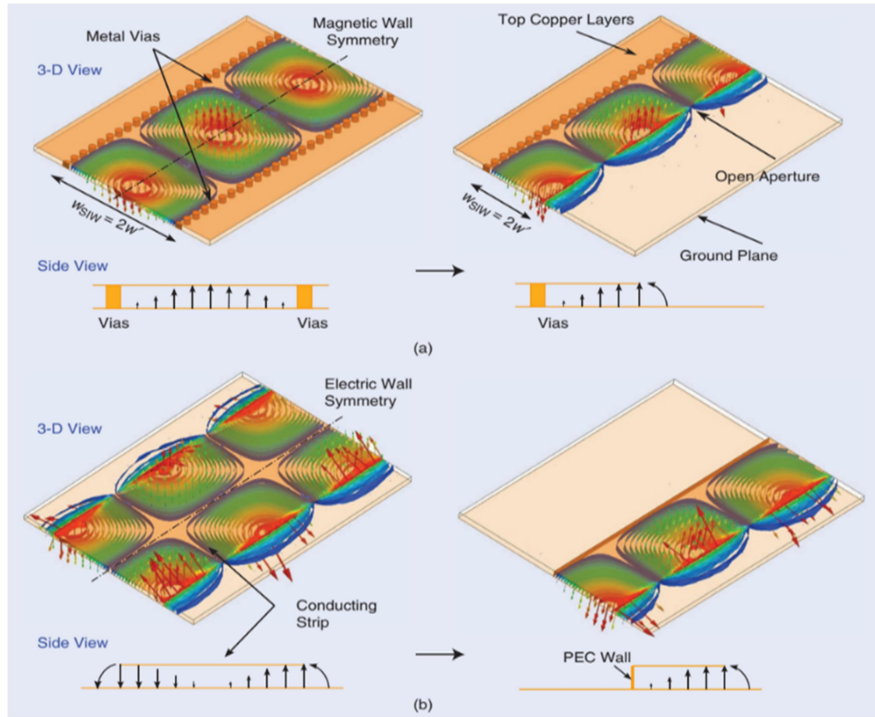


**Fig. 1.5. SIW and HMSIW Field Distributions**

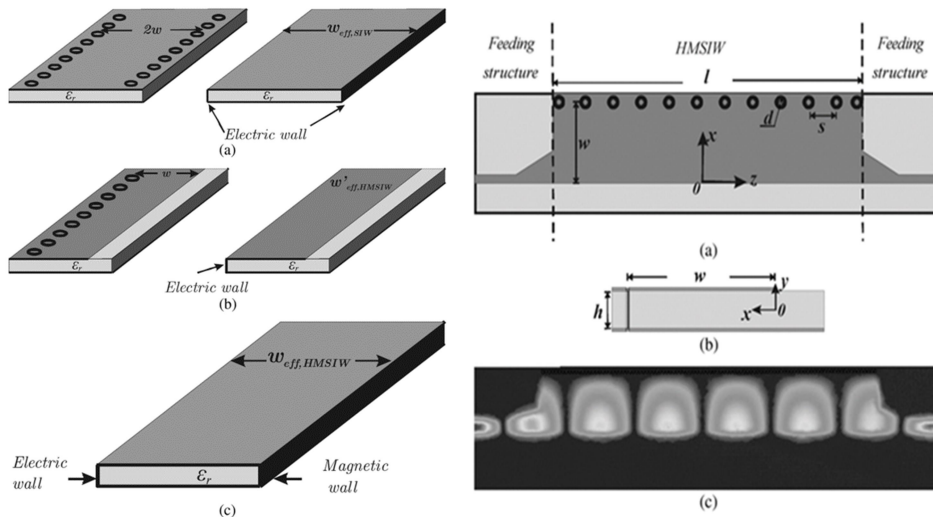


**Fig. 1.6. SIW to HMSIW conversion**

Due to the high width to height ratio, the open side aperture of the HMSIW is equivalent to a perfect magnetic wall [20]. Both the waveguide width and the surface area is reduced to half compared to the SIW, while keeping the propagation characteristics the same with dominant mode as  $TE_{1,0}$  [21].

### 1.3.2 Substrate Integrated Folded Waveguide (SIFW)

In SIW, a size reduction of a factor of  $\epsilon_r^{-1/2}$  is achieved compared to the classical RW. Whereas in substrate integrated folded waveguide (SIFW), based on the concept of folded waveguide [22], by using a dual-layer substrate, the waveguide width can be reduced up to  $(9\epsilon_r)^{-1/2}$ . These types of guides do not require internal vias and can be fabricated using the various multilayer fabrication techniques such as microwave laminates, LTCC and photoimageable thick- films [23]. A combination of HMSIW and folded technique forms a new waveguide called folded half mode substrate integrated waveguide (FHMSIW) which helps in further size reduction [24]. The SIFW layout is shown in Fig. 1.7.

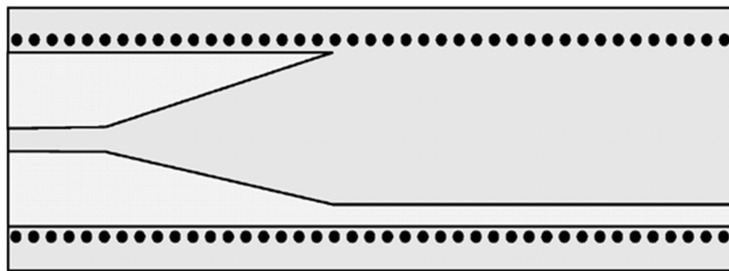


Fig. 1.7. Layout of SIFW

### 1.3.3 Substrate Integrated Slab Waveguide (SISW)

The RWs filled with a dielectric medium having periodically perforated air holes known as substrate integrated slab waveguide (SISW) is shown in Fig. 1.8. These are used for broader bandwidth applications. The electric field of  $TE_{1,0}$  mode is confined in the dielectric slab. So, the cut off frequency is rarely affected. But for the second mode electric field is concentrated more in the side portions so its cut off frequency is strongly increased [25,26].

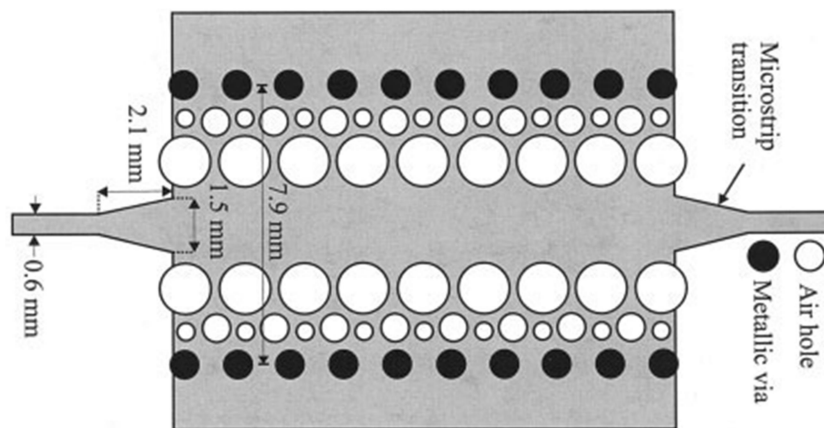


Fig. 1.8. Layout of SISW

### 1.3.4 Substrate Integrated Ridge Waveguide (SIRW)

To improve the bandwidth, another modification in the classical RW is introduced called substrate integrated ridge waveguide (SIRW) as in Fig. 1.9 by introducing a longitudinal metal ridge without any deterioration in the RF performances. The bandwidth is confined between the cut offs of  $TE_{1,0}$  mode and  $TE_{2,0}$  modes of the waveguide. A series of periodic metallized capacitive posts are arranged across the longer side of

the waveguide to establish the ridge. A bandwidth enhancement of 37% can be achieved compared to the 40% enhancement in the SISW [27].

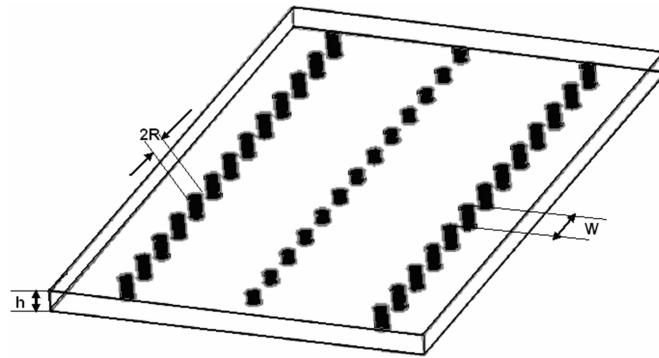


Fig. 1.9. Layout of SIRW

### 1.3.5 Quarter-Mode Substrate Integrated Waveguide (QMSIW)

The HMSIW can be further bisected into two parts along the symmetrical plane with one electric wall and two magnetic walls forms the quarter-mode substrate integrated waveguide (QMSIW) as shown in Fig. 1.10.

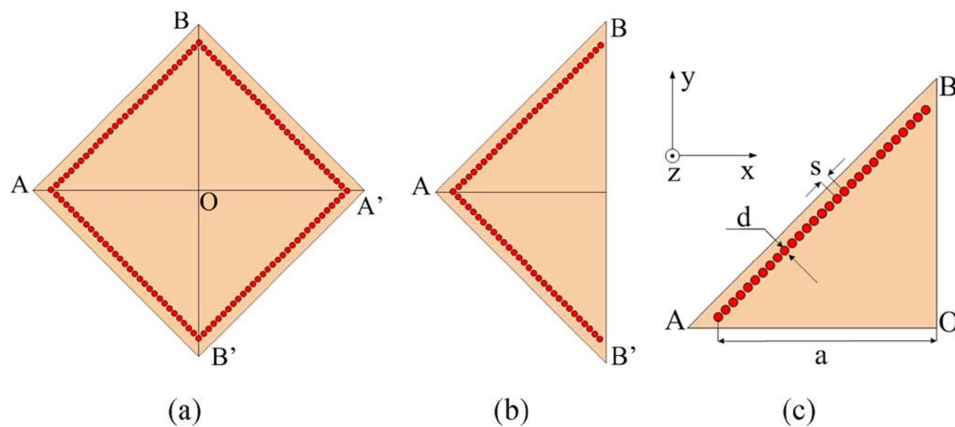


Fig. 1.10. SIW to QMSIW Conversion

The QMSIW field distribution is almost equivalent to that of the SIW. According to the analysis of QMSIW and through several designs it is verified that this guide is suitable for the realization of components like antennas, filters etc. [28].

#### 1.4 Overview of SIW Filters

Bandpass filters proved to be the one which is the most difficult to design and develop in practical case compared to other filter prototypes. The other filters like low pass and bandstop are less critical with its realization. The SIW provides lower loss than the conventional planar transmission structures at high frequencies like microstrip and coplanar waveguide (CPW) and it is of great interest in designing narrow and wideband bandpass filters. Both narrow and wide bandstop filters are also realized using SIW technology. Variety of filters in terms of passband characteristics, stopband characteristics, multiband nature, reconfigurable feature, better attenuation levels, compactness etc. are realized using SIW technology.

Properties	Microstrip <sup>1</sup> (50 $\Omega$ )	SIW <sup>1,2</sup>	Waveguide
Q-factor	42	462	4,613

<sup>1</sup>Substrate:  $\epsilon_r = 2.33$ ,  $\tan \delta = 5 \times 10^{-4}$ ,  $h = 10$  mils, copper foil  
<sup>2</sup>Width = 200 mils

**Fig. 1.11. Comparison of Q-factor of SIW with respect to that of 50  $\Omega$  microstrip line and standard waveguide at Ka-band.**



The SIW shows reasonable increase in the Q-factor compared to the microstrip lines as shown in Fig.1.11. This makes it perfect candidate for high Q filter realization. Popular SIW filter configurations include filters with inductive posts, iris filters, defected ground filters, filters with SIW cavity. Filter parameters such as selectivity, cost, compactness, sensitivity to environmental effects, power handling capability along with inband and out-of-band performances are to be taken care of for the better RF/microwave front end designs. This is inevitable for the efficient usage of the frequency spectrum resources and low cost enhancement of wireless system performance.

### **1.5 Split Ring Resonator (SRR)/ Complementary Split Ring Resonator (CSRR)**

The resonant structures utilized in the filters discussed in the thesis are mostly SRRs and CSRRs. The SRR is a planar magnetic resonator, which can be excited by an axial magnetic field whereas the CSRR is an electric resonator and can be excited by axial electric field. These are proposed by Pendry in 1999 [29]. These artificial structures known as metamaterials are initially studied by Veselago [30] and their lefthanded behaviors have been experimentally verified by Smith in 2001 [31].

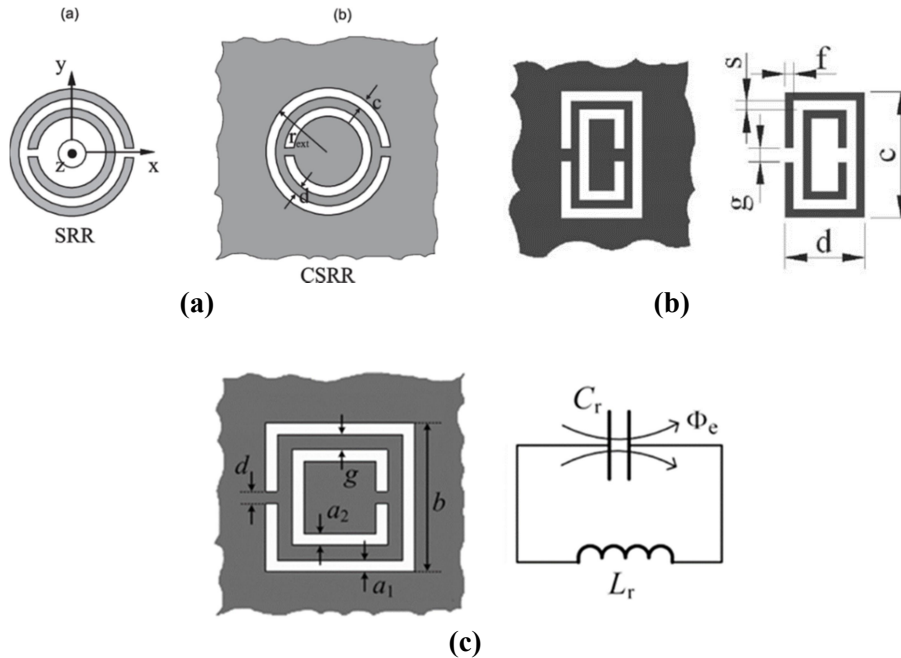


**Fig. 1.12. (a) Circular SRR and CSRR (b) Rectangular CSRR and SRR (c) CSRR and equivalent LC circuit**

Different types of SRR/CSRR shapes are used according to the applications in various field. The above Fig. 1.12 (a) shows circular SRR/CSRR, (b) represents rectangular SRR/CSRR, and (c) square CSRR with LC equivalent circuit.

A simple microstrip line loaded with SRR/CSRR can produce compact band reject filters. A microstrip transmission line generates magnetic field lines that close upon themselves around the line. If illuminated by a time-varying magnetic field with an appreciable component in its axial direction, the SRR gets excited. Due to the strong anisotropic electromagnetic nature, the SRR/CSRR is able to inhibit signal propagation in a narrow band in the vicinity of its resonant frequency.

If two arrays of SRRs are placed closely at both sides of the central microstrip line, giving rise to a negative- $\mu$  effect over a narrow band around the resonant frequency of the individual SRRs, inhibition of signal propagation over this band can be achieved.

The combination SRR/CSRR and SIW is a very good choice to develop bandpass as well as bandstop filters. The CSRR/SRRs etched in the center of the top layer or bottom layer of the SIW are mainly excited by the electric field induced by the SIW in the  $TE_{1,0}$  mode. For the SRR/CSRR loaded SIW, the SRR/CSRRs provide a stopband when they are resonant above the cut off frequency whereas this stopband switches to a passband when the SRR/CSRRs are resonant below the cut off frequency. The applications of this property is widely used in SIW filters to design bandstop, bandpass and ultra-wide bandpass filters.

## **1.6 Important filter specifications and parameters**

### **1.6.1 Filter Specifications**

#### **1.6.1.1 Frequency Specifications**

- Center frequency and bandwidth ( $f_0$  & BW) for BPF and BSF
- Cut off frequency ( $f_c$ ) for LPF and HPF
- Passband insertion loss
- Return loss and flatness (ripple level)
- Selectivity or skirt sharpness
- Out of band rejection levels
- Harmonic rejection.

### 1.6.1.2 Power handling capability

- Multipactor effects and voltage breakdown
- Environmental specifications
- Operational temperature limits
- Pressure and humidity environments
- Shock and vibration levels.

### 1.6.1.3 Mechanical Specifications

- Size, shape and weight
- Type of input/output connectors
- Mechanical mounting interfaces.

## 1.6.2 Filter Parameters

The functional requirements of a filter are specified in terms of filter parameters. The Fig.1.13 shows the important filter parameters in both time as well as frequency domain, considered in the design of various filters. The performance of these filters are assessed from these parameters.

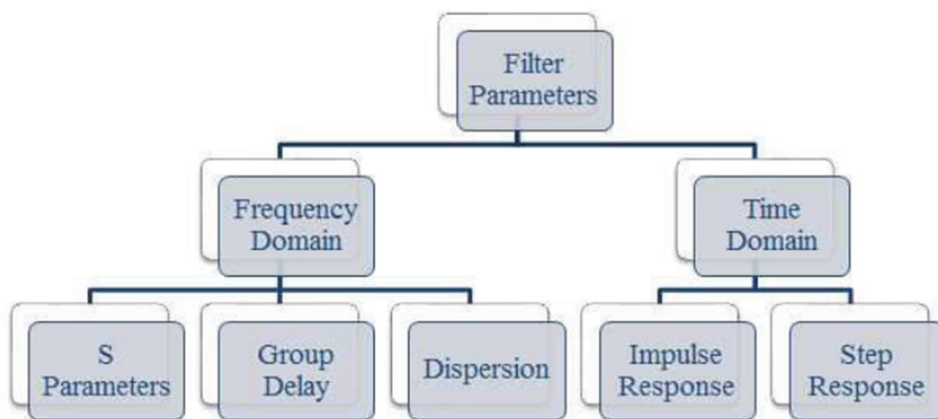


**Fig. 1.13. Important Filter Parameters**

### 1.6.2.1 Frequency domain parameters

Frequency domain parameters indicate how well a filter performs in frequency domain. Focus is given mainly on scattering (S) parameters (transmission and reflection parameters), group delay. These are the important factors that determines the transmission quality.

#### 1.6.2.1.1 S parameters

Z, Y and H parameters are used for low frequency characterization. At higher frequencies S parameters take precedence which are defined in terms of voltage travelling wave and are easy to measure. S parameters relate travelling waves to a network's reflection and transmission behavior. This does not require connections to undesirable loads (like open and short circuits required for Z and Y parameters). Moreover Z, Y and H parameters can be derived from S parameters if required. Performance characteristics like insertion loss, roll off rate, return loss and stopband attenuation of a filter can be obtained from S parameters.

#### 1.6.2.1.2 Group delay

Group delay is defined as the rate of change of transmission phase angle with respect to frequency.

$$\text{Group delay} = - \Delta\Phi/\Delta\omega$$

Where  $\Phi$  is the phase angle and  $\omega$  is the frequency. The unit of quantity on LHS works out to time when the angle is in radians and frequency is in radians/time (seconds, nanosecond, picosecond or whatever is convenient, depending on the length of the path).

Group delay evaluates the linear phase nature of the filter. A signal can contain a collection of different frequency components. If the phase of each of these components suffer a delay proportional to their corresponding frequencies, at any particular instant of time, the signal appears to be constituted of the same components. In other words, the envelope remains the same and there is no distortion. This is the case of flat or constant group delay. The group delay may also be referred to as envelope delay. The difference in group delay for signals spread out over a filter's passband is a measure for the phase distortion introduced by the filter.

Flat and consistent group delay (versus frequency) is important in communication systems and radar systems. In radar systems, distances are to be measured accurately using electromagnetic energy. The radar pulse is complex and its frequency content can span a bandwidth of 1 GHz or more. When the pulse is being processed, its spectrum has to be the same over the intended bandwidth of frequencies, otherwise distortion may cause inaccurate radar range measurements. Inductors, capacitors, transistors, amplifiers, transformers etc. can all contribute to eroding group delay flatness of a network.

Group delay consistency is extremely important in receivers such as mono pulse, where amplitude and phase tracking is required to achieve good null depths. Similar is the case with communication receivers where variation in group delay can cause distortion in received signals.

Group delay can be positive or negative depending on the phase shift over a range of frequencies considered. A transmission line loaded with resonators can exhibit combinations of negative and positive group delay. Negative group delay does not violate the principle of causality; instead, it only reshapes the waveform of the pulse. At the resonant frequencies of the resonators, there will be accumulation of charges at the resonators causing increased delay.

### 1.6.2.2 Performance parameters in frequency domain

The main performance parameters used in the design which are deduced from the S parameters are listed below.

- i) *Insertion loss*: Insertion loss can be defined as the ratio of the power delivered to the load impedance before insertion of the filter to the power delivered to the load impedance after insertion of the filter. This has to be kept as low as possible. The insertion loss can be determined from the transmission characteristics ( $S_{21}$ ) between the two cut off frequencies.
- ii) *Return loss*: The return loss of a filter is a measure of energy/power reflected at the ports instead of transmitting. Often a value of at least 10dB in the passband is insisted for return loss in most applications. It is extracted from the reflection parameters ( $S_{11}$ ).
- iii) *Cut off frequency*: The passband and stopband boundary points in the filter transmission characteristics are defined by cut off frequency.

- iv) *Roll off rate:* The roll off rate is the slope of the transfer characteristics ( $S_{21}$ ), at the passband edges or in the transition band. This determines the selectivity of the filter. Higher slope indicates better selectivity. A roll of rate steeper than 30 dB/ GHz is considered reasonable in most of the applications.
- v) *Stopband attenuation:* This indicates the signal suppression offered by a filter. This should be as high as possible. The FCC spectral mask suggests a stopband attenuation of 10 dB on either side for indoor applications and 20dB on either side for outdoor applications.

## 1.7 Motivation behind the current research

Mobile communication has become an indispensable part of the modern life. Different communication systems like GPS, UMTS, and WLAN have been implemented to meet various needs. These applications do not utilize the same frequency bands and the system requires separate filters in order to support different applications. In recent years, many problems arise since the number of systems on individual platforms grows, such as: co-site interference, cost, maintainability, reliability and weight. Therefore, the design of multifunctional filters for newly developed systems is of practical interest. In almost all multiple functionality systems that can simultaneously support devices operating at any of or combinations of these different frequency bands, printed filters have become an integral part. The printed filter technology has gained the attention of mobile wireless system designers due to its attractive features like light weight, ease of



fabrication and low cost of production. The fast development in the field of communication systems demands compact microstrip filters suitable for use in MMIC's, satellite mobile communication systems, personal communication systems, etc.

Mobile devices are the enabling centerpiece of digital convergence and the digital gateway for the real world to adapt to the ever demanding human needs. The society is now entering the era of 'wearable' mobile technology with smart glasses, and smart watches. Addition of mobile network components offers undeniable business benefits, both direct and indirect and wireless networking moves into the mainstream. Wireless technologies provide considerable savings in networking cost and a degree of flexibility not known in wired systems.

In the present scenario, there is a strong customer desire to have compact, portable, cheap, secured and easy to use devices with high data/video transfer capability within home and office environments. Sensors and embedded wireless controllers are increasingly needed in a variety of appliances and applications. PDA's and mobile computers are regularly connected to e-mail and internet services through wireless communications, and wireless local area networks for computers are becoming common in public areas like universities, airports etc.

A promising candidate in the upcoming wireless system is the SIW technology. With the advent of SIW, various types of filters in microwave and millimeter wave are realized with least complexity. The derivatives of SIW, like HMSIW, QMISW etc. are on its way to the upcoming

developments. By embedding different types of resonating elements SIW can easily be reformed for various applications. The SIW and its component filters are well suited in mobile cellular communication, satellite communication and in radar systems. Almost all communication systems require key building blocks such as bandpass filters and bandstop filters, with narrow as well as wider bandwidth, low insertion loss and flat group delay properties. High performance filters with adequate bandwidths are essential for current wireless communication systems.

The research aims to understand the design trade-offs and build optimum filters with the SIW technology incorporating different types of resonating elements. A top down design strategy is followed, where the SIW with appropriate cut off frequency is designed first. Then the corresponding passband is realized with low insertion loss. By proper optimization the stopband transmission zeros and attenuation levels are finalized. Equivalent circuit models are developed for the filters, which helps in identifying the circuit behavior in a better detail. The field distribution for different designed frequencies and the surface current distribution are also analyzed. Various parametric analysis have been carried out to understand the frequency dependence of different filter parameters. Proposed designs are simple, compact, planar, repeatable and reproducible with minimum turnaround time.

## **1.8 Thesis Organization**

### **1.8.1 Chapter 1 Introduction**

The thesis consolidates the entire work carried out into six chapters. The references relevant to each chapter are given after every chapter summary. Chapter one discusses about microwave communication systems, with emphasis on SIW technology and role of filters. It also details the different types and categories of SIW filters used in various applications, design methods, challenges etc. A section is set aside for deliberations about important filter parameters in frequency domain which are crucial in the performance analysis and hence looked into while designing.

### **1.8.2 Chapter 2 Literature Review**

This chapter presents a thorough review of literature on the development in the field of microwave filters, especially in the SIW class, giving special attention to planar bandstop and bandpass filters. Attempts have been made to cover all the seminal papers from microstrip as well as SIW filters theory and experiment. Different classes of filters in SIW technology from its beginning time till the present year is mentioned with its significant features. Various types of loop resonator filters based on their specific geometries with their gradual development have been studied to arrive at the motivation of the present thesis.

### **1.8.3 Chapter 3 Methodology**

Chapter three provides an overview of simulation software and optimization studies used for the design and development, fabrication

method adopted and the measurement setup used. Chapters four and five explain the step by step design and development of various SIW filters. This includes the geometry, simulation studies, field study at various frequency of interest, LC equivalent circuit model, measured results etc.

#### **1.8.4 Chapter 4 HMSIW narrow bandstop and bandpass filters**

In chapter four one bandstop filter and two bandpass filters are discussed. The bandstop filter is a realization of a narrow stopband with SIW and SRR. This structure is utilized in the first bandpass filter for its transmission zero generation. The second bandpass filter is the compact version of first one with the introduction of CSRR. A comparison chart with the reported filters is also given at the end.

#### **1.8.5 Chapter 5 SIW and HMSIW compact bandpass filters**

Chapter five discusses two moderately wideband filters. The first filter is a combination of a top loaded cross slot SIW and bottom loaded CSRRs. The filter is realized with reasonably good insertion and return losses. The second filter is a planar realization of the vertical loop loaded SIW. Both SIW and HMSIW filters are realized. In this case also compact filter with good insertion and return loss are described. HMSIW coupled vertical loop narrow bandstop filter is also discussed in this section.

#### **1.8.6 Chapter 6 Conclusions**

This chapter gives the conclusions drawn from the study with directions for future work. It describes the important findings of the thesis and the salient features of the proposed SIW filters.

**References**

- [1] Xiao-Ping Chen and Ke Wu, "Substrate Integrated Waveguide Filter: Basic Design Rules and Fundamental Structure Features," Article in IEEE Microwave Magazine, July 2014.
- [2] Richards P. L, "Resistor-transmission-line circuits," Proc. IRE, Vol. 36, pp. 217-220, 1948.
- [3] Mason W. P and Sykes R. A, "The use of coaxial and balanced transmission lines in filters and wide hand transformers for high radio frequencies," Bell Syst. Tech. J., Vol. 16, pp. 275-302, 1937.
- [4] Darlington S, "Synthesis of reactance 4-poles," J. Math. Phys., Vol. 18, pp. 257-353, 1939.
- [5] Ozaki H and Ishii J, "Synthesis of a class of stopline filters," IRE Trans. Circuit Theory, Vol. CT-5, pp. 104-109, 1958.
- [6] Cohn S. B, "Parallel-coupled transmission-line resonator filters," IRE Trans. Microwave Theory Tech., Vol. MTT-6 VD, pp. 223-231, 1958.
- [7] Cohn S. B, "Parallel-coupled transmission-line resonator filters," IRE Trans. Microwave Theory Tech., Vol. MTT-10, pp. 223-231, 1958.
- [8] Matthaci G. L, "Interdigital band-pass filters," IRE Trans. Microwave Theory Tech., Vol. MTT-10, pp. 479-491, 1962.
- [9] Fano R. M and Lawson A. W, "Microwave Transmission Circuits," ser. M.I.T. Rad. Lab. New York, McGraw-Hill, Vol. 9, ch. 9,10, 1948.
- [10] Matthaai G. L, Young L, and Jones E. M. T, "Microwave Filters, Impedance-matching networks and coupling structures," New York McDraw Hill, 1964.

- [11] Cohn S. B, “Microwave bandpass filters containing high-Q dielectric resonators,” IEEE Trans. Microwave Theory Tech., Vol. MTT-16, pp. 218-227, 1968.
- [12] Masse D. J and Pucel R. A, “A temperature-stable bandpass filter using dielectric resonators,” Proc. IEEE. Vol. 60, pp. 730-731, 1972.
- [13] Plourde J. K and Linn D. F, “Microwave dielectric resonator filters using Ba<sub>2</sub>Ti<sub>9</sub>O<sub>20</sub> ceramics,” IEEE MTT-S Int. Microwave Symp. Dig., Cat. No. 77CH1219-5, pp. 290-293, 1977.
- [14] Ren C. L, “Waveguide bandstop filter utilizing Ba<sub>2</sub>Ti<sub>9</sub>O<sub>20</sub> resonators,” IEEE MTT-S Int. Microwave Symp. Dig., Cat. No. 78CH-1375-7 MTT, pp. 227-229, 1978.
- [15] Tsui J. B, “Microwave Receivers with Electronic Warfare Applications,” New York: Wiley, 1992.
- [16] Hunter I. C, “Microwave Filters-Applications and Technology,” IEEE Trans. Microwave Theory and Tech. Vol. 50, pp. 794-805, 2002.
- [17] Atia A. E and Williams A. E, “New types of waveguide bandpass filters for satellite transponders,” Comsat Tech. Rev., Vol. 1, pp. 21-43, 1971.
- [18] M. Bozzi, A. Georgiadis, and K. Wu, “Review of substrate-integrated waveguide circuits and antennas,” IET Microw. Antennas Propag., Vol. 5, Iss. 8, pp. 909–920, 2011.
- [19] Wei Hong, Bing Liu, Yuanqing Wang, Qinghua Lai, Hongjun Tang, Xiao Xin Yin, Yuan Dan Dong, Yan Zhang, and Ke Wu, “Half Mode Substrate Integrated Waveguide: A New Guided Wave Structure for Microwave and Millimeter Wave Application,” IEEE Millimeter Waves Systems, 2006.

- [20] Qinghua Lai, Christophe Fumeaux, Wei Hong, and Rüdiger Vahldieck, "Characterization of the Propagation Properties of the Half-Mode Substrate Integrated Waveguide," *IEEE Trans. Microwave theory and Techniques*, VOL. 57, NO. 8, August 2009.
- [21] G. L. Chen, T. L. Owens, and H. Whealton, "Theoretical Study of the Folded Waveguide," *IEEE Trans. Plasma Science*, Vol. 16, No. 2, April 1988.
- [22] Nikolaos Grigoropoulos, Benito Sanz-Izquierdo, and Paul R. Young, "Substrate Integrated Folded Waveguides (SIFW) and Filters," *IEEE Microwave and Wireless Components Letters*, Vol. 15, No. 12, December 2005.
- [23] Guo Hua Zhai, Wei Hong, KeWu, Ji Xin Chen, Peng Chen, Jing Wei, and Hong Jun Tang, "Folded Half Mode Substrate Integrated Waveguide 3 dB Coupler," *IEEE Microwave and Wireless Components Letters*, Vol. 18, No. 8, August 2008.
- [24] Maurizio Bozzi, Dominic Deslandes, Paolo Arcioni, Luca Perregini, Ke Wu, Giuseppe Conciauro, "Efficient Analysis and Experimental Verification of Substrate-Integrated Slab Waveguides for Wideband Microwave Applications," *Wiley Periodicals, Inc.*, 2005.
- [25] Dominic Deslandes, Maurizio Bozzi, Paolo Arcioni and Ke Wu, "Substrate Integrated Slab Waveguide (SISW) for Wideband Microwave Applications," *IEEE MTT-S Digest*, 2003.
- [26] Wenquan Che, Cuixia Li, Peter Russer, and Y. L. Chow, "Propagation and Band Broadening Effect of Planar Integrated Ridged Waveguide in Multilayer Dielectric Substrates," *IEEE*, 2008.
- [27] Cheng Jin, and Zhongxiang Shen, "Compact Triple-Mode Filter Based on Quarter-Mode Substrate Integrated Waveguide," *IEEE Trans. Microwave Theory and Techniques*, Vol. 62, No. 1, January 2014.

- [28] Cheng Jin, Member, Rui Li, Arokiaswami Alphones, and Xiaoyue Bao, “Quarter-Mode Substrate Integrated Waveguide and Its Application to Antennas Design,” *IEEE Trans. Antennas and Propagation*, Vol. 61, No. 6, June 2013.
- [29] J. B. Pendry, A. J. Holden, D. J. Robbins, and W. J. Stewart, “Magnetism from Conductors and Enhanced Nonlinear Phenomena,” *IEEE Trans. Microwave Theory and Techniques*, Vol. 47, No. 11, November 1999.
- [30] V. G. Veselago, “Electrodynamics of materials with negative index of refraction,” *UFN*, 173:7 (2003), 790–794; *Phys. Usp.*, 46:7 (2003), pp. 764–768.
- [31] R. A. Shelby, D. R. Smith, S. Schultz, “Experimental Verification of a Negative Index of Refraction,” *American Association for the Advancement of Science, New Series*, Vol. 292, No. 5514, pp. 77-79, Apr. 6, 2001.

.....✎.....



# Chapter 2

## LITERATURE REVIEW

Contents	2.1	<i>Microwave filters</i>
	2.2	<i>Microstrip filters employing split ring resonators (SRR)/complementary split ring resonators (CSRR)</i>
	2.3	<i>Substrate integrated waveguide (SIW) bandstop, narrow and wide bandpass filters</i>
	2.4	<i>SRR and CSRR loaded SIW and half mode substrate integrated waveguide (HMSIW) filters.</i>

*This chapter starts with a brief review of microwave filters and continues with a comprehensive review of literature associated with the microstrip filters employing split ring resonators (SRRs)/complementary split ring resonators (CSRRs). The pioneer research work in the substrate integrated waveguide (SIW) technology are presented. SIW filter categories such as bandstop, narrow and wide bandpass filters are also studied with emphasis on compactness, stopband attenuation, insertion loss and return loss characteristics. The various techniques and methodologies employed by different researchers for achieving the desired characteristics are briefed. The recent works in the field of SRR and CSRR loaded SIW and half mode substrate integrated waveguide (HMSIW) filters are also described.*

## 2.1 Microwave filters

Microwave communication links are an important practical application of the microwave technology and are used to carry data, voice and video over distances ranging from intercity links to deep – space spacecraft. Filters find applications virtually in any type of communication, radar or test and measurement system. In some applications such as communication satellite and mobile communication devices, it is critical that filters be devised with small size, light weight, and lower cost along with stringent electrical characteristics. Planar filter geometries are well suited for meeting these requirements.

The recent advances in novel materials and fabrication technologies, including monolithic microwave integrated circuit (MMIC), microelectro mechanical systems (MEMS), micromachining, high-temperature superconductor (HTS) and low temperature co-fired ceramic (LTCC) technology stimulated the development of new types of filters. The substrate integrated waveguide (SIW) is a promising technology considering its advantages as a new microwave transmission media with the advantages of both the rectangular waveguides and planar transmission line. The upcoming filter realizations utilize SIW to a large extent for microwave as well as millimetre wave communications.

A survey of the major techniques used in the design of microwave filters is presented by Ralph Levy et al. [1]. It is shown that the basis for much fundamental microwave filter theory lies in the realm of lumped – element filters, which indeed are actually used directly for many applications at microwave frequencies as high as 18 GHz. Many types of

microwave filters are discussed with the objective of pointing out the most useful ones, especially for the newcomer to this area.

## **2.2 Microstrip filters employing split ring resonators (SRRs)/complementary split ring resonators (CSRRs)**

The electromagnetic behaviour of split ring resonator (SRR) and complementary split ring resonator (CSRR) coupled to planar transmission lines are analysed in literature. Coupling mechanism of these elements to the host transmission line are studied and analytical equivalent-circuit models are proposed for the isolated and coupled SRR/CSRRs [2, 3]. From these models, the stopband/passband characteristics of the analysed SRR/CSRR loaded transmission lines are derived.

A compact bandpass filter (BPF) using a combination of the coupled uniform impedance resonator (CUIR) and the single CSRR is investigated in [4]. Two transmission zeros of the proposed BPF can be controlled by tuning the dimension of CSRR at higher stopband. Here, the size of the proposed BPF has a reduction of 26%, compared with the size of the conventional parallel coupled BPF.

The propagation characteristics of a microstrip line loaded with an array of SRRs as superstrate is investigated [5]. The presence of SRRs over the microstrip line leads to an effective negative permeability in a narrowband, where the signal propagation is inhibited. The width and attenuation of the rejected frequency band depends on the height of the superstrate as well as its relative position with the microstrip line.

The use of SRR loaded waveguide for the design of a band-reject filter with adjustable bandwidth is reported [6]. The width of the stopband

can be adjusted by suitably positioning the SRR array in the waveguide. The rejection band can be made very narrow by placing the array at the electric-field minimum. The stopband attenuation depends on the number of unit cells in the array.

Bandpass filter design using metallic SRR at optical frequencies is theoretically investigated in [7]. The transmission and reflection coefficients of the SRR array is also analysed.

Design of a compact microstrip band reject filter is proposed [8]. The device consists of an open loop rectangular resonator (OLRR) coupled to a microstrip line. The transmission line has a U –bend which enhances the coupling with the OLRR element and reduces the size of the filter.

A comparative investigation of SRR and CSRR based band reject filters is performed [9]. These compact filters are obtained by loading simple  $50 \Omega$  microstrip lines with SRRs and CSRRs that have exactly the same shape and dimensions. Unlike the previous studies, the stopband characteristics of these filters, such as resonant frequency, bandwidth, sharpness, and amount of attenuation in the rejection region is based on the number of SRR or CSRR stages, are investigated in detail and comparative manner. Both the filter structure and S-parameters are shown in Fig. 2.1.

Inter-digital capacitance loaded loop resonators (IDCLLRs) are used to design microstrip band reject filters [10]. The analysed structures are based on the coupling of IDCLLRs to a conventional  $50 \Omega$  microstrip line. The main features of the IDCLLRs are small dimensions (much smaller than the wavelength at resonance) and more structural parameters (provide flexibility in design).

Novel configurations of CSRR with dual mesh- shaped couplings and defected ground structures (DGS) are introduced to design the high performance of wide passband and stopband BPF [11]. This paper presents low insertion loss (0.82 dB), symmetry and sharper transmission zero level (-51.88 dB), using DGS and alternative coupling of CSRR.

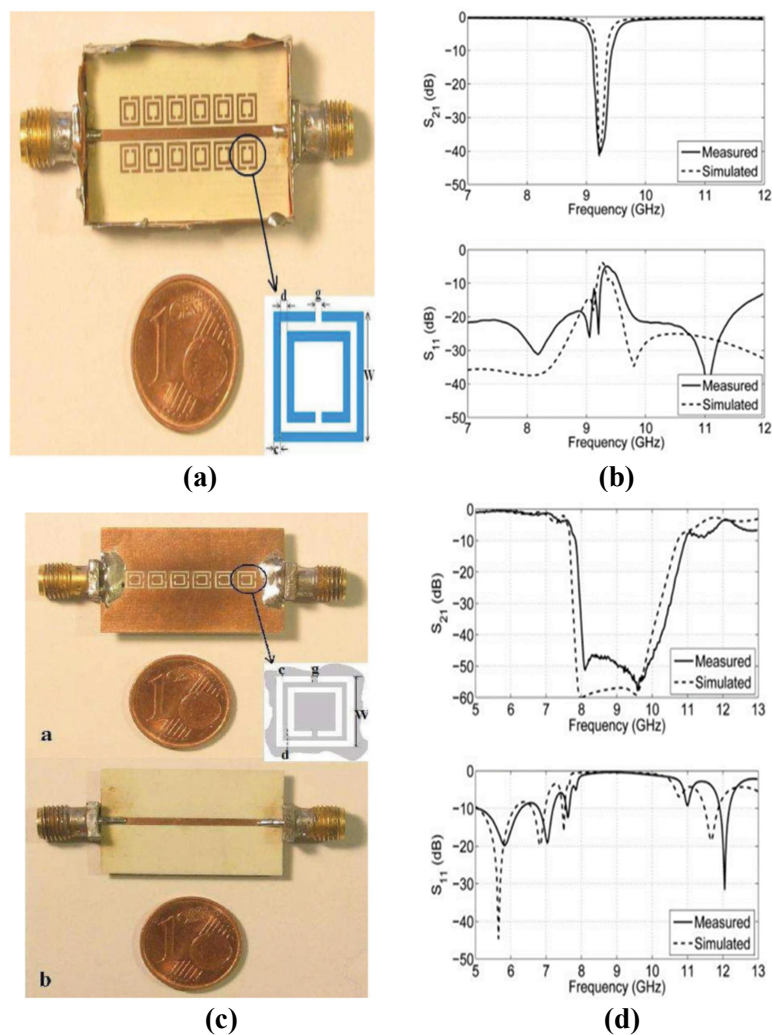


**Fig. 2.1. Microstrip line coupled SRR/CSRR Filter [9] (a) Fabricated Filter structure (SRR) (b) S-Parameters (c) Fabricated Filter structure (CSRR) (d) S-Parameters**

A novel compact microstrip bandpass filter using folded open loop resonator is presented in [12]. The resonator elements are placed in close proximity to parallel coupled microstrip lines. The presence of undesired harmonics is eliminated by properly modifying the configuration of the folded resonator. Another novel SRR configuration is proposed in [13]. The proposed resonator can generate two notches without increasing the physical size. A microstrip lowpass filter (LPF) is designed on the proposed resonator. The cut off frequency of the designed LPF is 3.7 GHz and the stopband with an attenuation level lower than 20 dB is obtained from 3.9 to 7.5 GHz. Miniaturized nested SRR structure is proposed in [14]. The nested SRR structure incorporates multiple SRRs in a compact nested structure, and has more split gaps than the conventional SRR structure. Compared with the conventional SRR, this nested SRR has better performance on miniaturization and high-Q value. This novel BPF is very compact and has good in- and out-band performances.

A microstrip bandstop filter (BSF) based on square SRR is proposed in [15]. The design steps consist of two parts. The first one consists of LPF characterized by a cut off frequency of 3.5 GHz. In the second part, square SRRs are used to pass from a LPF to bandstop filter. Finally the BSF is produced by an array of miniaturized loaded SRRs close to a microstrip line. High selectivity compact microstrip BPF with a flexibility controllable bandwidth, based on multi-path source-load couplings and a rectangular-type SRR is presented in [16]. The SRR is enclosed between the capacitively coupled source and load transmission feed lines, form the structure of the proposed BPF. The main advantage of this structure is its high selectivity due to the presence of multiple

transmission zeros. In addition, the bandwidth of the proposed filter can be flexibly controlled by varying the magnetic coupling gap between the SRR and the feed lines. The measured passband insertion and return loss are -0.83 dB and 27.23 dB respectively.

### **2.3 Substrate integrated waveguide bandstop, narrow and wide bandpass filters**

Infinite Rectangular waveguide periodically loaded by infinitely thin resonant irises is described in [17]. The result can be used for various applications such as waveguide filters and matching networks. New waveguide structure for millimeter-wave applications is proposed [18]. The dielectric waveguide with side walls of lined via-holes and edges of metallized planes are described and manufactured using lamination technique. New planar platform for microstrip to rectangular waveguide transition on the same substrate with taper is introduced [19]. A new generation of high- frequency integrated circuits is presented, which is called substrate integrated circuits (SICs) [20].

Current state- of- the art circuit design and implementation platforms based on the new concept are reviewed and discussed in detail. Different possibilities and numerous advantages of the SICs are shown for microwave, millimeter-wave and optoelectronics applications. Practical examples are illustrated with theoretical and experimental results for SIW, substrate integrated slab waveguide (SISW), and substrate integrated non radiating dielectric (SINRD) guide circuits. Future research and development trends are also discussed with reference to low cost innovative design of millimeter-wave and optoelectronic integrated circuits. The

integrated planar technique has been considered as a reliable candidate for low cost mass production of microwave and millimeter-wave circuits and systems. A new concept allows for a complete integration of planar circuits and waveguide filters synthesized on a single substrate by means of metallized post arrays [21].

Analysis of the synthesized integrated waveguide and design criteria are presented for the post pitch and diameter. A filter design method derived from a synthesis technique using inductive post is presented. An experimental three pole Chebyshev filter having 1 dB insertion loss and return loss better than 17 dB is demonstrated. A new method of analysis is presented in [22] for the determination of complex propagation constants in SIWs. This method makes use of the concept of surface impedance to model the rows of conducting cylinders, and the proposed model is then solved by combining method of moments and transverse resonance procedure. The proposed method is further applied to extract results in terms of parametric curves and graphs which demonstrate fundamental and interesting wave guidance and leakage properties of this type of periodic waveguide. Useful design rules are extracted from this analysis, suggesting that appropriate design parameters and regions should be carefully selected for practical applications.

A novel SIW equivalent inductive post filter is presented in [23] by using HFSS and equivalent circuit method. The filter is fabricated using standard PCB process. Excellent performance in selectivity, out of band rejection and passband insertion loss are shown.



A special planar negative coupling scheme including a magnetic coupling post-wall iris and a balanced microstrip line with a pair of metallic via-holes is studied in [24] detail. Two K-band fourth degree cross coupled bandpass filters with and without source-load coupling using the negative coupling structures are then proposed and designed. The two novel SIW filters having the same centre frequency of 20.5 GHz and respective bandwidth of 700 and 800 MHz are implemented on a single layer Rogers RT Duroid 5880 substrate with thickness of 0.58mm. The filters exhibit high selectivity, minimum insertion loss of 0.9, and 1.0 dB respectively.

A new topology of coupling between SIW circular cavities is designed [25] to produce particular filtering functions through combinations with the classical iris based coupling. This coupling is achieved by a grounded coplanar line etched at the top of cavities. This topology is used to realize a Ku-band third order filter.

A patent pending SIW bandpass filter with moderate fractional bandwidth and improved stopband performance are proposed and demonstrated [26] for a Ka- band satellite ground terminal. Non- physical cross-coupling provided by higher order modes in the oversized SIW cavities is used to generate the finite transmission zeros far away from the passband for improved stopband performance. Different input/output topologies of the filter are discussed for wide stopband applications. Design considerations including the design approach, filter configuration, and tolerance analysis are addressed. Two fourth-order filters with a passband of 19.2-21.2 GHz are fabricated on a single –layer Rogers

RT/Duriod 6002 with standard PCB process. Measurements over a temperature range of  $-20\text{ }^{\circ}\text{C}$  to  $+40\text{ }^{\circ}\text{C}$  show the passband remains almost unchanged.

An overview of the latest status and future trends of academic and industrial research on SIW technology is presented [27]. The historical development of SIW components and circuits is briefly outlined. The hot research topics such as development of numerical techniques for the modelling and design of SIW components, the investigation of novel compact and broadband interconnects, the determination of design solutions for loss minimization etc. are also discussed. Future research trends including implementation of SIW components at high frequency (60-350 GHz) and the integration of complete systems-on-substrate (SoS) is detailed.

A novel SIW dual-mode filter is proposed in [28]. By using an orthogonal input feed line and two slot lines for disturbing degenerate modes, two transmission zeros are created. The propagation properties of the half mode substrate integrated waveguide (HMSIW) are studied theoretically and experimentally in [29].

Two equivalent models of the HMSIW are introduced. With the first model, equations are derived to approximate the field distribution inside and outside the HMSIW. Using the second model, an approximate closed-form expression is deduced for calculating the equivalent width of an HMSIW that takes into account the effect of the fringing fields. The obtained design formulas are validated by simulations and experiments. Furthermore, the attenuation characteristics of the HMSIW are studied

using the multiline method in the frequency range of 20 - 60 GHz. A numerical investigation is carried out to distinguish between the contributions of the conductive, dielectric, and radiation losses. As a validation, the measured attenuation constant of a fabricated HMSIW prototype is presented and compared with that of a microstrip line and SIW. The conventional HMSIW structure, its variations and its antenna applications are reviewed in [30].

Review of SIW circuits and antennas are given in [31]. The operating principles, loss mechanisms, size and bandwidth are detailed. SIW passive circuit configurations such as filters, couplers, transitions and its electromagnetic modelling are reviewed. The SIW active circuits such as oscillators, mixers and amplifiers are also discussed. Different types of SIW antennas are also mentioned. Another review on the SIW approach to microwave and millimetre wave circuit is in [32]. In this SIW is depicted as a structure which has proven the capability to integrate within a monolithic microwave integrated circuit (MMIC) approach, allowing the development of high Q and low loss component that cannot be implemented in quasi-TEM transmission media like the stripline, microstrip line and coplanar waveguide. Micromachining has demonstrated the capabilities of the SIW approach within the framework of monolithic integrated passive components, while SIW implementations in flexible substrates will pave the way to low cost, consumer electronic products that could not be realized in conventional quasi- TEM transmission lines. One more review on recent advances in theory and applications of SIW is in [33]. The SIW structure, its recent progress and analysis, progress in

passive as well as active circuits, SIW antennas, reconfigurability, SoS concept etc. are reviewed.

The SIW filters are reviewed in [34-36]. The first paper [34] discusses the basic design considerations and challenges. The design guidelines and fundamental properties of SIW is being described. Filter components like SIW resonators and direct coupled SIW cavity resonator filters are also discussed. In the second paper [35] SIW filter with finite transmission zeros, dual mode SIW filters, wideband SIW filters, multiband SIW filters, reconfigurable filters and the art of miniaturization of SIW filters are discussed. The SIW cavity filters and its miniaturization is given in [36]. Different types of miniaturized SIW cavities such as folded SIW cavity, half-mode SIW cavity, and quarter-mode SIW cavity are discussed. In the new SIW material category paper-based SIW filters, textile based SIW filters and SIW filters based on 3D printing are detailed.

Novel SIW and HMSIW structures for bandpass filter and switchable bandpass filter applications are proposed [37]. The SIW resonators are realized by etching the electrically coupled complementary resonators on the surface of the SIW and the resonances are generated below the characteristic waveguide cut off frequency. By using a floating capacitor with mechanical switches loaded on the HMSIW resonators, a 1-bit HMSIW switchable bandpass filter is demonstrated.

The design of a microwave bandpass filter with frequency-dependent coupling is implemented in [38]. The proposed filter implements a four-pole generalized Chebyshev filtering function with two transmission

zeros. Resonators are arranged in extended box configuration with dispersive coupling on a main signal path, which produces an extra zero in comparison to classical approaches. The frequency dependent coupling is implemented as a shorted stub with an additional septum made from via holes. Such modification allows better control of the position of the transmission zero.

Novel SIW BPFs combined with planar resonators is proposed in [39]. According to specific topologies, microstrip lines with different electrical lengths are introduced into their designs. Their corresponding phase-shift characteristics are used to obtain the desired couplings between SIW cavities and the microstrip resonator. Two third-order filter samples are realized. One has single transmission zero below the passband and the other possess a quasi-elliptic response. Further, a fourth-order filter is developed by effectively super positioning two individual third-order topologies. It shows better frequency selectivity and flat in-band group delay.

The advances in the electromagnetic modelling of SIW components are described in [40]. In particular, the modelling of different aspects discussed, namely the dispersion characteristics, the losses, and the overall device simulation. The different modelling approaches, based on semi-analytical formulas, full-wave simulations and equivalent circuits are presented.

A millimeter wave BPF using SIW is proposed in [41]. A BPF with three resonators is formed by etching slots on the top metal plane of the single SIW cavity. The filter is investigated with the theory of electric

coupling mechanism. The design procedure and design curves of the coupling coefficient (K) and quality factor (Q) are given and discussed. The extracted K and Q are used to determine the filter circuit dimensions. In order to prove the validity SIW BPF operating at 140 GHz is fabricated in a single circuit layer using LTCC technology.

A novel multi-layer third-order SIW BPF with improved lower stopband performance is proposed [42].  $TE_{201}$ - mode in folded-SIW cavity is utilized to implement negative cross coupling, and the  $TE_{101}$ - mode is taken as a non-resonating node (NRN) for implementing bypass coupling. A circular aperture etched on the middle metal layer is used to realize coupling between source and the second SIW cavity. Then, three transmission zeros located below the passband can be obtained to improve stopband attenuation. Meanwhile, better spurious suppression performance above passband is achieved. A filter sample is designed and fabricated with multilayer LTCC technology.

An open-structure eigenvalue problem of SIW cavity structures is investigated in detail by using a finite-difference frequency-domain method, and the quality (Q) factor of such SIW cavities is given [43]. Based on the concept of a defected ground structure (DGS), a new class of SIW cavity bandpass filters are designed, fabricated and measured around 5.8 GHz. With their fabrication on standard PCB boards, such filters present the advantages of high-Q factor, high power handling capability, and small size.

Millimeter wave bandpass filter with three cascaded uniform slotted-SIW-based EBG units is constructed and designed at 40 GHz. [44].

The propagation constants of three different types of electromagnetic bandgap (EBG) units are discussed and compared with their passbands and stopbands performance. The slotted-SIW unit shows a very good lower stopband and upper stopband performance. The extracted coupling coefficient (K) and quality factor (Q) are used to determine the filter circuit dimensions. The structure is fabricated in a single circuit layer using LTCC and measured at 40 GHz.

Design of planar SIW and HMSIW BPF loaded with periodic array of longitudinal slots are proposed in [45]. The proposed method introduces simple periodic reactive slots which have the property to create the resonance to obtain stopband at multiple frequencies. Transmission zeros as well as insertion loss of the BPFs designed by using these techniques are relatively easy to control. The property of these periodic slots is further analysed to reach a concrete conclusion which provides the design engineers luxury to choose stopbands as per individual applications. Major spectrum of microwave X-band and Ku-band are covered with minimum insertion loss.

A novel perturbation approach using additional metalized via-holes for implementation of the dual-band or wide-band dual-mode SIW filters is proposed [46]. The independent perturbation on the first resonant mode  $TE_{101}$  can be constructed by applying the proposed perturbation approach, whereas the second resonant mode  $TE_{102}$  is not affected. In order to experimentally verify the design method, four two-cavity dual-band SIW filters, which have different numbers of perturbation via-holes in each cavity, and a two cavity dual-band SIW filter, which includes four via-

holes and eight reconfigurable states in each cavity, are designed and experimentally assessed. The measured results indicate that the available frequency-ratio range from 1 to 1.3 can be realized by using four two-cavity dual-band SIW filters.

The properties of dual mode resonance in planar SIW-based rectangular cavities are investigated and discussed [47]. A specific mode combination of dual mode cavity presents a unique frequency response feature. With the aid of an optimization process or software, it is convenient to cascade a number of cavities with coupling apertures to form a filter. A three-cavity pseudo-elliptic SIW filter based on  $H_{203}$  and  $H_{104}$  hybrid resonance is designed and fabricated on Rogers TMM3 substrate.

A quasi-elliptic filter with slot coupling and nonadjacent cross coupling based on the SIW cavity is proposed [48]. The slots etched on the top metal plane of SIW cavity are used to produce electrical coupling, and the cross coupling is realized by the microstrip transmission line above the SIW cavity. The coupling strength is mainly controlled by the width and height of the slot. The length of the open-ended microstrip line controls the sign of the cross coupling. The cross coupling with different signs is used in the filter to produce a pair of transmission zeros (TZs) at both sides of the passband. In order to prove the validity, a fourth-order SIW quasi-elliptic filter with TZs at both sides of the passband is fabricated in a two-layer printed circuit board. The measured insertion loss at a center frequency of 3.7 GHz is 1.1 dB. The return loss within the passband is below -18 dB with a fractional bandwidth of 16%.



A lossy filter with resistive coupling is proposed [49] based on SIW resonators, where nonresonating nodes are not required to simplify the realization. The sensitivity analysis of S-parameter to the resistive coupling coefficient is carried out to determine the parameters of coupling structure and mounted resistors. When resistive couplings are added to the structure, the measured 0.2 dB passband bandwidth increases from 198 to 256 MHz, compared with the case without resistive couplings. At a sacrifice on the additional insertion loss of 1.1 dB, the passband flatness and selectivity are improved significantly. The lossy SIW filter can provide a smaller in-band insertion loss than the microstrip counterparts, because the unloaded Q-factor of SIW resonators is higher than that of microstrip resonators. Moreover, a simple topology and a lesser insertion loss are obtained in the proposed resistively coupled SIW filter than those of the lossy filter synthesized with lossy coupling matrix.

High-performance, W-band SIW filters have been investigated [50] by using the low-cost PCB technology. Two types of SIW BPFs including cascaded quadruplet (CQ) and cascaded triplet (CT) filters are studied. The coupling matrix theory has been used to synthesize initial geometries, and the aggressive space mapping (ASM) algorithm was adopted as fast and low computation cost optimization method for realizations of investigated filters. A fin-line SIW-WR10 waveguide transition was developed for experiments. As demonstrations, two W-band prototypes having a 2.5% fractional bandwidth centered at 80 GHz are fabricated on a 0.508 mm-thick RO5880 substrate. This work mainly demonstrates that high-performance W-band planar filters can be realized by utilizing

the low-cost commercial PCB technology, and some design rules are recommended.

A highly selective inline SIW filter based on novel stepped-impedance non-resonating node (NRN) is presented [51]. The stepped impedance NRN is realized by inserting a stepped-impedance substrate integrated coaxial line resonator into the volume of a third-order SIW filter. It introduces extra signal transmission path between source and load. Thus, one more transmission zero (TZ) is produced compared with conventional NRN that further improves the selectivity of the filter. Also, the proposed filter achieves a compact circuit size as the stepped impedance NRN is embedded in the SIW cavity without occupying extra layout. To validate the proposed concept, a prototype filter with two TZs locating at both the lower and upper stop-bands, is designed.

A single-cavity dual-mode BPF design based on SIW resonator is proposed [52]. The proposed resonator has various types of inductive loading, such as symmetrical/asymmetrical, thin and narrow slots which are used to achieve a compact circuit size. The structure has also a new perturbation arrangement for dual-mode SIW resonators depending on the movement of narrow slots. A multilayer approach for suppressing the higher order modes of SIW BPFs is presented in [53]. Rectangular SIW resonators in multilayer substrate can be vertically coupled with magnetic and/or electric coupling by the proposed apertures etched on the middle metal layer. Harmonic passbands produced by the first higher-order mode  $TE_{102}$  can be suppressed, thanks to the proposed weak coupling or mixed coupling schemes in connection with the  $TE_{102}$  mode.

Compared with conventional horizontally coupled filter, the proposed filters also show a compact physical size. To demonstrate the proposed design method, two double-layered SIW BPFs are fabricated and measured. A dual-plane resonant cell wideband BPF is proposed [54] and designed on SIW cavities using U-shaped slots and H-shaped fractal DGS. The U-shaped slots etched on the top metal layer of the SIW cavity are used to constitute a multi-mode resonator and the H-shaped fractal DGS etched on the bottom metal layer can greatly improve the filter performance while keeping the overall size of the filter circuit to be much compact. The proposed filter can lead to a size reduction of approximately one-third compared with traditional SIW filters using U-shaped slots on the top metal plate of the SIW cavity. The measured 3 dB bandwidth is from 7.15 to 11.25 GHz, representing a fractional bandwidth of 44.6% at a center frequency of 9.2 GHz.

A dual-band BPF is proposed [55] in SIW technology. A single cavity that supports both  $TE_{101}$  and  $TE_{201}$  resonating modes is used for the design. The two passbands are created by the two modes. To improve the selectivity, one bypass coupling path is introduced which provides an additional transmission zero. The procedures to control the passband center frequencies as well as their bandwidths are presented. A prototype narrowband BPF with center frequencies of two passbands as 10 GHz and 11 GHz is fabricated for space applications. The 3 dB fractional bandwidths are 3% and 1.6% respectively.

Novel quasi-elliptic BPF in air-filled SIW technology is presented [56]. It is based on a dual-mode cavity resonator and features a frequency

response with two poles and two transmission zeros. This structure exploits the properties of the air-filled SIW, which has been recently proposed to realize integrated interconnects and allows for reduced losses. The geometry of the air-filled area in the SIW resonator allows controlling the passband of the filter, by setting the frequency of the first and second cavity modes. The position of the input/output microstrip lines, conversely, permits to modify the location of the transmission zeros.

A compact dual-mode SIW BPF with good skirt selectivity and bandwidth is proposed [57]. The position of the perturbation has an important role in deciding the passband in dual mode filter. The skirt selectivity of the filter was improved with a perfect electric conductor (PEC) covering for the perturbation on one side without altering the dual mode function. Two transmission zeros were present on either side of the passband with rejection values of -25.309 dB and -29.71 dB at 22.4 GHz and 25.7 GHz respectively. The transfer characteristics of the proposed design satisfies the frequency range of K band and hence can be used for RADAR and satellite communication applications. A comparative study of miniaturized inductive post and iris SIW BPFs are proposed [58].

Implementation of slow wave requires a double layer topology, which results in physically separating the electric and magnetic fields. This helps in miniaturization. Application of slow wave technique improved the insertion loss by 0.23% for the inductive post filter and 7.53% for iris filter. Slow wave factor (SWF) and group delay are found to be better in the iris filter. The inductive post filters are 38.1% and

61.36% miniaturized in size and area, and iris filters, 56.35% and 72.72% respectively. The Q factor of the miniaturize iris and inductive post filters are found to be 918.45 and 755.15 respectively.

A highly selective narrowband BPF employing SIW technology is presented [59]. Higher order  $TE_{301}$  resonators are used to utilize their high unloaded Q-factors. A midline feeding scheme together with a bypass coupling provides three TZs. Two of the zeros can be placed at band edges for high selectivity. A three-pole BPF with 3 dB fractional bandwidth of 1.1% at  $f_0= 8.25$  GHz is fabricated. It provides at least 35 dB attenuation over 2 GHz above and below the passband.

A network consisting of SIW, cavity resonator coupled to a stripline to give a bandstop response is proposed [60]. The fabricated filter is compact and operating at 9 GHz. A SIW bandstop filter on thick substrate is introduced [61]. The increased substrate height permits partial-height via holes to act as resonators whose interaction provides a wide range of possible coupling coefficients that result in wideband bandstop filters. In contrast to ridged all-metal waveguide filters, SIW filters with partial-height via holes maintain a small profile, low manufacturing cost and they can be integrated with other planar circuitry such as microstrip or coplanar waveguide. The design method of the bandstop filter relies on the well-known extracted-pole technique which allows designers to independently control the locations of reflection zeros. The parameters of the lowpass equivalent circuit of the filters are extracted and used for the initial design of the physical dimensions of the filter. A prototype bandstop filter is designed for a center frequency of 10.74 GHz

and a bandwidth of 1.58 GHz. Tolerance analyses demonstrate the influence of manufacturing inaccuracies on the filter performance.

The design and experiment of the half mode substrate integrated waveguide (HMSIW) BPFs are investigated [62]. Three-pole and five-pole HMSIW filters are simulated by using CST software and fabricated with a single layer standard PCB process. Different external coupling approaches are adopted in the design of the two filters. Low insertion loss and good selectivity are achieved. A planar HMSIW BPF filter is proposed [63].

It is realized by cascading a lowpass filter and a high pass filter. A transmission line with HMSIW on the circuit board has the characteristics of high pass, while a periodic uniform photonic bandgap structure (PBG) array has the characteristic of bandstop. Combining these two structures, a novel compact broadband BPF is fabricated and measured. The results show that the proposed BPF has wide bandwidth from 11.8 GHz to 23.8 GHz, all the measured insertion loss are less than 2.1 dB. The BPF achieves a wide stopband with 34 dB attenuation low to 5 GHz and 27 dB attenuation up to 35 GHz.

A novel, inductive post HMSIW BPF is presented [64]. The filter keeps the advantage of SIW filter but with a reduction of nearly one-half in size. A triangular shaped resonator which is one eighth of a square SIW cavity is used to design a novel miniaturized C-band BPF [65]. With the proposed one eighth SIW resonator (ESIWR) and new coupling structures, a conventional SIW filter can be reduced in size by about 87.5%. A four

pole ESIWR filter with a center frequency of 5.8 GHz and a fractional bandwidth of 8% is implemented. Fourth-order HMSIW filter with dual-mode resonator is etched on the top metal layer of HMSIW cavity [66], so the size can be reduced greatly. The filter has compact size and wide stopband in comparison with conventional SIW filters. Microstrip resonators and cavity resonators are integrated in one filter to achieve the goal of smaller size and better performance.

Compact ultra-wideband (UWB) BPF with two notched-band is presented and implemented [67]. Combining HMSIW and nonuniform periodic half circle-shaped DGS, a compact UWB BPF with high selectivity is realized. Modified electromagnetic bandgap (EBG) structures are studied and employed to introduce two notch bands, which is placed near the feedline to achieve the notchband.

Novel BPF using modified HMSIW technique is reported [68]. The via-fences are deployed as impedance inverters for the proposed filter to reduce its footprints, which are extracted by using full-wave electromagnetic simulator HFSS for the filter design. A BPF having a center frequency of 10.03 GHz and a passband from 9.78 to 10.3 GHz is designed. A HMSIW-DGS cell and its embedded form are proposed to miniaturize a BPF [69]. Both cells can purchase wideband frequency response and low insertion loss, as well as simple and easy fabrication. By cascading two of them according to design requirement, X-band BPF is designed and measured to meet compact size, low insertion loss, good return loss, second harmonic suppression, and linear phase.

A compact BPF employing novel ridged HMSIW [RHMSIW] and planar mixed electric and magnetic coupling is presented [70]. The RHMSIW is proposed by integrating a ridge into the HMSIW, where the ridge introduces a large capacitance in the cavity and hence leads to a lower cut off frequency and more compact size compared to the conventional HMSIW. Based on the RHMSIW, a fourth-order filter with the mixed coupling is designed and fabricated. The mixed coupling is realized by using an embedded open-ended strip line combined with an inductive window between adjacent RHMSIW cavities. Two transmission zeros are achieved in the upper stopband by using the mixed coupling.

Novel class of SIW filters based on perforations of the dielectric substrate is presented [71]. The air-hole perforations allow the local modification of the characteristic impedance of the SIW as well as its cut off frequency, thus permitting the easy design of filtering structures. Four-pole filters operating at 3.6 GHz, based on conventional and HMSIW, have been designed and validated. The proposed approach provides high flexibility, low sensitivity to fabrication inaccuracy, and simple design rules.

The propagation properties of RHMSIW are analysed and RHMSIW coupling topologies to implement compact wideband filters are explored [72]. The propagation constant and the cut off frequency of the RHMSIW are discussed. Two types of ultra-wideband RHMSIW coupling topologies are proposed by employing the evanescent-mode HMSIW and RHMSIW structures. To improve the stopband performance while keeping a small size, another novel mixed-coupled RHMSIW topology is



developed to introduce transmission zeros in filters by combining the evanescent-mode coupling with the slot coupling. Wideband RHMSIW filters are designed and fabricated with these coupling topologies.

A type of BPF based on HMSIW loaded with dielectric rods is designed and developed [73]. The proposed filter can operate below the characteristic cut off frequency of HMSIW, thus compact size can be achieved. Some slots etched on HMSIW are used in the filter development to reduce coupling effects between dielectric rods. Furthermore, an ultra-wide out-of-band rejection contributed to the slots is obtained.

Tri-band two-way filtering power divider structure is proposed [74] based on HMSIW. Dual-band filtering power divider is realized by etching semicircular slots on HMSIW. The third passband is achieved by loading open-stub without affecting two other passbands. The return loss is less than -20 dB in each passband with 3 dB fractional bandwidth of 3.75%, 9.3% and 0.61%. The design of wide BPFs for Ku and Ku/K band applications are investigated [75]. It has wide passband with miniaturization of size using folded SIW (FSIW) technique. The filter is designed by introducing a C slot and E slot in central metallic septum of FSIW respectively. The fabricated E slot filter achieved enhancement in bandwidth with dual-band operating in Ku band (14.35 GHz-16.76 GHz) and K band (18.06 GHz-19.61 GHz) respectively.

A novel BPF and tunable BPF are designed based on HMSIW embedded with complementary resonators [76]. Various passband

characteristics are observed, and lumped equivalent circuit analysis models are developed. The configuration of the proposed BPF is an open structure, and it is easy to load the active devices and build the bias/control networks on the signal plane. The tunable BPF is presented based on the proposed novel BPF loaded with semiconductor varactor diodes, and it has good spurious suppression characteristics and excellent out of band rejection.

A simple method for designing a triple-mode BPF is presented [77]. Triple-mode is achieved by using HMSIW cavity. Three perturbation metal vias were introduced for shifting resonant modes. The resonant frequencies of these modes can be adjusted by the location and the diameter of perturbation vias properly. In order to improve the out-of-band rejection, the CPW-to-SIW transition is added. A novel method is proposed [78] to design wideband BPF with compact size. Combining HMSIW and periodic dumbbell shaped DGS, two compact wideband BPFs with different HMSIW-microstrip transitions are tested. Two HMSIW filters are proposed [79] by introducing wide U slot in the conventional SIW structure. In the first case, lower industrial, scientific and medical radio (ISM) band HMSIW filter is designed by extending the center stub, thereby controlling the resonant frequency and bandwidth. In the second case higher ISM band HMSIW filter is designed by shorting the extended stub using via.

Triple-mode semi-hexagonal HMSIW cavity is utilized to implement a novel BPF [80] which has the advantages of compact size, low insertion loss, and high selectivity in upper and lower passband. To realize a triple-

mode filter, the first resonant mode is shifted to near the next two modes using a via hole perturbation. Two microstrip open stubs connected to open edge of HMSIW resonator are introduced to generate two transmission zeros in the lower passband. The position of transmission zeros could be controlled by adjusting the coupling gap between the microstrip open stub resonators. By etching an E-shape slot on the top plate of HMSIW resonator, two other transmission zeros are produced in the upper passband. A wideband planar six-pole BPF, which has the advantage of wide bandwidth and small size, is also proposed and fabricated by cascading two triple-mode resonators.

A half mode substrate integrated folded waveguide (HMSIFW) and a HMSIFW partial H-plane BPF are proposed [81]. The proposed filter employs H-plane slot of open-ended evanescent waveguide and H-plane septa of short-ended evanescent waveguide as admittance inverter and impedance inverter respectively. The filter has the advantages of convenient integration, compact size, low cost, mass-production and ease of fabrication. In order to validate the new proposed topology, a four-pole ultra-narrowband BPF, with quarter wavelength resonators, is designed and fabricated using standard PCB process.

The significant miniaturization of slotted HMSIW filters by incorporating a capacitive ridge is reported [82]. Based on this concept, two-pole and four-pole slotted BPFs are designed and tested. Compared to the previously reported slotted HMSIW filters, the proposed structure has a smaller footprint, lower insertion loss and a larger stopband. A BPF using HMSIW and modified U-shaped DGS slot-pairs is presented [83].

As both loaded into HMSIW, the modified DGS, compared with the original one, can contribute to improve the upper-side selectivity and expansion of the stopband.

## 2.4 SRR and CSRR loaded SIW and HMSIW filters

A novel BPF based on SIW and CSRRs are presented [84]. Three different CSRR cells are etched in the top plane of the SIW for transmission zero control. The filter structure as well as the S-parameters are shown in Fig. 2.2. A demonstration BPF is designed and tested. An ultra-wideband BPF based on a novel CSRR and HMSIW is proposed [85]. Sharpened rejection skirts and widened upper stopband are achieved due to the two resonant frequencies of the proposed CSRR. The fabricated filter along with the insertion and return loss characteristics are shown in Fig. 2.3. A SIW with square CSRRs etched on the waveguide surface is investigated [86]. This proposed structure allows the implementation of a forward-wave passband propagating below the characteristic cut off frequency of the waveguide. By changing the orientation of the CSRRs, which are incorporated in the waveguide surface and can be interpreted in terms of electric dipoles, varied passband characteristics are observed.

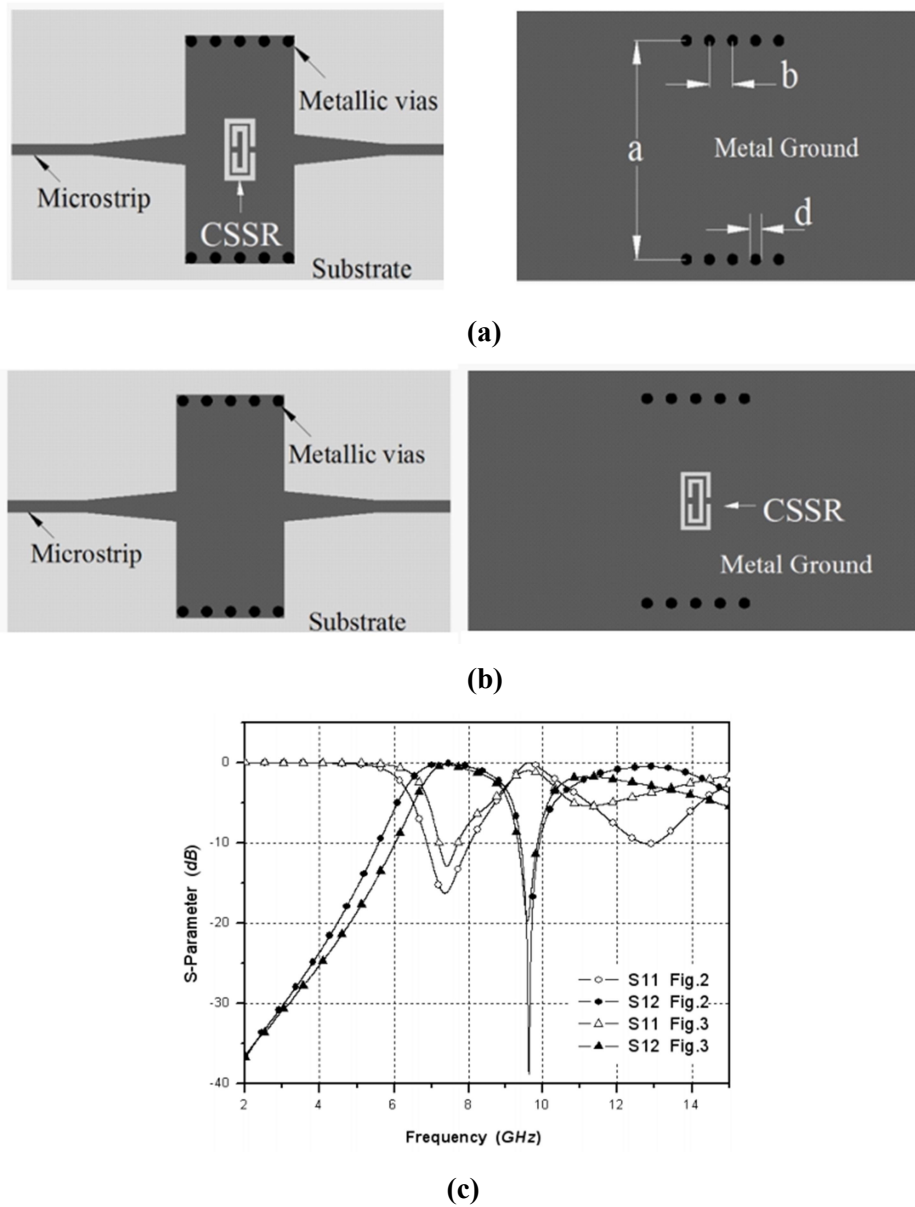


**Fig. 2.2. CSRR Embedded SIW Filters [84] (a) Top loaded CSRR (b) Bottom loaded CSRR (c) S-Parameters**

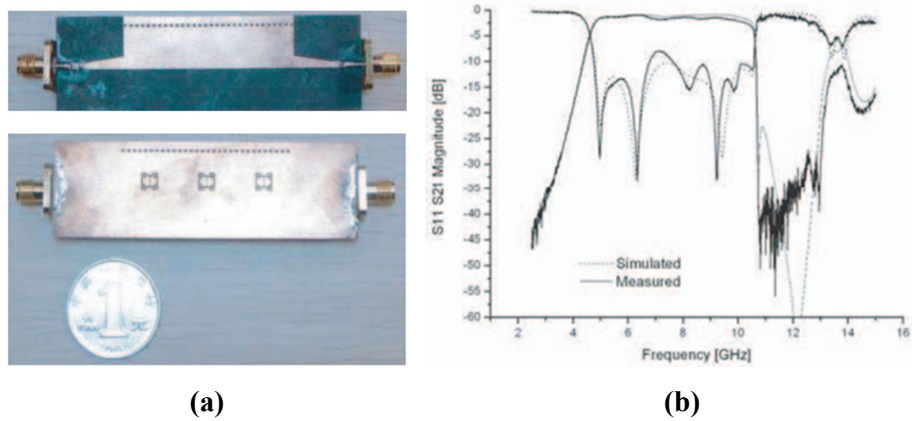


**Fig. 2.3. Ultra- Wideband HMSIW-CSRR filter [85] (a) Filter Structure (b) S-Parameters**

A detailed explanation of the generation and variations of the passbands has been illuminated. The application of this waveguide and CSRR combination technique to the design of miniaturized waveguide BPFs characterized by transmission zeros is then illuminated. Filter design methodology is examined. These proposed filters exhibit high selectivity and compact size due to the employment of the subwavelength resonators and an evanescent-wave transmission. By slightly altering the configuration of the CSRRs, the propagation of TE<sub>10</sub> mode can be suppressed and filters with improved selectivity and stopband rejection can be obtained. The Different types of SRR orientations, corresponding S-parameters, Narrow bandpass filter structure and its insertion and return loss characteristics are shown in Fig. 2.4.

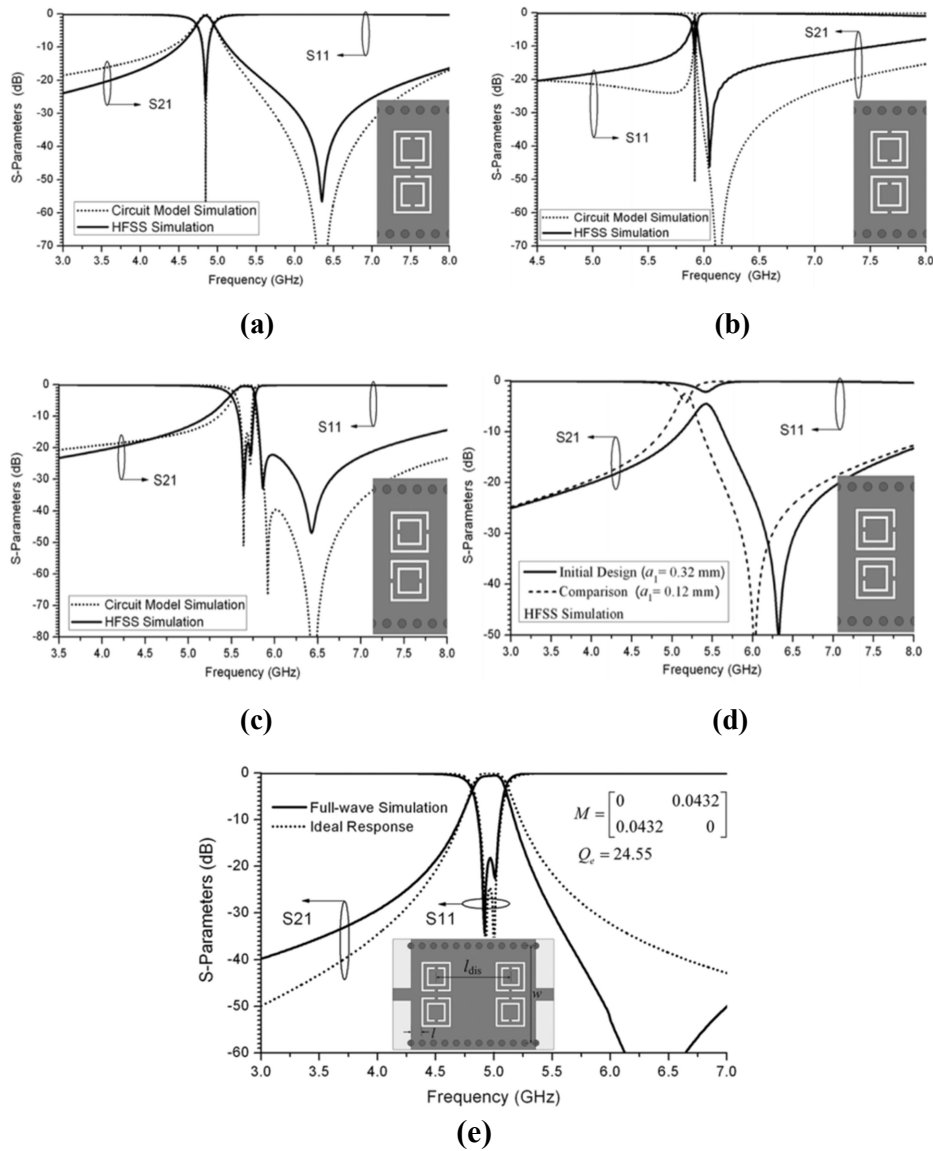


Fig. 2.4. Square SRR loaded SIW Bandpass Filter [86] (a)-(d) Different types of SRR orientations and corresponding S-Parameters (e) Four SRR loaded narrow bandpass filter

Single and dual band BPFs using CSRRs are implemented in [87]. Forward wave propagation is achieved below the characteristic cut off frequency of the waveguide due to evanescent wave transmission. Modified CSRRs are utilized to implement the filters.

A miniaturized BPF utilizing CSRR array loaded HMSIW is proposed [88]. By etching several CSRRs on the bottom metal plane of the HMSIW, a pass is realized below the cut off frequency of the HMSIW. The application of the HMSIW and CSRR combination technique for the design of miniaturized BPF is then illuminated by the equivalent circuit model. Another HMSIW miniaturization mode is depicted in [89]. The HMSIW etched with CSRRs can be regarded as the one filled with a dielectric material with higher permittivity. With specific CSRR arrays introduced, the CSRR-loaded structure can be 15% more compact than the original one. Moreover, the above CSRRs can also be used to enhance the rejection skirt of the BPF in this article. Finally, a compact and sharp rejection ultra-wideband BPF with designed notch-band is observed.

A compact planar BPF is presented [90] by the combination of three different electromagnetic structures, saying, SIW, square CSRR, and dumbbells slot. The resonator is formed by a SIW cavity loaded with some CSRRs on its top metal plane, causing a stopband with a very sharp rejection. Meanwhile, several dumbbells are etched on the bottom plane of SIW just below each CSRR to enhance the coupling. Double-sided parallel stripline (DSPSL) is also used to excite the SIW and guarantee good propagation between these two different structures. An x-band



prototype is designed and fabricated for demonstration. A new type of evanescent-mode SIW BPF is presented [91] with CSRRs introduced on the top or bottom metal planes of the waveguide. Both positive and negative coupling are obtained between CSRRs by changing their locations and orientations. In comparison with conventional SIW filters, the proposed filters are compact since their passbands are below the cut off frequency of the waveguide. A third and a fourth-order cross-coupled filter prototypes were designed using standard PCB technology. They operate at the same central frequency of 3.8 GHz, with their fractional bandwidths of 15% and 20%. The proposed filters have a wide upper stopband as the cut off frequency of  $TE_{1,0}$  mode in SIW is much higher than the central frequency.

Electrically tunable evanescent mode HMSIW resonators are implemented [92] for S-band applications. The tunable filter with its S-parameters are shown in Fig. 2.5. An HMSIW loaded with a CSRR achieves evanescent wave is applied here. A variable capacitor connected to one of the conductors of the CSRR changes its effective capacitance to ground, resulting in frequency tuning of the resonator. Three different configurations are investigated with varactor diode connected between the ground and three different contact points of the CSRRs. The external quality factor is slightly affected by the frequency tuning. More than 15% tunability is achieved around 3.4 GHz.

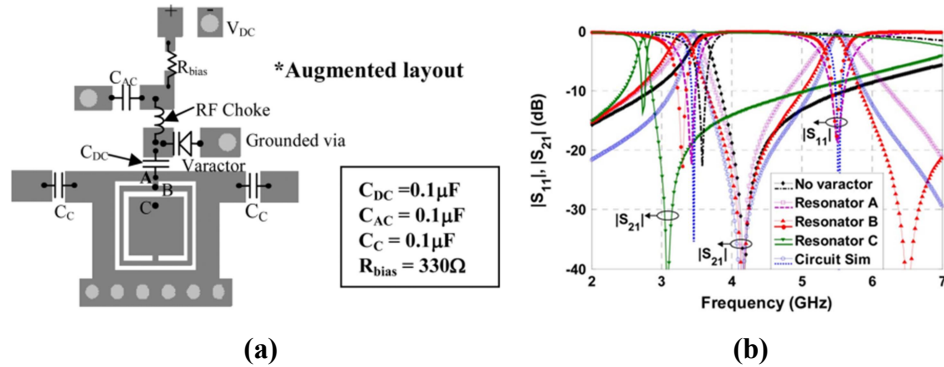


**Fig. 2.5. Electrically Tunable CSRR loaded SIW Filter [92] (a) Filter Structure (b) S-Parameters**

Novel dual-band BPFs are implemented [93] for 3.5 GHz and 5.8 GHz operation by using HMSIW loaded with CSRR and a capacitive metal patch. Forward electromagnetic wave transmission below the characteristic cut off frequency is achieved at two arbitrary frequency bands. Relatively independent control of the resonant frequencies, external Q factor and mutual coupling are possible. A dual band resonator and a two-pole miniaturized BPF are demonstrated. The external and internal mutual coupling variations are fully investigated. A reconfigurable HMSIW BPF loaded by CSRR is investigated [94]. The proposed HMSIW-CSRR structure allows the implementation of a forward-wave passband propagating below the characteristic cut off frequency of the waveguide. By changing the effective capacitance to ground of the CSRR, frequency tuning of the resonator is observed without other external circuit. The proposed filter exhibits improved selectivity due to the employment of the pseudo-S defected structure to generate transmission zero at the lower stopband. A hexagon shaped CSRR loaded HMSIW filter is investigated in [95]. By changing the radius of the

hexagon shaped CSRR, which is incorporated in the top plane of waveguide, the passaband can be tuned easily.

A bandstop filter employing half CSRR (HCSRR) loaded HMSIW is presented [96]. The experimental results indicate that the novel HCSRR shows almost the same resonant characteristics but half the size contrast with the original CSRR. Then the proposed HCSRR is etched on the middle of the HMSIW and a compact bandstop filter is obtained. A compact BPF exhibiting an ultra-wide out-of-band rejection is studied [97]. A combination of EBG-loaded HMSIW and composite right/left-handed (CRLH) HMSIW is used in this development. The proposed filter operates below the characteristic cut off frequency of HMSIW. The filter with a miniaturized size is then implemented with two slots etched on HMSIW to reduce coupling effects between EBG structures and interdigital capacitors. Defected microstrip structures (DMS) as feed lines are used to obtain an ultra-wide out-of-band rejection. Measured results show that this effective stopband can cover up to 10.3 times the design center frequency for a rejection level of 20 dB.

A modified CSRR loaded HSMIW BPF is proposed [98]. The modified CSRR is realized by using horizontal-asymmetrical stepped-impedance (SI) structure in the conventional CSRR, can enhance the equivalent capacitance and inductance of the CSRR and consequently shift the resonant frequency downwards. Therefore, for the same operation frequency, the SICSRR can occupy smaller size than the conventional CSRR, which provides a promising method to achieve size-reduction in microwave circuits. To verify the effectiveness of miniaturization

introduced from the proposed HMSIW-SICSRR resonator, a two-pole BPF is implemented.

Triple-mode BPFs on SIW is proposed [99]. Two degenerate modes of an SIW rectangular cavity and one resonant mode of a CSRR are employed to implement these filters. As a primary advantage, the CSRR mode is utilized instead of the fundamental mode of the SIW cavity to provide with an attractive capacity in easily controlling the frequency band of the designed SIW filters through the dimensions of this CSRR. Moreover, the positions of transmission zeros can be properly adjusted by the metallic via. Finally, three examples of SIW multimode BPFs are designed, fabricated and tested to verify the effectiveness of the proposed approach.

Open CSRRs (OCSRRs) loaded SIW is utilized for the realization of a novel BPF [100]. The OCSRRs can be interpreted in terms of electric dipoles and they are good candidates to behave as electric scatters. By loading OCSRRs on the waveguide surface, a forward-wave passband propagating below the waveguide cut off frequency is generated. The resonance frequency of the OCSRR is approximately half of the resonance frequency of the CSRR. Therefore, the electrical size of this particle is larger than the CSRR and the OCSRRs are more appropriate for the SIW miniaturization. A bandpass response with a sharp rejection frequency band is obtained by properly manipulating the structure of the elements. By changing the orientation of the OCSRRs, two type of unit cells are proposed. Moreover, by resizing the OCSRRs, resonance frequency can be shifted and bandwidth can be tuned by coupling between two OCSRRs.

Compared with some other reported BPFs, with SIW technique, the presented BPF has great improvements on size reduction and selectivity.

The concept of stepped-impedance resonators (SIRs) technique is used to miniaturize the physical size of the conventional CSRRs is utilized in the proposed [101] SIW filter. The proposed metamaterial unit-cells consists of two modified rings so that in these unit-cells, the slot lines in the conventional CSRRs are replaced by the stepped-impedance slot lines. The electrical size of SIR-CSRR are larger than the conventional CSRR. To investigate the performance of the proposed SIR-CSRR unit-cells in the size reduction, three SIW filters loaded by SIR-CSRR unit-cells with different configurations are designed. By loading the SIR-CSRRs on the substrate of the waveguide, an additional forward-wave passband propagating below the initial cut off frequency of the waveguide is produced. Consequently, by using the proposed SIR-CSRR unit-cells instead of the conventional CSRRs, miniaturization with arbitrary ratio are achieved. A dual-band SIW BPF based on CSRRs is proposed [102].

It consists of an SIW dual-mode cavity loaded by two additional CSRRs on its top layer. Both  $TE_{102}$  and  $TE_{201}$  modes in the cavity can be excited by the proper positions of the feeding lines. Two additional CSRRs are etched on the top layer coupled with the  $TE_{102}$  and  $TE_{201}$  modes respectively to achieve the dual-frequency operation. Four transmission zeros are generated in the vicinity of the passbands to improve the selectivity. To validate the design concept, a dual-band SIW BPF operating at 7.89 and 8.89 GHz is designed.

A shunt RLC resonant circuit obtained from a broadside-coupled open SRR (BC-OSRR) is proposed [103]. This BC-OSRR cell allows a parallel connection with planar waveguides. Hence, it has been applied to a HMSIW section. The analysis of the frequency response and electromagnetic field distribution of the HMSIW structure loaded with an appropriate BC-OSRR cell have shown two main behaviours. The first characteristic is a highpass frequency response inherent to the HMSIW and the second is a transmission zero in the passband of the HMSIW, which is due to the resonance of the BC-OSRR cell. The first- and second-order prototypes have been designed and fabricated. The measured bandstop HMSIW filters using BC-OSRR achieve a 3 dB stopband bandwidth around 10% with more than 21 dB insertion loss. This BC-OSRR cell with low undesired radiation loss can be a new alternative for the implementation of compact bandstop filters in the planar technology.

An extended doublet BPF is proposed [104] using a SIW cavity with a CSRR etched on its top metal plane. Thus, a single-layer BPF with two transmission zeros is realized successfully, with no additional area or layers occupied. A novel SIW bandpass filter with circular cavity is proposed [105].

The dual-iris coupling method to load CSRRs into HMSIW is used to implement a novel BPF [106]. Two circular cavities based on SIW are connected via connect hole. The width of the hole can control the coupling between resonators. Two different CSRRs are loaded at input and output feed line to produce transmission zeros and improve the characteristics of the stopband. By modifying traditional CSRRs through nesting method

combined with step impedance structure, a nested stepped-impedance CSRR (NSICSRR) structure with higher equivalent capacitance and inductance of CSRR is obtained. Based on the traditional single-iris coupling method, a dual-iris coupling method is developed. An NSICSRR is loaded into HMSIW by using the dual-iris coupling method, which can reduce the resonant frequency of the structure. In order to verify the effectiveness of the technology above in realizing the miniaturization of HMSIW filter, a second-order HMSIW filter is designed and measured.

## References

- [1] Ralph Levy, Richard V. Snyder, and George Matthaei, "Design of Microwave Filters," *IEEE Trans. Microwave Theory and Techniques*, Vol.50, No.3, March 2002.
- [2] Juan Domingo Baena, Jordi Bonache, Ferran Martin, Ricardo Marques Sillero, Francisco Falcone, Txema Lopetegi, Miguel A. G. Laso, Joan Garcia-Garcia, Ignacio Gil, Maria Flores Portillo, and Mario Sorolla, "Equivalent-Circuit Models for Split-Ring Resonators and Complementary Split-Ring Resonators Coupled to Planer Transmission Lines," *IEEE Trans. Microwave Theory and Techniques*, Vol.53, No.4, April 2005.
- [3] Filiberto Bilotti, Alessandro Toscano, Lucio Vegni, Koray Aydin, Kamil Boratay Alici, and Ekmel Ozbay, "Equivalent-Circuit Models for Design of Metamaterials Based on Artificial Magnetic Inclusions," *IEEE Trans. Microwave Theory and Techniques*, Vol.55, No.12, December 2007.
- [4] Hung-Wei Wu, Yan-Kuin Su, Min-Hang Weng, and Cheng-Yuan Hung, "A Compact Narrow-Band Microstrip Bandpass Filter with a Complementary Split-Ring Resonator," *Article in Microwave and Optical Technology Letters / Vol.48, No.10 October 2006.*

- [5] C. K. Anandan, C. S. Nimisha, B. Jitha, P. Mohanan, and K. Vasudevan, "Transmission Properties of Microstrip Lines Loaded with Split Ring Resonators as Superstrate," *Microwave and Optical Technology Letters / Vol.48, No.11* November 2006.
- [6] B. Jitha, C. S. Nimisha, C. K. Anandan, P. Mohanan, and K. Vasudevan, "SRR Loaded Waveguide Band Rejection Filter with Adjustable Bandwidth," *Microwave and Optical Technology Letters / Vol.48, No.7* July 2006.
- [7] A. Zarifkar, A. Rahmani, "Optical Bandpass Filter Design using Split Ring Resonators," *Progress In Electromagnetics Research M, Vol. 2,* 93-103, 2008.
- [8] B. Jitha, P. C. Bybi, C. K. Anandan, P. Mohanan, and K. Vasudevan, "Microstrip Band Rejection Filter using Open Loop Resonator," *Microwave and Optical Technology Letters / Vol.50, No.6* June 2008.
- [9] V. Oznazi, V. B Erturk, "A Comparative Investigation of SRR- AND CSRR-Based Band-Reject Filters: Simulations, Experiments, and Discussions," *Microwave and Optical Technology Letters / Vol.50, No.2* February 2008.
- [10] Y. Peng, W. X. Zhang, "Microstrip Band-Reject Filter Based on Inter-Digital Capacitance Loaded Loop Resonators," *Progress In Electromagnetics Research Letters, Vol. 8,* 93-103, 2009.
- [11] J. C. Liu, H. C Lin, "Complementary Split Ring Resonators with Dual Mesh-Shaped Couplings and Defected Ground Structures for Wide Pass-Band and Stop-Band BPF Design," *Progress In Electromagnetics Research Letters, Vol. 10,* 19-28, 2009.
- [12] B. Jitha, P. C. Bybi, C. K. Anandan, P. Mohanan, and K. Vasudevan, "Compact Bandpass Filter using Folded Loop Resonator with Harmonic Suppression," *Progress In Electromagnetics Research Letters, Vol. 14,* 69-78, 2010.



- [13] Yang Yang, Xi Zhu, and Nemaï C. Karmakar, "Microstrip Lowpass Filter Based on Split Ring and Complementary Split Ring Resonators," *Microwave and Optical Technology Letters* / Vol. 5, No. 7, July 2012.
- [14] Yong Liu, Xiaohong Tang, Zhongxun Zhang, and Xiaolong Huang, "Novel Nested Split-Ring-Resonator (SRR) for Compact Filter Application," *Progress In Electromagnetics Research*, Vol. 136, 765-773, 2013.
- [15] Badr Nasiri, Ahmed Errkik, Jamal Zbitou, Abdelali Tajmouati, Larbi El Abdellaoui, and Mohamed Latrach, "A New Compact Microstrip Band-stop Filter by Using Square Split Ring resonator," Article in *International Journal Microwave and Optical Technology*, Vol.12, No.5, September 2017.
- [16] Eun-Seong KIM, Kishor Kumar Adhikari, and Nam-Young KIM, "Split Ring Resonator-based Bandpass Filter with Multi-Transmission Zeros and Flexibly Controllable Bandwidth Using Multipath Source-Load Couplings," *Radioengineering*, Vol. 27, No. 4, December 2018.
- [17] T. E Rozzi, M. S Navarro, "Propagation in a Rectangular Waveguide Periodically Loaded with Resonant Irises," *IEEE Trans. Microwave Theory and Techniques*, Vol. MTT-28, No.8, August 1980.
- [18] H. Uchimura, T. Takenoshita, and M. Fuji, "Development of the Laminated Waveguide," *IEEE MTT-S International Microwave Symposium Digest*, 1998.
- [19] Dominic Deslandes, Ke Wu, "Integrated Microstrip and Rectangular Waveguide in Planar Form," *IEEE Microwave and Wireless Components Letters*, Vol. 11, No. 2, February 2001.
- [20] Ke Wu, Dominic Deslandes, and Yves Cassivi, "The Substrate Integrated Circuits – A New Concept for High-Frequency Electronics and Optoelectronics," *Conference Paper Proceedings*, November 2003.

- [21] Dominic Deslandes, Ke Wu, "Single-Substrate Integration Technique of Planar Circuits and Waveguide Filters," IEEE Trans. Microwave Theory and Techniques, Vol. 51, No.2, February 2003.
- [22] Dominic Deslandes, Ke Wu, "Accurate Modelling, Wave Mechanisms, and Design Considerations of a Substrate Integrated Waveguide," IEEE Trans. Microwave Theory and Techniques, Vol. 54, No.6, June 2006.
- [23] Yuandan Dong, Yuanqing Wang, and Wei Hong, "A Novel Substrate Integrated Waveguide Equivalent Inductive-Post Filter," Wiley Periodicals, Inc. Int J RF and Microwave CAE 18: 141-145, 2008.
- [24] Xia0 -Ping Chen, Ke Wu, "Substrate Integrated Waveguide Cross-Coupled Filter with Negative Coupling Structure," IEEE Trans. Microwave Theory and Techniques, Vol. 56, No.1, January 2008.
- [25] Benjamin Potelon, Jean-Francois Favennec, Cedric Quendo, Eric Rius, and Juan-Carlos, "Design of a Substrate Integrated Waveguide (SIW) Filter Using a Novel Topology of Coupling," IEEE Microwave and Wireless Components Letters, Vol. 18, No. 9, September 2008.
- [26] Xiao-Ping, Ke Wu, and Daniel Drolet, "Substrate Integrated Waveguide Filter with Improved Stopband Performance for Satellite Ground Terminal," IEEE Trans. Microwave Theory and Techniques, Vol. 57, No.3, March 2009.
- [27] Maurizio Bozzi, Luca Perregrini, Ke Wu, and Paolo Arcioni, "Current and Future Research Trends in Substrate Integrated Waveguide Technology," Radioengineering, Vol. 18, No. 2, June 2009.
- [28] R. Q. Li, X. H. Tang, and F. Xiao, "Substrate Integrated Waveguide Dual-Mode Filter Using Slot Lines Perturbation," Electronics Letters Vol. 46, No. 12, June 2010.

- [29] Qinghua Lai, Christophe Fumeaux, Wei Hong, and Rudiger Vahldieck, "Characterization of the Propagation Properties of the Half-Mode Substrate Integrated Waveguide," *IEEE Trans. Microwave Theory and Techniques*, Vol. 57, No.8, August 2009.
- [30] Nghia Nguyen-Trong, Christophe Fumeaux, "Half-Mode Substrate-Integrated Waveguides and Their Applications for Antenna Technology," *IEEE Antennas & Propagation Magazine*, December 2018.
- [31] M. Bozzi, A. Georgiadis, "Review of Substrate-Integrated Waveguide Circuits and Antennas," *IET Microw. Antennas Propag.*, Vol. 5, Iss. 8, 2011.
- [32] G. Ghione, "A Review on the Surface Integrated Waveguide (SIW): Integrating a Rectangular Waveguide in a Planar (M)MIC," *Conference on Substrate Integrated Waveguides and Related Technology*, Bari, 15 Maggio 2015.
- [33] Abhishek Sahu, Vijay K. Devabhaktuni, Rabindra K. Mishra, and Peter H. Aaen, "Recent Advances in Theory and Applications of Substrate-Integrated Waveguide: A Review," *Wiley Periodicals, Inc. Int J RF and Microwave CAE* 26:129-145, 2016.
- [34] Xiao-Ping Chen, Ke Wu, "Substrate Integrated Waveguide Filter," *IEEE Microwave Magazine*, August 2014.
- [35] Xiao-Ping Chen, Ke Wu, "Substrate Integrated Waveguide Filter," *IEEE Microwave Magazine*, October 2014.
- [36] Cristiano Tomassoni, Maurizio Bozzi, "Substrate Integrated Waveguide Cavity Filters: Miniaturization and New Materials for IoT Applications," *Radioengineering*, Vol. 26, No. 3, September 2017.
- [37] Q.-Y. Xiang, Q.-Y. Feng, X.-G. Huang, and D.-H. Jia, "Substrate Integrated Waveguide (SIW) Filters and Its Application to Switchable Filters," *Progress In Electromagnetics Research Symposium Proceedings*, August 19-23, 2012.

- [38] Lukasz Szydlowski, Natalia Leszczynska, Adam Lamecki, and Michal Mrozowski, "A Substrate Integrated Waveguide (SIW) Bandpass Filter in A Box Configuration with Frequency-Dependent Coupling," IEEE Microwave and Wireless Components Letters, Vol. 22, No. 11, November 2012.
- [39] Wei Shen, Wen-Yan Yin, Xiao-Wei Sun, and Lin-Sheng Wu, "Substrate-Integrated Waveguide Bandpass Filters With Planar Resonators for System-on-Package," IEEE Trans. Components, Packing and Manufacturing Technology, Vol. 3, No.2, February 2013.
- [40] Maurizio Bozzi, Marco Pasian, and Luca Perregrini, "Modeling of Losses in Substrate Integrated Waveguide Components," IEEE, 2014.
- [41] Sai Wai Wong, Kai Wang, Zhi-Ning Chen, and Qing-Xin Chu, "Design of Millimeter-Wave Bandpass Filter Using Electric coupling of Substrate Integrated Waveguide (SIM)," IEEE Microwave and Wireless Components Letters, Vol. 24, No. 1, January 2014.
- [42] Ping-Juan Zhang, Min-Quan Li, "Substrate Integrated Waveguide Filter with Improved Stopband Performance Using LTCC Technology," Progress In Electromagnetics Research C, Vol. 54, 155-162, 2014.
- [43] Yu Lin Zhang, Wei Hong, Ke Wu, Ji Xin Chen, and Hong Jun Tang, "Novel Substrate Integrated Waveguide Cavity Filter With Defected Ground Structure," IEEE Trans. Microwave Theory and Techniques, Vol. 53, No. 4, April 2005.
- [44] Sai-Wai Wong, Rui Sen Chen, Kai Wang, Zhi-Ning Chen, and Qing-Xin Chu, "U-Shape Slots Structure on Substrate Integrated Waveguide for 40-GHz Bandpass Filter Using LTCC Technology," IEEE Trans. Components, Packaging and Manufacturing Technology, Vol. 5, No. 1, January 2015.

- [45] Sourav Moitra, Partha Sarathee Bhowmik, “Modelling and analysis of Substrate Integrated Waveguide (SIW) and Half-Mode SIW (HMSIW) Band-pass Filter Using Reactive Longitudinal Periodic Structures,” *Int. J. Electron. Commun. (AEU)*, 2016.
- [46] Yongle Wu, Yuqing Chen, Lingxiao Jiao, Yuanan Liu, and Zabih Ghassemlooy, “Dual-Band Dual-Mode Substrate Integrated Waveguide Filters with Independently Reconfigurable TE<sub>101</sub> Resonant Mode,” *Scientific Reports*, 2016.
- [47] Yu Tang, Ke Wu, and Nazih Khaddaj Mallat, “Development of Substrate Integrated Waveguide Filters for Low-Cost High-density RF and Microwave Circuit Integration: Pseudo-Elliptic Dual Mode Cavity Band-Pass Filters,” *Int. J. Electron. Commun. (AEU)*, 2016.
- [48] Sai-Wai Wong, Rui-Sen Chen, Jing-Yu Lin, Lei Zhu, and Qing-Xin Chu, “Substrate Integrated Waveguide Quasi-Elliptic Filter Using Slot-Coupled and Microstrip-Line Cross-Coupled Structures,” *IEEE Trans. Components, Packaging and Manufacturing Technology*, Vol. 6, No. 12, December 2016.
- [49] Bin Gao, Lin-Sheng Wu, and Jun-Fa Mao, “Flat-Passband Substrate Integrated Waveguide Filter with Resistive Couplings,” *Progress In Electromagnetics Research C*, Vol. 62, 1-10, 2016.
- [50] Zhang-Cheng Hao, Wen-qi Ding, and Wei Hong, “Developing Low-Cost W-Band SIW Bandpass Filters Using the Commercially Available Printed-Circuit-Board technology,” *IEEE Trans. Microwave Theory and Techniques*, Vol. 64, No. 6, June 2016.
- [51] Zhaosheng He, Chang Jiang You, Supeng Leng, and Xiang Li, “Compact Inline Substrate Integrated Waveguide Filter with Enhanced Selectivity Using New Non-Resonating Node,” *Electronics Letters*, Vol. 52, No. 21, October 2016.

- [52] Ceyhun Karpuz, Gulfem Balasu Firat, Pinar Ozturk Ozdemir, Ahmet Ozek, and Ali Kursad Gorur, "Design of Dual-Mode Substrate Integrated Waveguide Filter using Inductive Slots," Proceedings of the Asia-Pacific Microwave Conference 2016.
- [53] Dinghong Jia, Quanyuan Feng, Qianyain Xiang, and Ke Wu, "Multiplayer Substrate Integrated Waveguide (SIW) Filters With Higher-Order Mode Suppression," IEEE Microwave and Wireless Components Letters, Vol. 26, No. 9, September 2016.
- [54] Jun-Ping Liu, Zhi-Qing Lv, and Xiang An, "Compact Substrate Integrated Waveguide Filter Using Dual-Plane Resonant Cells," Microwave and Optical Technology Letters / Vol. 58, No. 1, January 2016.
- [55] Arani Ali Khan, Mrinal Kanti Mandal, "Dual-Band Substrate Integrated Waveguide Filter with Independently Controllable Bandwidth," Proceedings of the Asia-Pacific Microwave Conference 2016.
- [56] Cristiano Tomassoni, Lorenzo Silvestri, Maurizio Bozzi, Luca Perregrini, and Anthony Ghiotto, "A Dual-Mode Quasi-Elliptic Filter in Air-Filled Substrate Integrated Waveguide Technology," Proceedings of the EUMC, 2017.
- [57] Ananya Parameswaran, S. Raghavan, "Novel SIW Dual Mode Band Pass Filter with High Skirt Selectivity," International Conference for Convergence in Technology, 2017.
- [58] Ananya Parameswaran, Athira P, and S. Raghavan, "Miniaturizing SIW Filters with Slow Wave Technique," Int. J. Electron. Commun. (AEU) 84, 2018.
- [59] Arani Ali Khan, Mrinal Kanti Mandal, "Narrowband Substrate Integrated Waveguide Bandpass Filter with High Selectivity," IEEE Microwave and Wireless Components Letters, Vol. 28, No. 5, May 2018.

- [60] Badrul Hisham Ahmad, Ian C. Hunter, “Design and Fabrication of a Substrate Integrated Waveguide Bandstop Filter,” Proceedings of the 38th European Microwave Conference, 2008.
- [61] Yuanqing Wang, Wei Hong, Yuandan Dong, Bing Liu, Hong Jun Tang, Jixin Chen, Xiaoxin Yin, and Ke Wu, “Half Mode Substrate Integrated Waveguide (HMSIW) Bandpass Filter,” IEEE Microwave and Wireless Components Letters, Vol. 17, No. 4, April 2007.
- [62] Mahbubeh Esmacili<sup>1</sup>, Jens Bornemann<sup>1</sup>, Peter Krauss, “Substrate Integrated Waveguide Bandstop Filter using Partial-Height Via-Hole Resonators in Thick Substrate,” IET Microw. Antennas Propag., Vol. 9, Iss. 12, pp. 1307–1312, 2015.
- [63] C.-L. Zhong, J. Xu, Z.-Y. Yu, M.-Y. Wang, and J.-H. Li, “Half Mode Substrate Integrated Waveguide Broadband Bandpass Filter,” Progress In Electromagnetics Research Letters, Vol. 4, 131-138, 2008.
- [64] Xiaochuan Zhang, Jun Xu, Zhiyuan Yu, and YuLiang Dong, “C-BAND Half Mode Substrate Integrated Waveguide (HMSIW) Filter,” Microwave and Optical Technology Letters / Vol. 50, No. 2, February 2008.
- [65] Guang Yang, Wei Liu, and Falin Liu, “A Compact C-band Bandpass Filter Using One Eighth Substrate Integrated Waveguide Resonator,” IEEE Conference paper Proceedings May 2012.
- [66] M. Zhou, M. X. Yu, J. Xu, X. C. Zhang, and M. Y. Wang, “Compact Half-Mode Substrate Integrated Waveguide (HMSIW) Filter with Dual-Mode Microstrip Resonator,” Progress In Electromagnetics Research C, Vol. 33, 29-41, 2012.
- [67] Liu Hao, Xu Ziqiang, Wu Bo, and Liao Jiakuan, “Compact HMSIW UWB Bandpass Filter Using DGS and EBG Technology with Two Notched-band,” International Workshop on Microwave and Millimeter Wave Circuits and System Technology, 2013.

- [68] Zhang-Cheng Hao, Xin -Ping Huo, “A Bandpass Filter Using Modified Half Mode Substrate Integrated Waveguide Technique,” Wiley Periodicals, Inc., International Journal of RF and Microwave Computer-Aided Engineering, 2014.
- [69] Yong Mao Huang, Zhenhai Shao, Zhaosheng He, Chang Jiang You, and Di Jiang, “A Bandpass Filter Based on Half Mode Substrate Integrated Waveguide-to-Defected Ground Structure Cells,” International Journal of Antennas and Propagation, 2015.
- [70] Liwen Huang, Hao Cha, “Compact Ridge Half-Mode Substrate Integrated Waveguide Bandpass Filter,” IEEE Microwave and Wireless Components Letters, Vol. 25, No. 4, April 2015.
- [71] Lorenzo Silvestri, Enrico Massoni, Maurizio Bozzi, Luca Perregrini, Cristino Tomassoni, and Angela Coves, “A New Class of SIW Filters Based on Periodically Perforated Dielectric Substrate,” Proceedings of the 46<sup>th</sup> EUMA Conference, 2016.
- [72] Liwen Huang, Hao Cha, and Yi Li, “Compact Wideband Ridge Half-Mode Substrate Integrated Waveguide Filters,” IEEE Trans. Microwave Theory and Techniques, vol. 64, No. 11, November 2016.
- [73] Qiao-Li Zhang, Bing-Zhong Wang, “A Dielectric Loaded Bandpass Filter Based on Half-Mode Substrate Integrated Waveguide,” IEEE Conference paper Proceedings, 2017.
- [74] Xu Wang, Ling-Qin Meng, Wei Wang, and Dan-Dan Lv, “HMSIW Tri-Band Filtering Power Divider,” Progress In Electromagnetics Research Letters, Vol. 68, 17-24, 2017.
- [75] Nithin Muchhal, Arnab Chakraborty, Manoj Vishwakarma, and Shweta Srivastava, “Slotted Folded Substrate Integrated Waveguide Band Pass Filter with Enhanced Bandwidth for Ku/K Band Applications,” Progress In Electromagnetics Research M, Vol. 70, 51-60, 2018.



- [76] Q.-Y. Xiang, Q.-Y. Feng, and X.-G. Huang, "Half-Mode Substrate Integrated Waveguide (HMSIW) Filters and its Application to Tunable Filters," *J. of Electromagn. Waves and Appl.*, Vol. 25, 2043–2053, 2011.
- [77] Zicheng Wang, Tao Yang, and Jun Dong, "A Compact Triple-Mode Bandpass HMSIW Filter," *Progress in Electromagnetics Research Letters*, Vol. 48, 39{43, 2014.
- [78] Q. Y. Song, H. R. Cheng, X. H. Wang, L. Xu, X. Q. Chen and X. W. Shi, "Novel Wideband Bandpass Filter Integrating HMSIW with DGS," *J. of Electromagn. Waves and Appl.*, Vol. 23, 2031–2040, 2009.
- [79] Ramalingam Sandhya, Hyder Ali Umma Habiba, "Miniaturised ISM Band HMSIW Band-Pass Filter Loaded with Wide U Slot," *The Journal of Engineering*, December 2017.
- [80] Tahsin Khorand, Mohammad Sajjad Bayati, "Novel Half-Mode Substrate Integrated Waveguide Bandpass Filters using Semi-Hexagonal Resonators," *Int. J. Electron. Commun. (AEÜ)* 95, 2018.
- [81] Z. G. Wang, X. Q. Li, S. P. Zhou, B. Yan, R. M. Xu, and W. G. Lin, "Half Mode Substrate Integrated Folded Waveguide (HMSIFW) and Partial H-Plane Bandpass Filter," *Progress In Electromagnetics Research, PIER* 101, 203{216, 2010.
- [82] Thomas R. Jones, Mojgan Daneshmand, "Miniaturized Slotted Bandpass Filter Design Using a Ridged Half-Mode Substrate Integrated Waveguide," *IEEE Microwave and Wireless Components Letters*, Vol. 26, No. 5, May 2016.
- [83] Yong Mao Huang, Tao Huang, and Zhenhai Shao, "Size-Reduced Bandpass Filter Using HMSIW and Modified U Shaped DGS Slot-Pairs," *IEEE Conference paper Proceedings*, 2015.

- [84] X.-C. Zhang, Z.-Y. Yu, and J. Xu, "Novel Band-Pass Substrate Integrated Waveguide (SIW) Filter based on Complementary Split Ring Resonators (CSRRS)," *Progress in Electromagnetics Research*, PIER 72, 39-46, 2007.
- [85] L. Qiang, Y.-J. Zhao, Q. Sun, W. Zhao, and B. Liu, "A Compact UWB HMSIW Bandpass Filter based on Complementary Split-Ring Resonators," *Progress In Electromagnetics Research C*, Vol. 11, 237-243, 2009.
- [86] Yuan Dan Dong, Tao Yang, and Tatsuo Itoh, "Substrate Integrated Waveguide Loaded by Complementary Split-Ring Resonators and Its Applications to Miniaturized Waveguide Filters," *IEEE Trans. Microwave Theory and Techniques*, Vol. 57, No. 9, September 2009.
- [87] David E. Senior, Xiaoyu Cheng, Melroy Machado, and Yong-Kyu Yoon, "Single and Dual Band Bandpass Filters Using Complementary Split Ring Resonator Loaded Half Mode Substrate Integrated Waveguide," *IEEE Conference Paper Proceedings*, 2010.
- [88] Li Qiang, Quan Sun, Wei Zhao, Wen-Bo Qin, and Ji-Kang Wang, "A Miniaturized Bandpass Filter Based on Half-Mode Substrate Integrated Waveguide Loaded by Complementary Split-Ring Resonators," *Proceedings of IEEE International Conference on Ultra-Wideband (ICUWB2010)*, 2010.
- [89] Li Qiang, Hong-Min Lu, Wei Zhao, Hong-Bo Qin, and Bing Liu, "Half Mode Substrate Integrated Waveguide Miniaturization using Complementary Split Ring Resonators," *Microwave and Optical Technology Letters* / Vol. 53, No. 5, May 2011.
- [90] Kuan Deng, Zengxu Guo, Chao Li, and Wenquan Che, "A Compact Planar Bandpass Filter with Wide Out-Of-Band Rejection Implemented By Substrate-Integrated Waveguide and Complementary Split-Ring Resonator," *Microwave and Optical Technology Letters* / Vol. 53, No. 7, July 2011.

- [91] Q.-L. Zhang, W.-Y Yin. And S, He, “Evanescent-Mode Substrate Integrated Waveguide (SIW) Filters Implemented with Complementary Split Sing Resonators,” *Progress In Electromagnetics Research*, Vol. 111, 419-432, 2011.
- [92] David E. Senior, Xiaoyu Cheng, and Yong-Kyu Yoon, “Electrically Tunable Evanescent Mode Half-Mode Substrate-Integrated-Waveguide Resonators,” *IEEE Microwave and Wireless Components Letters*, Vol. 22, No. 3, March 2012.
- [93] David E. Senior, Xiaoyu Cheng, and Yong Kyu Yoon, “Dual-Band Filters using Complimentary Split-Ring Resonator and Capacitive Loaded Half-Mode Substrate-Integrated-Waveguide,” *IEEE Conference Paper Proceedings*, 2012.
- [94] Zhu-Dan, Feng Wei, Li Zhang, and Xiaowei Shi, “Compact Reconfigurable HMSIW Bandpass Filter Loaded by CSRR,” *Progress In Electromagnetics Research Letters*, Vol. 84, 115–121, 2019.
- [95] Di Jiang, Yuehnag Xu, Ruimin Xu, and Weigan Lin, “A Novel Bandpass Filters using Complementary Split Ring Resonator Loaded Half Mode Substrate Integrated Waveguide,” *ACES JOURNAL*, Vol. 28, No. 2, February 2013.
- [96] Yang Cai, Zuping qian, Wenquan Cao, Yingsong Zhang, and Liu Yang, “HMSIW Bandstop Filter Loaded with Half Complementary Split-Ring Resonator,” *Electronics Letters*, Vol. 51, No. 8 pp. 632-633, April 2015.
- [97] Qiao-Li Zhang, Bing-Zhong Wang, De-Shuang Zhao, and Ke Wu, “a Compact Half-Mode Waveguide Bandpass Filter with Wide Out-of-Band Rejection,” *IEEE Microwave and Wireless Components Letters*, Vol. 26, No. 7, July 2016.

- [98] Yong Mao Huang, Zhenhai Shao, Wei Jiang, Tao Huang, and Guoan Wang, "Half-Mode Substrate Integrated Waveguide Bandpass Filter Loaded with Horizontal-Asymmetrical Stepped-Impedance Complementary Split-Ring Resonators," *Electronics Letters*, Vol. 52, No. 12 pp. 1034-1036, June 2016.
- [99] Zheng Liu, Gaobiao Xiao, and Lei Zhu, "Triple-Mode Bandpass Filters on CSRR-Loaded Substrate Integrated Waveguide Cavities," *IEEE Trans. Components, Packaging and Manufacturing Technology*, Vol. 6, No. 7, July 2016.
- [100] Mostafa Danaeian, Kambiz Afrooz, Ahmad Hakimi, and Ali-Reza Moznebi, "Compact Bandpass Filter Based on SIW Loaded by Open Complementary Split-Ring Resonators," *Wiley Periodicals, Inc. Int J RF and Microwave CAE*, Vol. 26 No. 8, October 2016.
- [101] Mostafa Danaeian, Kambiz Afrooz, and Ahmad Hakimi, "Miniaturization of Substrate Integrated Waveguide Filters using Novel Compact Metamaterial Unit-Cells based on SIR Technique," *Int. J. Electron. Commun. (AEU)* Vol. 84, 62-73, 2018.
- [102] Hao Zhang, Wei Kang, and Wen Wu, "Dual-Band Substrates Integrated Waveguide Bandpass Filter Utilising Complementary Split-Ring Resonators," *Electronics Letters*, Vol. 54, No. 2 pp. 85-87, January 2018.
- [103] Juan Hinojosa, Marcello Rossi, Adrian Saura-Rodenas, Alejandro Alvarez-Melcon, and Felix Lorenzo Martinez-Viviente, "Compact Bandstop Half-Mode Substrate Integrated Waveguide Filter Based on a Broadside-Coupled Open Split-Ring Resonator," *IEEE Trans. Microwave Theory and Techniques*, Vol. 66, No. 6, June 2018.
- [104] Lin-Sheng Wu, Xi-Lang Zhou, Wei, and Wen-Yan Yin, "An Extended Doublet Substrate Integrated Waveguide (SIW) Bandpass Filter with a Complementary Split Ring Resonator (CSRR)," *IEEE Microwave and Wireless Components Letters*, Vol. 19, No. 12, December 2009.

- [105] Chuanyun Wang, Xiaoyan Zhang, Xuehui Guan, Jing Wan, and Haiwen Liu, “A Novel Substrate Integrated Waveguide Circular Cavity BandPass Filter Loaded with Complementary Split Ring Resonator,” ICMMT Proceedings, 2010.
- [106] Bo Yin, Zhangyao Lin, Honggang Hao, Wei Luo, and Wen Huang, “Miniaturized HMSIW Bandpass Filter Based on the Coupling of Dual-Iris with Nested Stepped-Impedance CSRRs,” Progress In Electromagnetics Research Letters, Vol. 84, 115–121, 2019.

.....✂.....



# Chapter 3

## METHODOLOGY

### Contents

- 3.1 *Simulation and Optimization*
- 3.2 *Filter Fabrication*
- 3.3 *Filter Measurement*

---

*The experimental and simulation methodology utilized for the analysis of the proposed filters are described in this chapter. Photolithographic process is used to fabricate different filter geometries while the filter characterization is done with the help of Rohde & Schwarz ZVB20 network analyser. The finite integration technique (FIT) based CST Microwave Studio is used to perform the parametric analysis of the filter geometry.*

---

### 3.1 Simulation and Optimization

Designing and prototyping are made easy with the availability of a wide variety of commercially available Electromagnetic (EM) field solvers. They optimize the design and help to reduce the cost of production. Fig. 3.1 shows classifications of popular EM solvers.

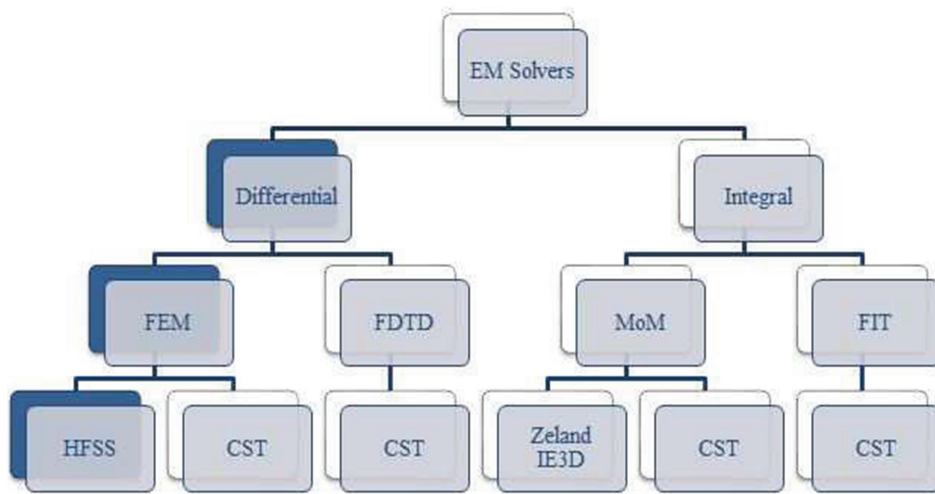


**Fig. 3.1. Classification of popular EM solvers**

EM simulation has long been an essential modelling tool for RF/microwave design. Electromagnetic field solvers simulate the structure behaviour by solving (a subset of) Maxwell's equations directly. They are commonly used in the design of MMIC's and printed circuit boards when a solution from first principles is needed, or the highest accuracy is required. They help to learn the circuit behaviour under varying design aspects and thus save costly prototyping. All these CAD products provide analysis tools of unparalleled power and flexibility and can be selected based on the structure at hand.



Depending on the formulation of Maxwell's equations (differential/integral) there are two classes of solution methods. Differential equation based and integral equation based [1]-[3].

Different types of electromagnetic simulation solvers are part of the CST Studio Suite<sup>®</sup>. They use the finite element method (FEM), the finite integration technique (FIT), and the transmission line matrix method (TLM) for various mode of solutions. These are known for their powerful high frequency simulation works. Additional solvers for specialized applications are also available in the suite. The electrically large or highly resonant structures can be simulated using the additional solvers. There are simulation methods available for the low frequency, charged particle, electronics and multiphysics tasks. The proper integration of the different types of solvers in CST Studio Suite provides the best and easy selection of the most suitable method for given problem, by offering specialized and reliable simulation tools [4]. The filter structure modelled using CST Microwave Studio is shown in Fig. 3.2.

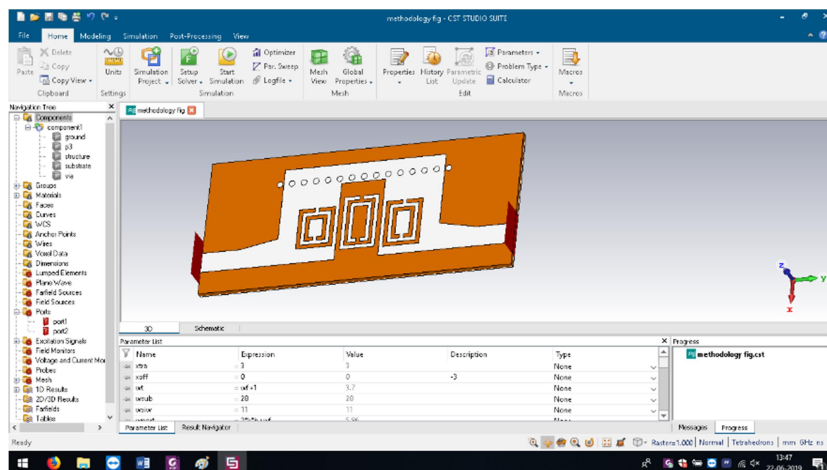


**Fig. 3.2. Modelled Structure in CST MW Studio Window**

The FIT is a spatial discretization scheme to numerically solve electromagnetic field problems in time and frequency domain. Efficient numerical simulations utilize the resulting matrix equations of the discretized fields. It preserves basic topological properties of the continuous equations such as conservation of charge and energy. FIT was proposed in 1977 by Thomas Weiland and has been enhanced continually over the years. This method covers the full range of electromagnetics (from static up to high frequency) and optic applications and is the basis for commercial simulation tools. So FIT is a numerical simulation method for approximation-free solutions of Maxwell's equations in their integral form [5]. The simulated S-parameter plots of the simulated structure is shown in Fig. 3.3.

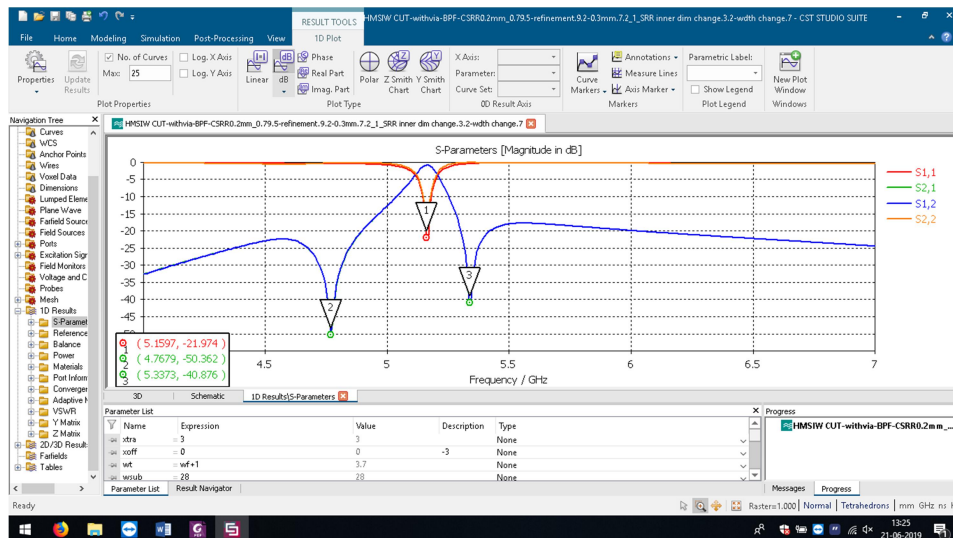


Fig. 3.3. S-Parameter Plots of Simulated Structure

### **3.1.1 Frequency Domain Solver**

The finite element method (FEM) based simulation procedure is carried out in the frequency domain solver that provides one of the best simulation environments among the many simulation software available in the market. The frequency domain solver is a multi-purpose 3D full-wave solver method. It is an efficient way for the simulation of large multi-port systems such as connectors and arrays since the frequency domain solver calculates all ports at the same time. The resonant structures and filters can be simulated with its high-speed feature of model-order reduction (MOR).

The first step in simulating a structure in CST requires the definition of the geometry of the structure by giving the material properties and boundaries for 3D or 2D elements available in CST window. The next step is to draw the intended architecture using the drawing tools available in the software. The designed structure is excited using the suitable port excitation schemes. The next step involves the assigning of the boundary scheme. A radiation boundary filled with air is commonly used for radiating structures.

Now the simulation engine can be invoked by giving the proper frequency of operation and the number of frequency points. Finally, the simulation results such as scattering parameters, port surface characteristic impedance, 3D static and animated field (electric or magnetic) plots on any surface, surface current distributions (Fig. 3.4), radiation pattern are displayed and visualised in various forms like 2D/3D Cartesian/Polar plots, Smith charts and data tables. The vector as well as the scalar

representation of E, H, J values of the device under simulation gives good insight into the structure under analysis.

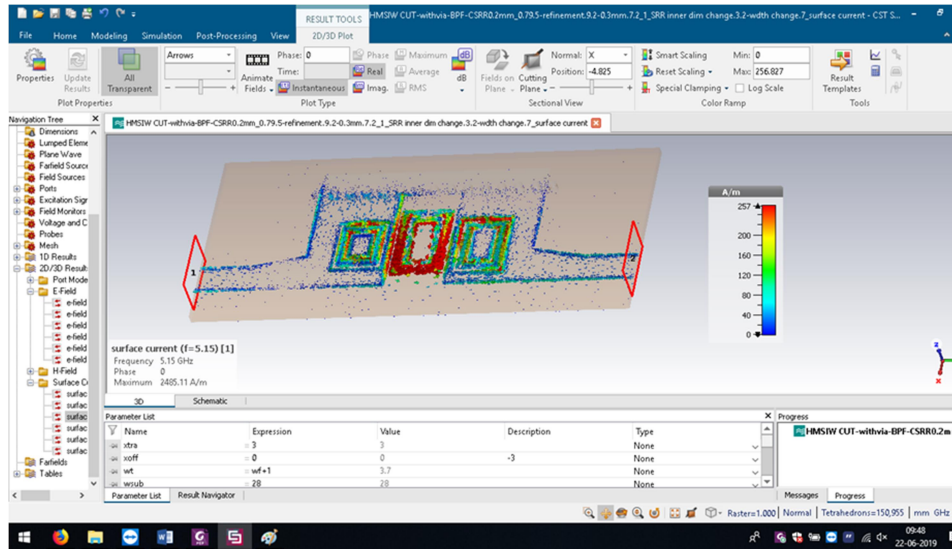


**Fig. 3.4. Surface current distribution of the SRR in simulated structure**

### 3.2 Filter Fabrication

Different resonators designed for constructing bandpass and bandstop filters are based on split ring resonators or complementary split ring resonators (SRR/CSRRs) along with substrate integrated waveguide (SIW). The optimized filters are fabricated using the standard photolithographic technique. This is a chemical etching process by which the unwanted regions of the metal layers are removed so that the intended design is obtained.

Depending on the design of the filter, uniplanar or biplanar, single or double sided substrate is used. Selection of the most suitable substrate for an application is a matter of prime importance. The dielectric constant,

loss tangent and thickness of the substrate have a pronounced effect on the fabricated filter performance. Right material chosen can provide excellent performance. The dimensions of the substrate integrated waveguide (SIW) and the resonator elements in the filter are inversely proportional to the square root of the material's dielectric constant; in short, materials with higher dielectric constants make it possible to design and fabricate smaller filters for a given frequency. Dielectric loss tangent is another important circuit material parameter for filter circuits. Quite simply, low values of loss tangent indicate materials capable of achieving low insertion loss. This means high quality factor (Q), which translates into the potential for a filter with sharper transitions from passband to stopband [6].

The filters are fabricated on low loss Rogers RT Duroid substrate with a dielectric constant of 2.2, thickness of 0.79 mm and loss tangent of 0.0009.

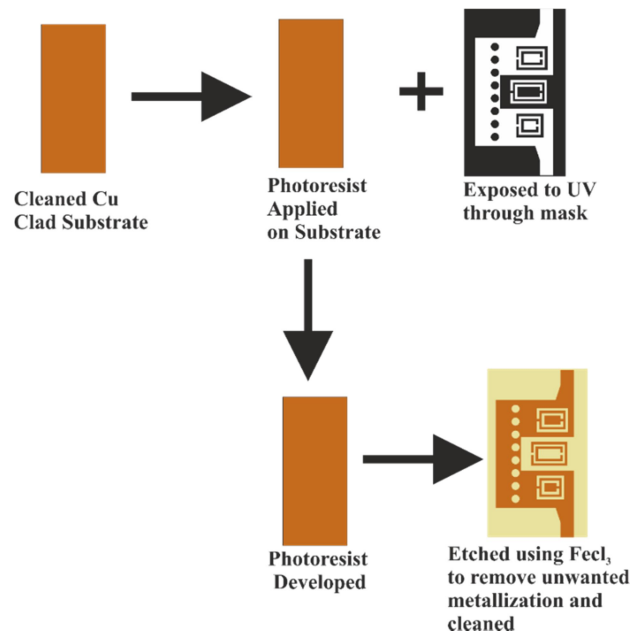


**Fig. 3.5. Various steps involved in the photolithography process**

### 3.2.1 Photolithography

Photolithography is a process of transferring geometrical shapes from a photolithographic mask to the surface of a substrate which results in optical accuracy. After the proper selection of the substrate a computer aided design of the structure was made and a negative mask of geometry is generated. The precise fabrication of a prototype falling within the microwave frequency is very essential. With the help of a high resolution laser printer, the computer aided designed filter geometry was printed on a transparent sheet for the use as the mask.

The copper clad substrate of suitable dimension was cleaned with solvents like acetone to remove any chemical impurities and dried. Thereafter, a thin layer of negative photoresist material was coated over the substrate using a high-speed spinner. This substrate is then exposed to UV light through the carefully aligned mask. Extreme care is taken to ensure that the region between the copper clad and the mask remains dust free. The UV exposure results in the hardening of the photoresist layer. Subsequently, the substrate was immersed in a developer solution and followed by ferric chloride treatment to remove the unwanted copper. The substrate is cleaned to remove the hardened photoresist using acetone solution. The photolithography process is illustrated in Fig. 3.5.

### 3.3 Filter Measurement

A short description of equipment and facilities used for the measurements of filter characteristics are presented in this section.

The measurements are taken utilizing the facilities at Microwave Research Laboratory, under the Department of Electronics, CUSAT. The vector network analyser, Rohde & Schwarz ZVB20 is utilized for the characterization of the fabricated passive filters. The network analyser works in the range 10 MHz – 20 GHz.

The experimental setup is shown in Fig. 3.6. Network analysis is concerned with accurate measurement of ratios of the reflected signal to the incident signal and the transmitted signal to the incident signal. The accuracy of measurements depends on how well we terminate the load port. It is to be terminated in perfect  $Z_0$ . The characteristic impedance of  $50 \Omega$  is chosen for microwave systems as an average value between those corresponding to minimum loss/ length ( $77 \Omega$ ) and maximum power handling ( $30 \Omega$ ) of a 10mm coaxial cable. When DUT is connected to the network analyser, the imperfect matching of the test port should be carefully accounted for. One port calibration is done for reflection measurements and two port calibration for transmission measurements. This is done in the frequency range of interest. For filter measurements both test ports are to be calibrated for reflection and transmission, so as to measure full two-port scattering matrices (S- parameters) for the device. For two port calibration, measurement of known standards is taken. There are four standards; Short, Open, Load and Through. The definitions of these standards are available with the calibration kit [7].



Fig. 3.6. Experimental setup

The measurements for insertion loss, return loss, group delay, magnitude and phase are taken for the fabricated prototypes using the network analyzer. The generalized internal block diagram of a network analyser is shown in Fig. 3.7.

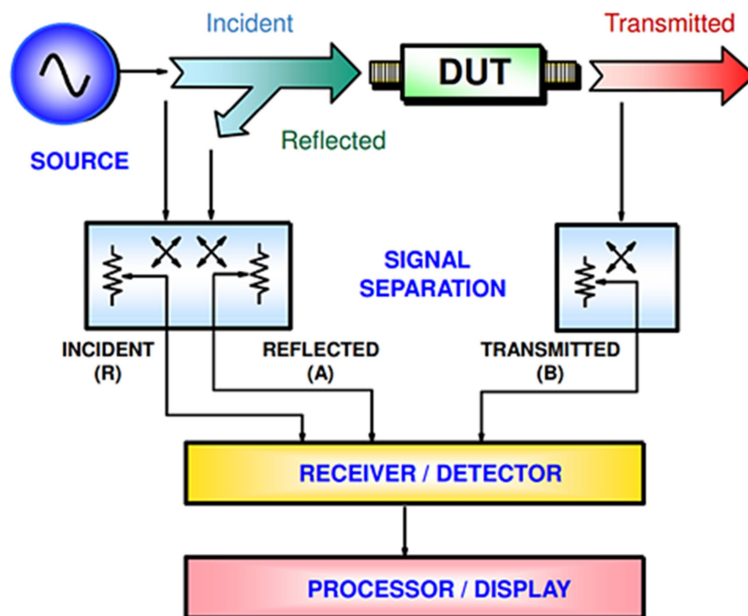


Fig. 3.7. Network Analyser- Generalized Internal Block Diagram



### 3.4 Summary of the chapter

This chapter details the tools and techniques used in the research. It begins with briefing of the various EM simulation software available in the market with an emphasis on CST MW studio and its FIT method. The role of substrate materials on the performance and the fabrication method (photolithography) adopted in this work are elaborated in the subsequent sections and finally the vector network analyser and the measurement setup used are explained.

#### References

- [1] A Vasylychenko, Y Schols, W De Raedt and G.A.E Vandenbosch, “Quality Assessment of Computational Techniques and Software Tools for Planar-Antenna Analysis”, *Antennas and Propagation Magazine*, IEEE vol.51, pp. 23-28, Feb. 2009.
- [2] Guy A. E. Vandenbosch and Alexander Vasylychenko, “A Practical Guide to 3D Electromagnetic Software Tools Katholieke Universiteit Leuven, Belgium, [www.intechopen.com](http://www.intechopen.com).
- [3] Luca Pierantoni, Marco Farina et.al, “Comparison of the Efficiency of Electromagnetic Solvers in the Time-and Frequency-Domain for the Accurate Modeling of Planar Circuits and MEMS”, *IEEE MTT-S Digest*, pp. 891-894.
- [4] <http://www.cst.com>.
- [5] <http://microwave101.com>.
- [6] Russell Hornung, “Insertion Loss and Loss tangent”, *Application Notes*, [www.arlon-med.com](http://www.arlon-med.com).
- [7] <http://www.rohde-schwarz.com>.

.....✂.....



## Chapter 4

### HMSIW NARROW BANDSTOP AND BANDPASS FILTERS

- |                 |  |
|-----------------|--|
| <i>Contents</i> | 4.1 <i>Bandstop filter using HMSIW and SRR</i> |
|                 | 4.2 <i>HMSIW bandpass filter</i>               |
|                 | 4.3 <i>Compact HMSIW bandpass filter</i>       |
|                 | 4.4 <i>Summary of the chapter</i>              |

*The design procedure of HMSIW bandstop filter and two types of HMSIW narrowband bandpass filters are described in this chapter. The bandstop filter utilizes broadside coupled SRR for the narrow stopband generation. The first bandpass filter utilizes SRRs for both passband and stopband generations. In the second type, SRR is used for passband generation, CSRR embedded in the HMSIW is used for stopband generation. This technique results in the size reduction of the bandpass filter.*

## 4.1 Bandstop Filter using HMSIW and SRR

This section introduces a bandstop filter with the HMSIW coupled with rectangular SRR. The proposed structure is simple with a narrow stopband at the resonant frequency of SRR. The filter is realized on the Rogers RT 5880 substrate ( $\epsilon_r = 2.2$ ,  $h = 0.79\text{mm}$ ) with an overall dimension of  $40 \times 1.7 \text{ mm}^2$ .

This work aims at the development of narrow stopband filter in the X-band region. Design approach followed and various planar components identified for the design are elaborated in chapters 1- 3. Analysis of the literature shows that split ring resonators (SRR) or complementary split ring resonators (CSRR) are good candidates for bandstop/bandpass filters. Different combinations of SRR/CSRRs are utilized for the realization of various filters discussed in chapter 4 and 5.

### 4.1.1 Geometry

The layout of the HMSIW bandstop filter is shown in Fig. 4.1. The SRR schematic is shown in Fig. 4.2. Half Mode SIW is fed using a tapered microstrip line. The bandstop filter is designed by placing SRRs near to the open end side of the HMSIW. The ground plane of the HMSIW is kept unaltered. The interactions between the HMSIW fields and the SRR inhibits the propagation at the SRR resonant frequency and narrow stopband is observed. The optimized filter parameters are shown in Table 4.1. The SRR parameters shown in Table 4.2 are optimized using simulation for the particular stopband.

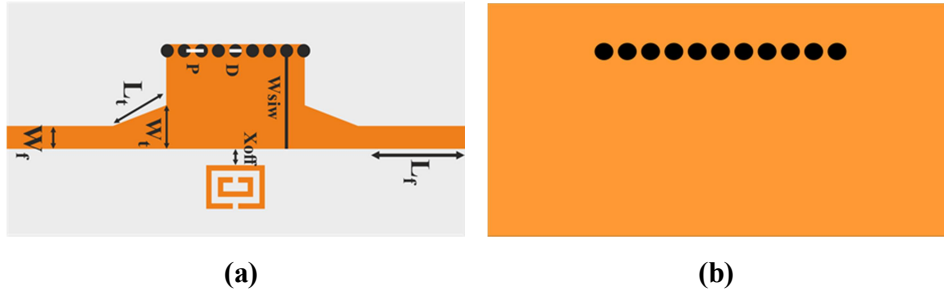


**Fig. 4.1. Filter Layout (a) Top View (b) Bottom View**

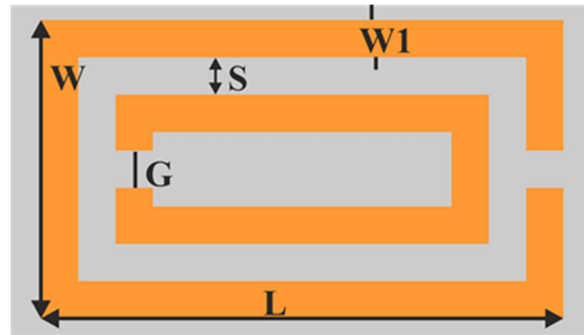


**Fig. 4.2. SRR Schematic**

**Table 4.1. Filter Parameters**

Filter Parameters							
$L_f$	$L_t$	$W_t$	$W_f$	$X_{off}$	$W_{siw}$	$D$	$P$
10	5	4	2.1	0.2	8.4	0.8	1.2

**Table 4.2. SRR Dimensions**

SRR Dimensions				
$L$	$W$	$S$	$G$	$W_1$
4.8	1.85	0.4	0.5	0.2

### 4.1.2 Design Evolution

The design evolution of the filter is described in the following section. The SIW and HMSIW with a cut off frequency of 6 GHz with its simulated S- parameters are shown in Fig. 4.3 and Fig. 4.4. The microstrip line accompanied by SRR with its simulated results is shown in Fig. 4.5. Different SRR orientations with respect to the HMSIW open side is shown as well as its surface current distributions are shown in the following figures. A narrow stopband is observed in Fig. 4.6, Fig. 4.9 and Fig. 4.10 orientations while no proper stopband response in Fig. 4.7.

A comparison of the surface current distribution of the SRR orientations of Fig. 4.6 and Fig. 4.7 is shown in Fig. 4.8. A proper stopband at 9.88 GHz is observed due to the surface current distribution in Fig. 4.8 (a) whereas no proper stopband due to the surface current distribution in Fig. 4.8 (b). By increasing the number of SRRs the stopband bandwidth can be increased as shown in Fig. 4.11.

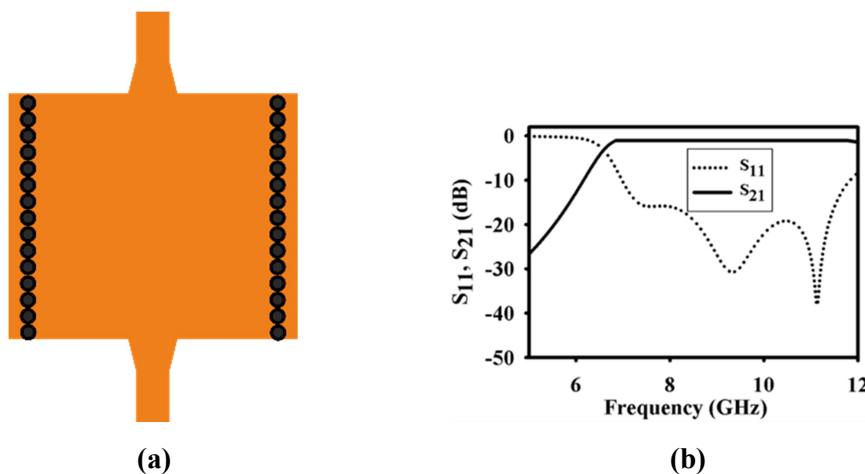


Fig. 4.3. (a) SIW (6 GHz cutoff frequency) (b) S-Parameters

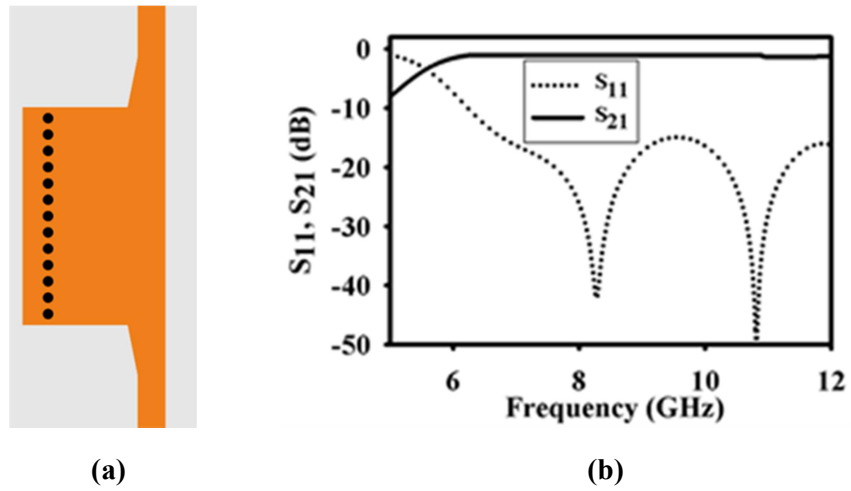


Fig. 4.4. (a) HSIW (6 GHz cutoff frequency) (b) S-Parameters

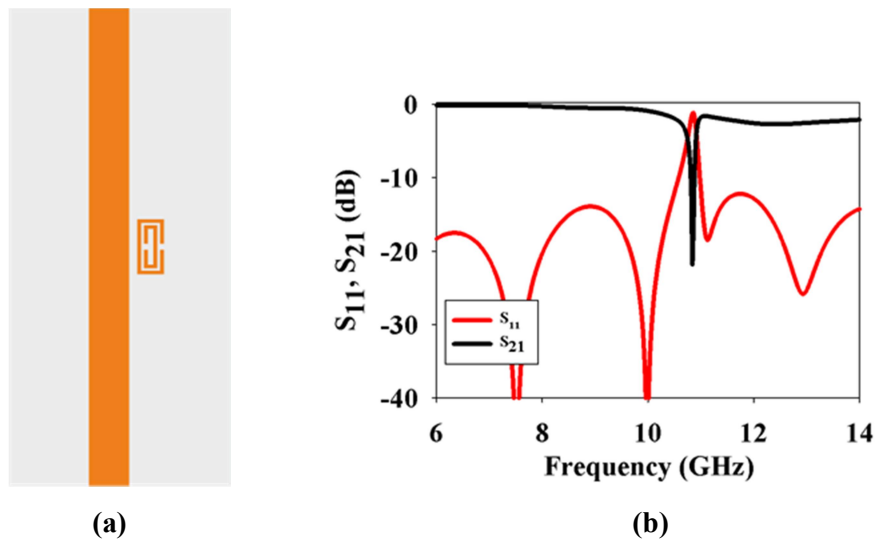


Fig. 4.5. (a) Microstrip Line with SRR (b) S-Parameters

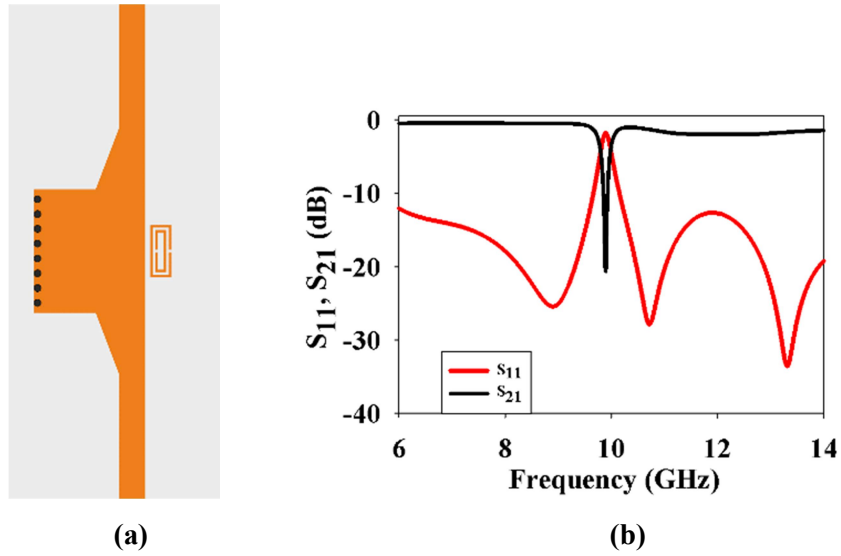


Fig. 4.6. (a) HSIW with SRR (Outer Ring Slit Orientation 1)  
(b) S-Parameters

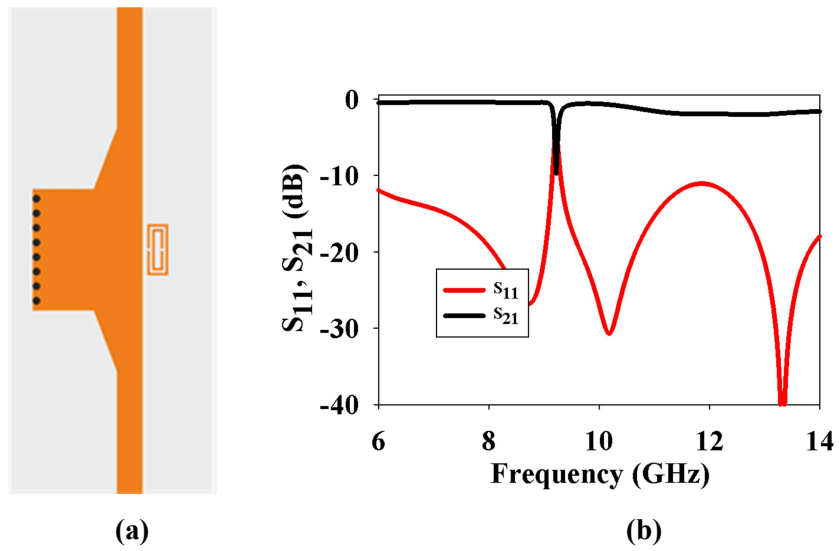


Fig. 4.7. (a) HSIW with SRR (Outer Ring Slit Orientation 2)  
(b) S-Parameters



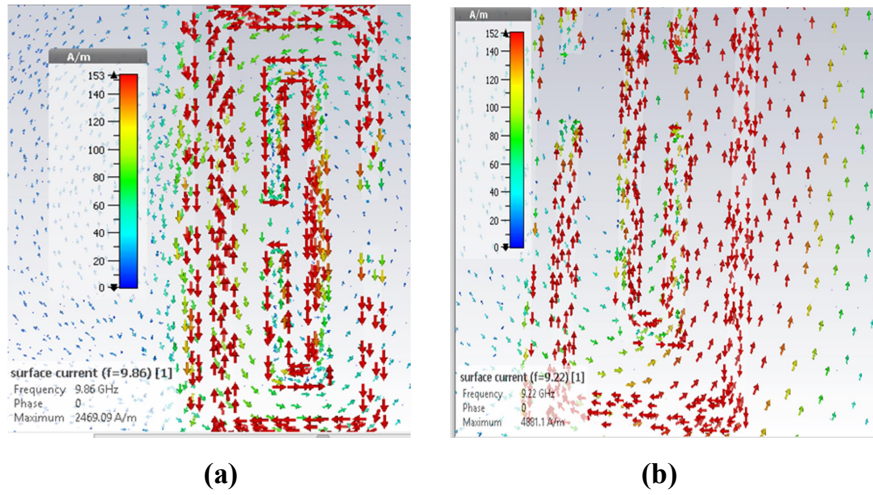


Fig. 4.8. Surface Current Distributions Corresponding to (a) Fig. 4.6 (b) Fig. 4.7

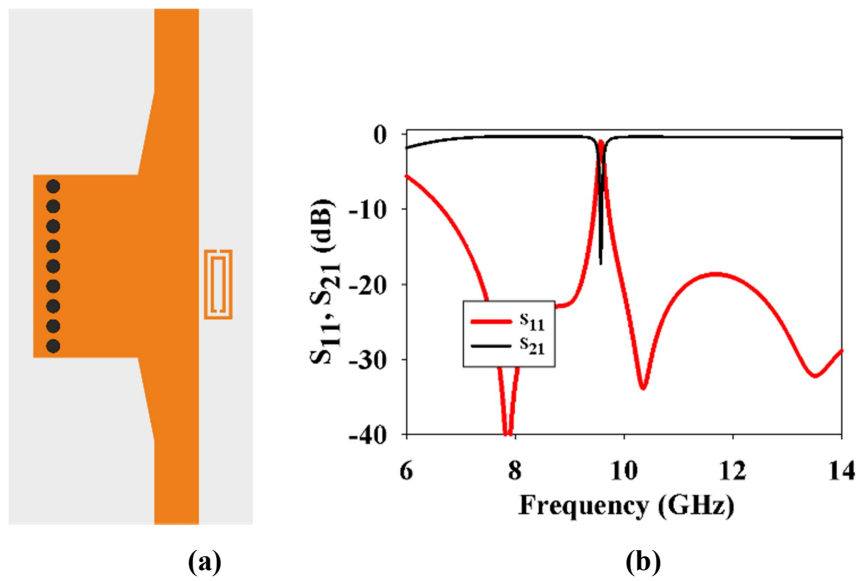


Fig. 4.9. (a) HSIW with SRR (Outer Ring Slit Orientation 3) (b) S-Parameters

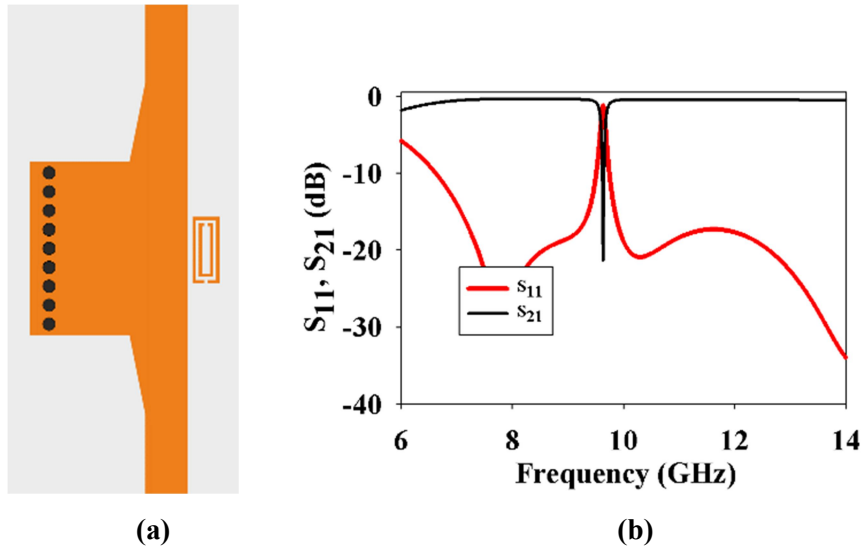


Fig. 4.10. (a) HSIW with SRR (Outer Ring Slit Orientation 4)  
(b) S-Parameters

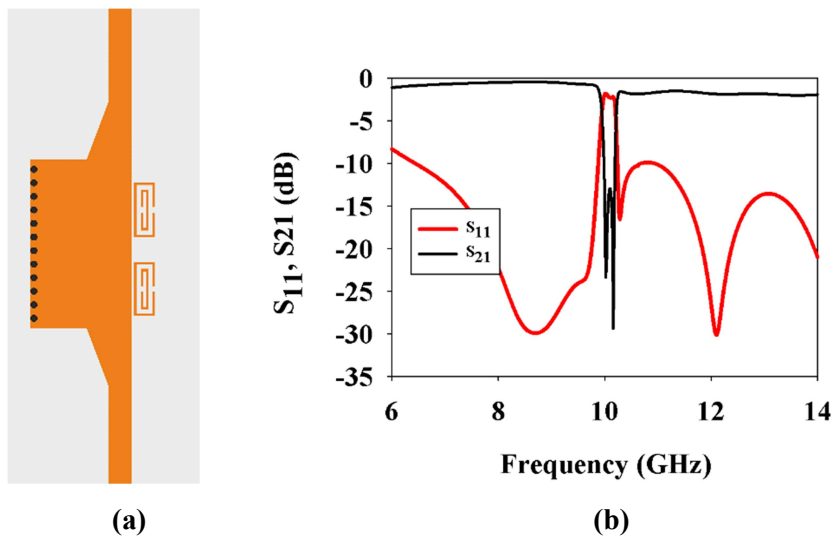
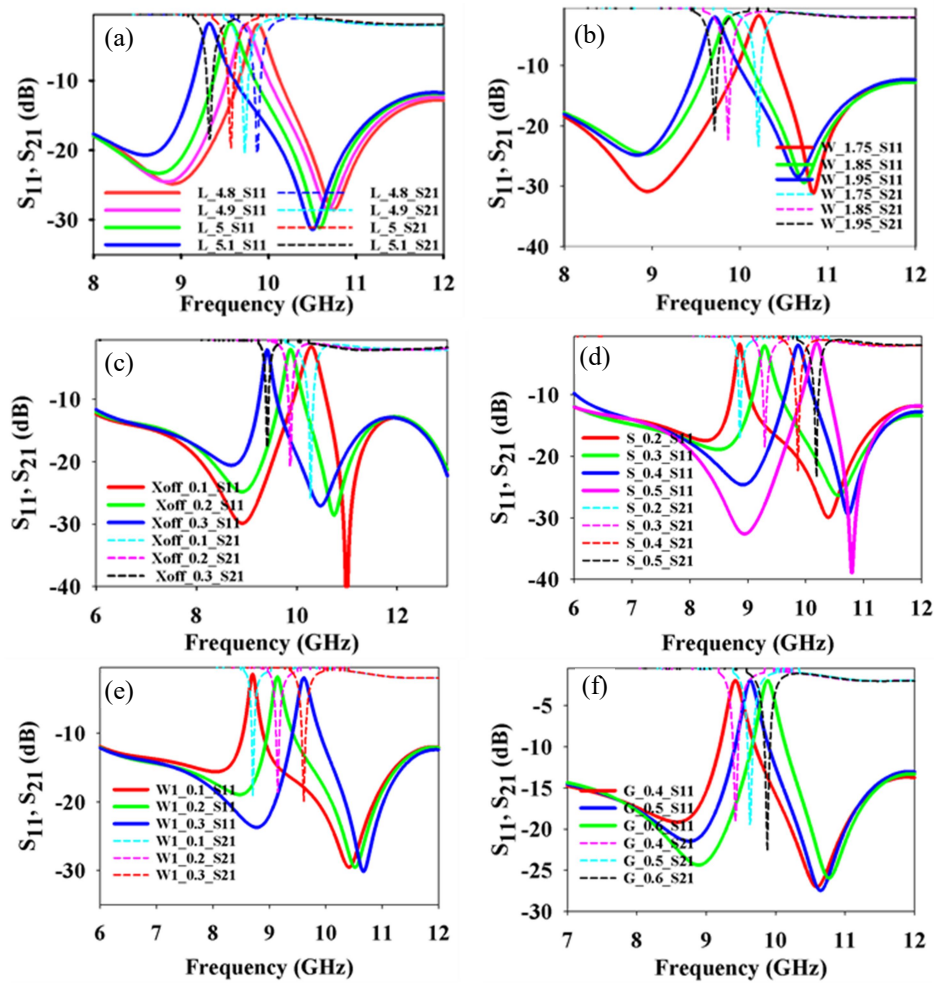


Fig. 4.11. (a) HSIW with two SRRs (b) S-Parameters

### 4.1.3 Simulation and Analysis

A Parametric analysis is carried out to analyze the filter behaviour on varying the dimensions of the constituent elements. Fig. 4.12 shows the parametric analysis of the filter. Increase in the parameters  $L_{SRR}$ ,  $W_{SRR}$  and  $X_{off}$  shows lower frequency shift and  $S$ ,  $W_{cut}$  and  $W_1$  shows higher frequency shift.



**Fig. 4.12. Parametric Simulation of SRR Dimensions (a) Outer Loop Length (L) (b) Outer Loop Width (W) (c) Offset Distance ( $X_{off}$ ) (d) Gap between Rings (S) (e) SRR Loop conductor width ( $W_1$ ) (f) Gap in the SRR Loop Slit (G)**

#### 4.1.4 Fabrication and Measurement

The Fig. 4.13 (a) shows the photograph of the fabricated filter with the SMA connectors. Standard photolithography is used for the fabrication process and the S parameter measurements are taken using Rohde & Schwarz ZVB20 vector network analyzer. The measured result in comparison with the simulated result shows good agreement as shown in Fig. 4.13 (b). A small variation in  $S_{11}$  level is due to the fabrication tolerances of the small sized SRR.

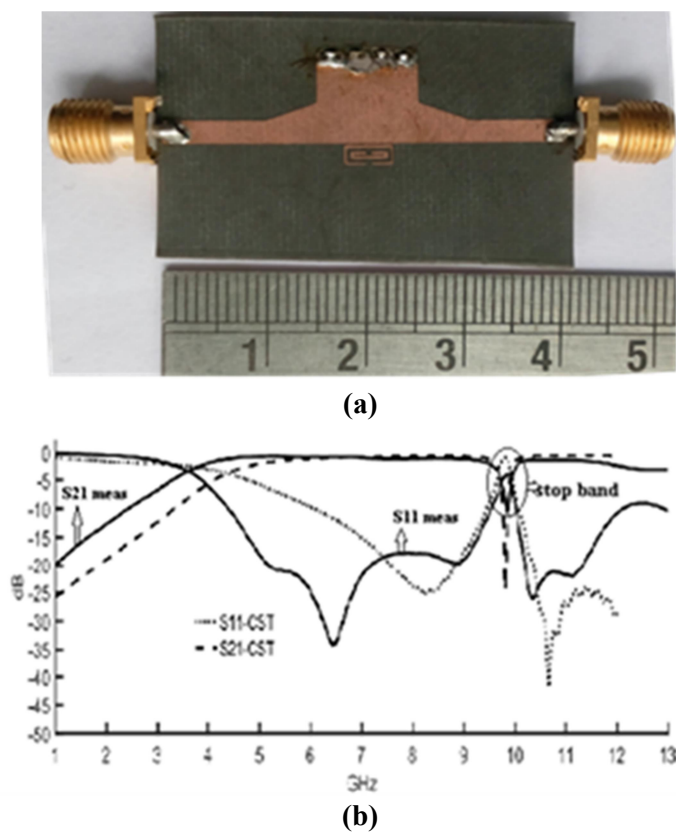


**Fig. 4.13. (a) Photograph of Fabricated Bandstop Filter  
(b) Insertion and Return Loss Characteristics**

## 4.2 HMSIW bandpass filter with SRRs

The SRRs play different role in the realization of this filter depending upon their location. The SRR placed in the HMSIW discontinuity, couples the passband frequency. The edge coupled SRRs establish stopbands at its resonant frequencies. A filter with overall size of 20X35 mm<sup>2</sup> is realized on Rogers RT duroid 5880 with  $\epsilon_r = 2.2$  and substrate thickness of 0.79 mm with good insertion and return loss characteristics.

### 4.2.1 Geometry

The proposed structure describes a narrowband filter utilizing SRR for the passband and for obtaining two transmission zeros on either side of the passband. The standard HMSIW structure with a discontinuity inserted with SRR and two edge coupled SRRs on either side form the filter structure. The top and bottom view of the filter structure with 50  $\Omega$  feed line and tapering for impedance transformation is shown in Fig. 4.14. The SRR schematic is shown in Fig. 4.15. The filter parameters and the optimized SRR dimensions are shown in Table 4.3 and Table 4.4.

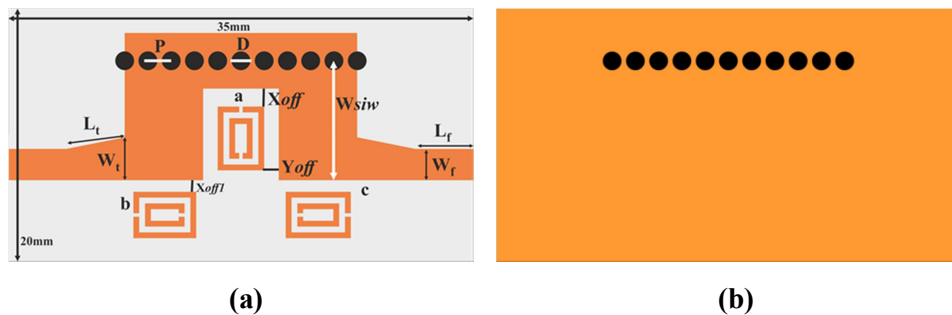


Fig. 4.14. Filter Layout (a) Top View (b) Bottom View

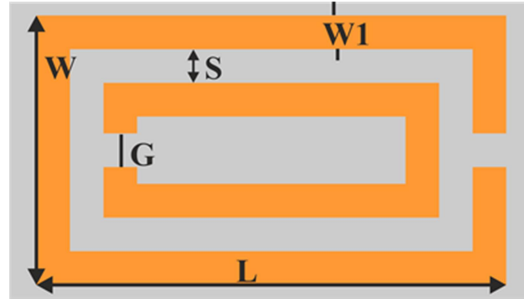


Fig. 4.15. SRR Schematic

Table 4.3. Filter Parameters

Filter Parameters (mm)									
Lf	Lt	Wf	Wt	Wsiw	Xoff	Xoff1	Yoff	D	P
5	5	2.7	3.7	8.4	0.3	1.25	0.6	0.8	1.2

Table 4.4. SRR Dimensions

SRR Dimensions (mm)					
SRR Name	W1	S	G	La, Lb, Lc	Wa, Wb, Wc
SRR (a)	0.3	0.3	0.3	4.3	2.45
SRR (b)	0.3	0.3	0.3	4.2	2.45
SRR (c)	0.3	0.3	0.3	4.4	2.45

### 4.2.2 Design evolution

The HMSIW with a cut off frequency of 6 GHz is designed and simulated in CST MW Studio as shown in Fig. 4.16 (a) and the simulated S-parameters are shown in Fig. 4.16 (b). The input and output lines are tapered to match with 50 $\Omega$  line. A small discontinuity is introduced in it as shown in Fig.4.17 (a) and the response is shown in Fig. 4.17 (b). The

Parametric simulation for different HMSIW cut widths is shown in Fig. 4.18. SRR is inserted in the gap to get the desired narrow passband.

The simulation results corresponding to various SRR orientations are shown in Fig. 4.19, Fig. 4.20 and Fig. 4.22 to Fig. 4.25. The SRR orientations shown in Fig. 4.19 and Fig. 4.22 shows a narrow passband while the orientations in Fig. 4.20, Fig. 4.23, Fig. 4.24, and Fig. 4.25 didn't give proper passband response. The selected SRR orientation for the passband generation is shown in Fig. 4.26. The surface current distribution corresponding to SRR orientations in Fig. 4.19 and Fig. 4.20 is shown in Fig. 4.21. The SRR orientation shown in Fig. 4.19 shows a passband with a center frequency at 9.2476 GHz while SRR orientation in Fig. 4.20 has no trace of a passband at that frequency. This characteristic is evident from the surface current distributions shown in Fig. 4.21 (a) and (b). As the SRR orientation shown in Fig. 4.20 has a tendency of forming a passband at 17.216 GHz which is shown with the surface current distribution of 4.21 (c).

To sharpen the stopband edges we need more resonating elements. As shown in Fig. 4.27 two SRRs are introduced into the structure near the open end of the HMSIW so that the fields of both the structures can interact well. These two SRRs are resonating at different frequencies which act as notch filters giving transmission zeros on either side of the passband. The structure with an additional covering in the HMSIW discontinuity is also simulated as shown in Fig. 4.28. But that variation shows an inferior stopband characteristics compared to the above discussed filter structure.

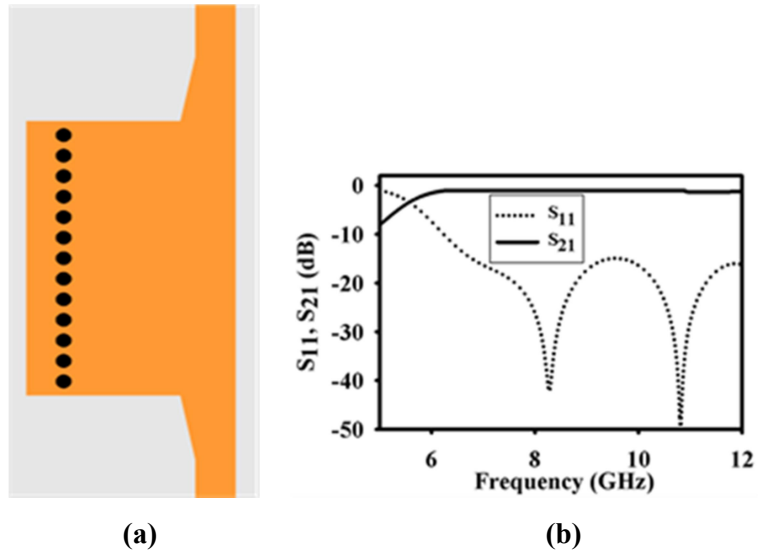


Fig. 4.16. (a) HSIW (6 GHz cutoff frequency) (b) S-Parameters

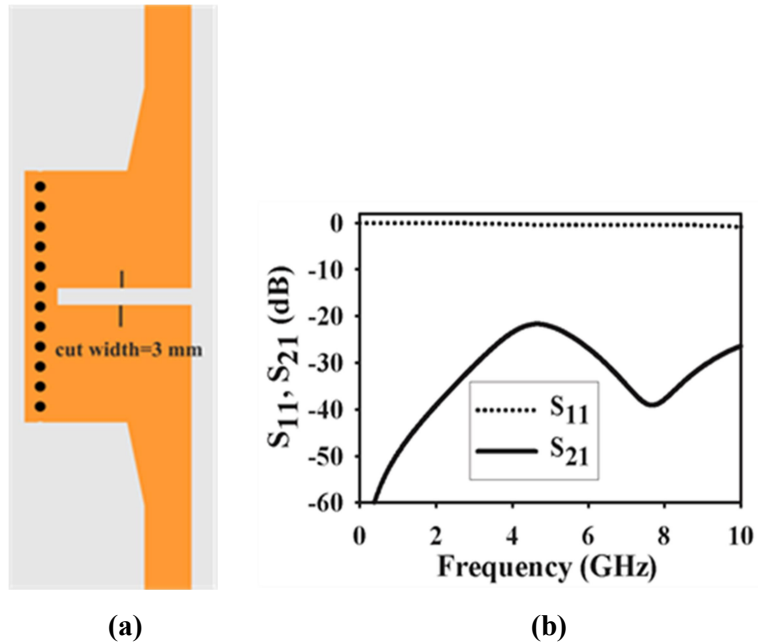


Fig. 4.17. (a) HSIW with a well-defined Discontinuity (b) S-Parameters



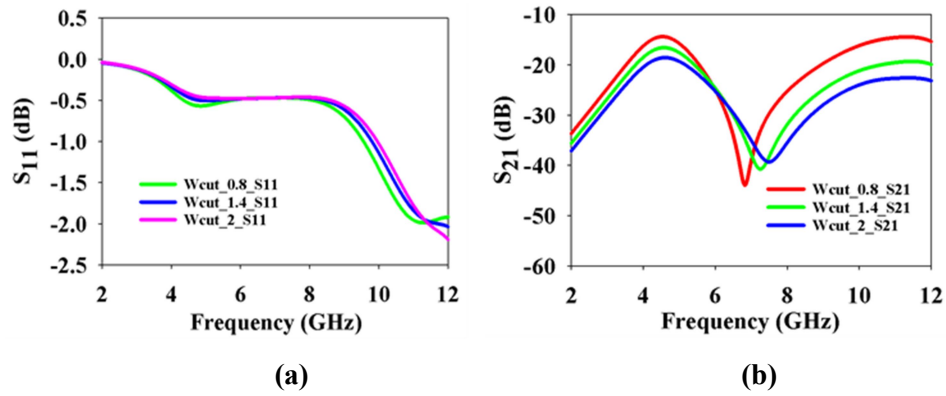


Fig. 4.18. Parametric Simulations for various HMSIW Discontinuity Widths (Wcut) (a)  $S_{11}$  (b)  $S_{21}$

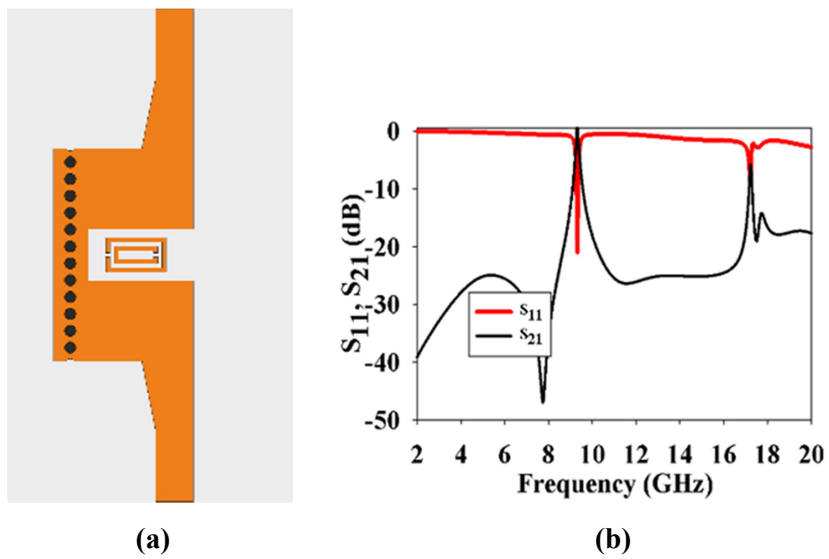


Fig. 4.19. (a) HMSIW with SRR at center (Outer Ring Slit Orientation 1) (b) S-Parameters

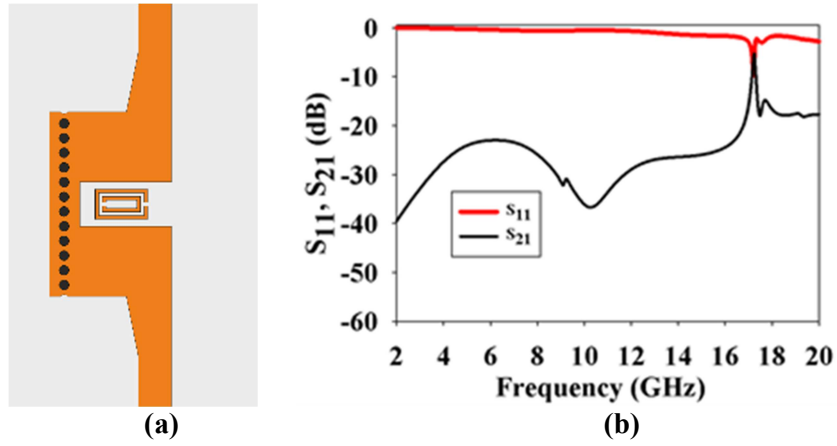


Fig. 4.20. (a) HMSIW with SRR at center (Outer Ring Slit Orientation 2) (b) S- Parameters

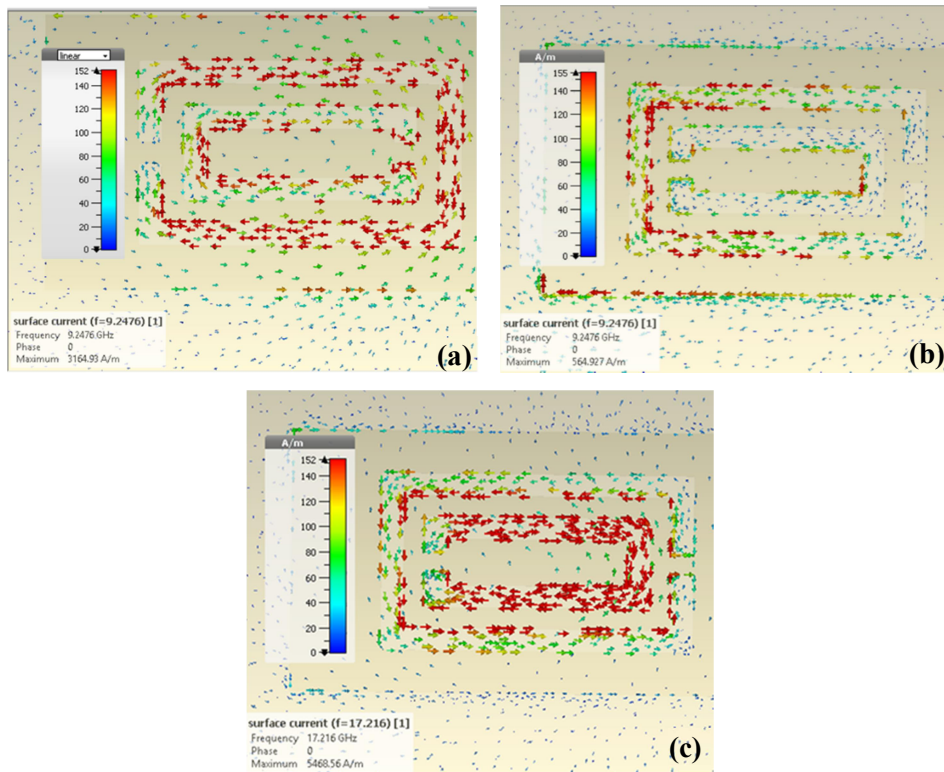
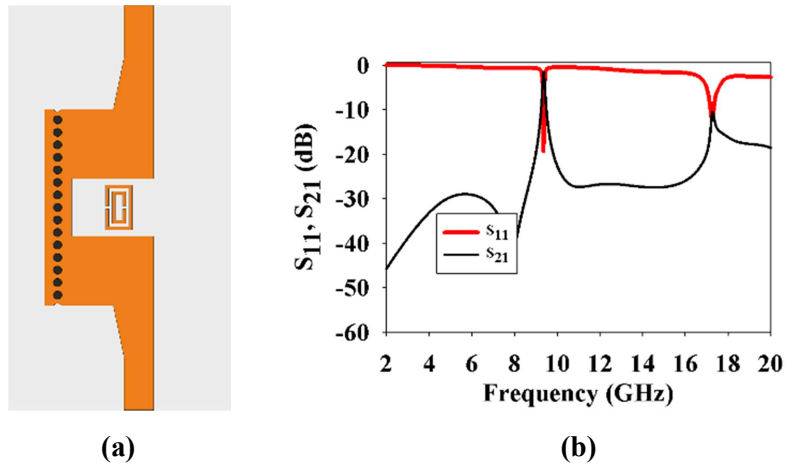
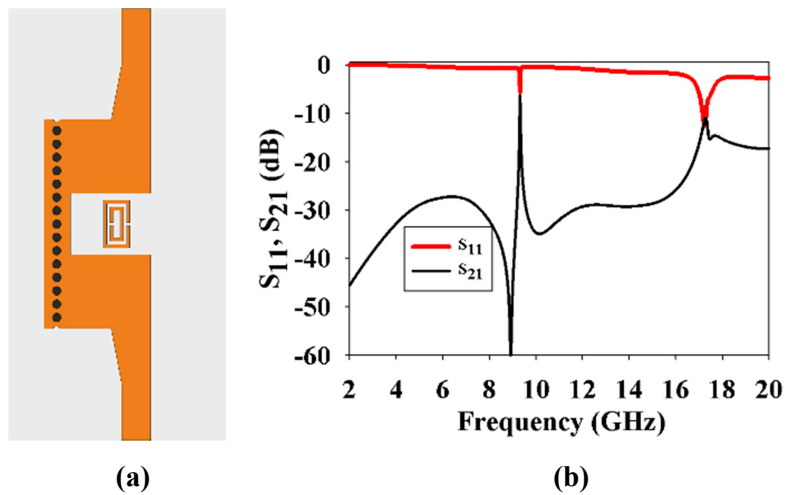


Fig. 4.21. Surface Current Distributions of SRR Orientations of (a) Fig. 4.19 (b) Fig. 4.20 at f = 9.2476 GHz (c) Fig. 4.20 at f = 17.216 GHz



**Fig. 4.22.** (a) HMSIW with SRR at center (Outer Ring Slit Orientation 3)  
(b) S- Parameters



**Fig. 4.23.** (a) HMSIW with SRR at center (Outer Ring Slit Orientation 4)  
(b) S- Parameters

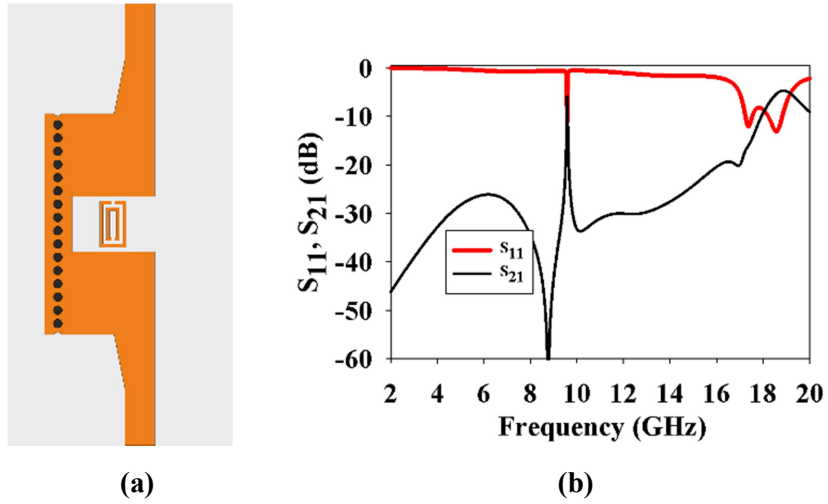


Fig. 4.24. (a) HMSIW with SRR at center (Outer Ring Slit Orientation 5)  
(b) S- Parameters

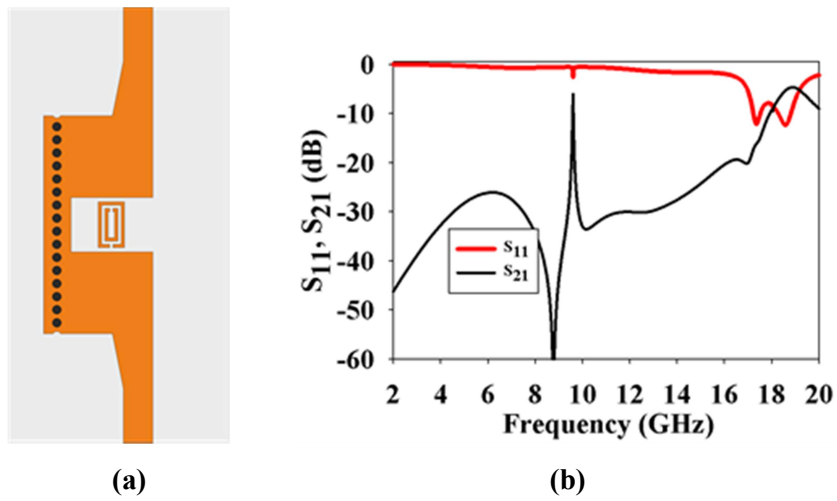
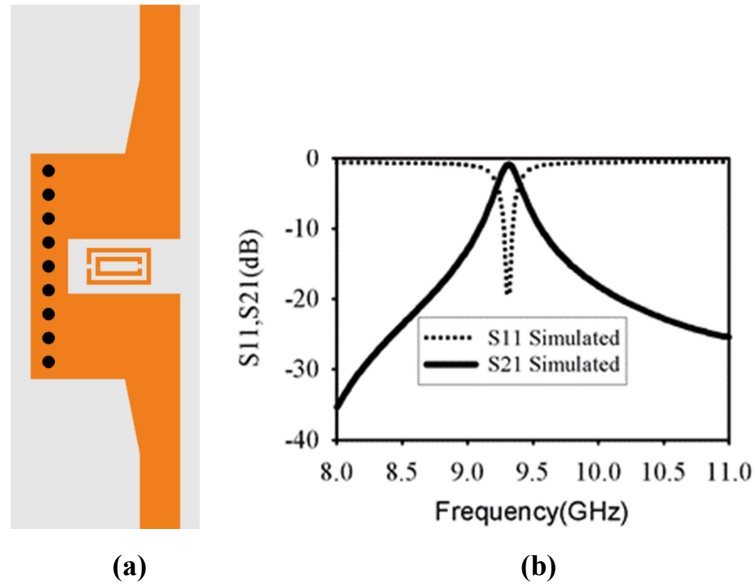
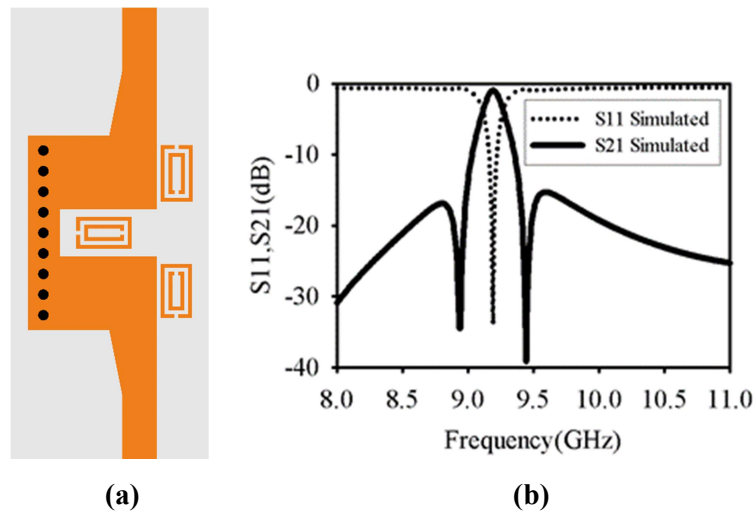


Fig. 4.25. (a) HMSIW with SRR at center (Outer Ring Slit Orientation 6)  
(b) S- Parameters



**Fig. 4.26. (a) HMSIW with SRR at center (Selected for filter design) (b) S- Parameters**



**Fig. 4.27. (a) Filter Structure (Selected for Fabrication) (b) S- Parameters**

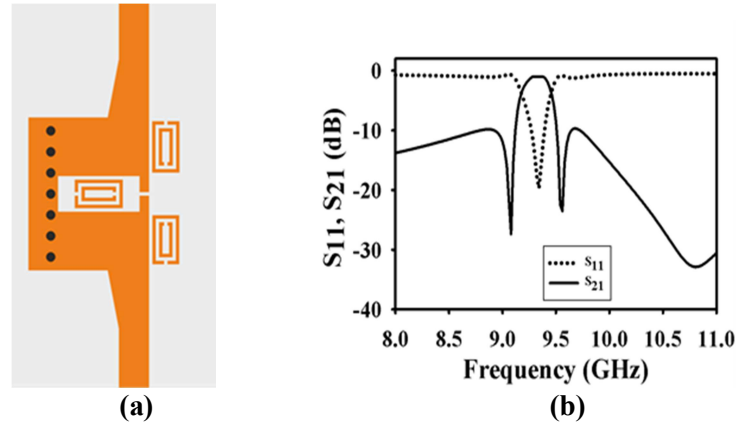


**Fig. 4.28. (a) Filter Structure (b) S- Parameters  
(with covering in HMSIW discontinuity)**

### 4.2.3 Simulation and Analysis

The surface current distribution for the lower transmission zero (9.19 GHz), center frequency (8.93 GHz) and upper transmission zero (9.44 GHz) is shown in Fig. 4.29 (a), (b), (c) respectively. From the figure it is clear that the corresponding SRRs are excited for the designed frequency. The electric field distribution at 9.19 GHz is as shown in Fig. 4.30 and it shows overall field distribution and excitation of the SRRs in the filter structure.

The parametric analysis of SRR dimension variation,  $X_{\text{off}}$  and  $Y_{\text{off}}$  are shown in Fig. 4.31 (a), (b) and (c). As the SRR dimensions increase, the passband and the transmission zeros shifts to the lower frequency band. From the LC equivalent circuit, it is clear that  $X_{\text{off}}$  represents capacitor C1 and  $Y_{\text{off}}$  capacitor C2. For the given filter the variation of  $X_{\text{off}}$  shows an upward frequency shift on S21 transmission zeros up to the designed value and a downward shift after that. The variation of  $Y_{\text{off}}$  shifts the stopband level downward as it increases. As  $Y_{\text{off}}$  increases the out of band rejection on both sides improves. Both the cases show a passband frequency shift also.

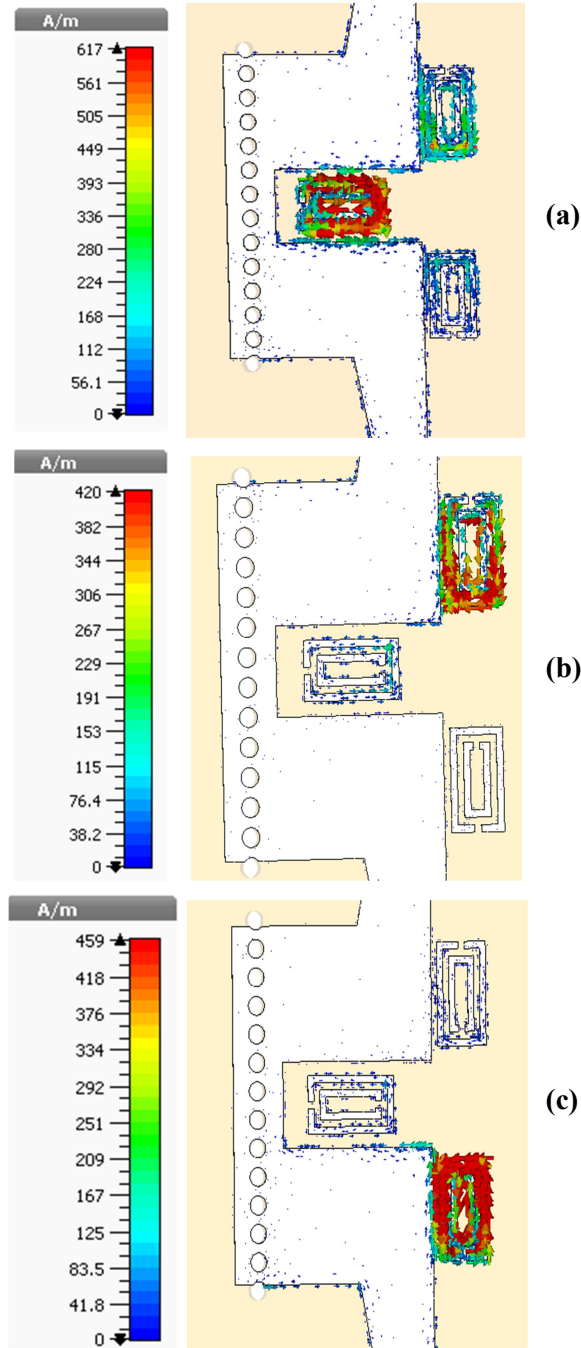


**Fig. 4.29.** Surface Current distributions (a) at 9.19 GHz (b) 8.93 GHz (c) at 9.44 GHz

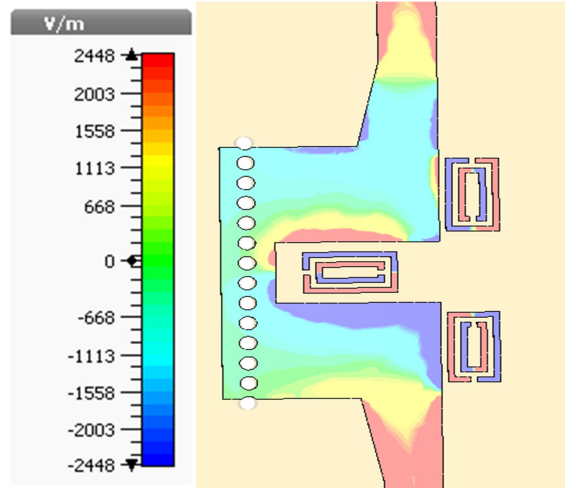


Fig. 4.30. Electric field distribution at 9.19GHz

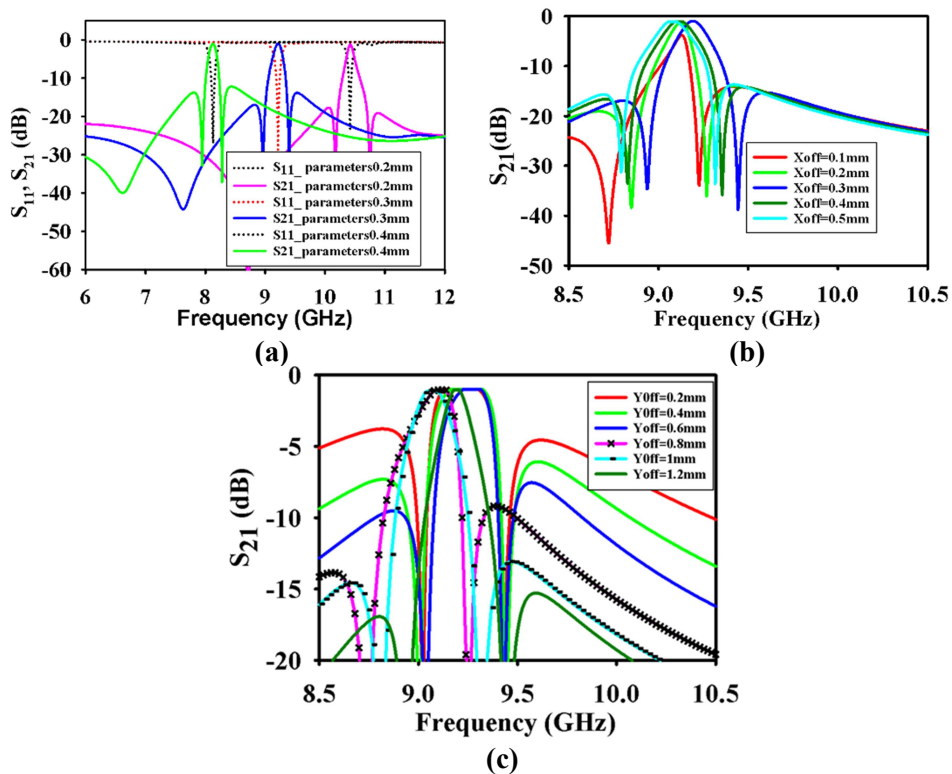
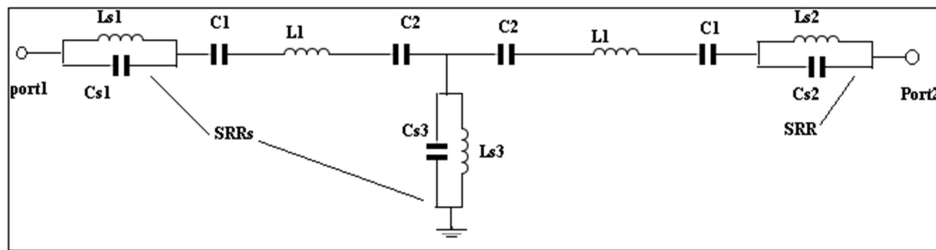


Fig. 4.31. Parametric Simulations (a) All SRR dimensions at 0.2 mm, 0.3 mm, 0.4 mm (b)  $X_{off}$  (c)  $Y_{off}$



### 4.2.3.1 Lumped element model

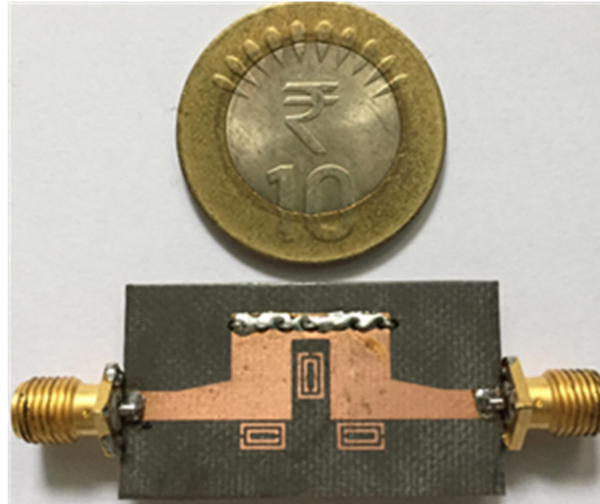
The equivalent circuit model is shown in Fig. 4.32. The three parallel LC circuits ( $L_{S1}$ & $C_{S1}$ ,  $L_{S2}$ & $C_{S2}$ , and  $L_{S3}$ & $C_{S3}$ ) represent the three SRRs in the filter structure. The inductor L1 represents the HMSIW sections, the capacitor C1 indicates gap capacitance to the edge coupled SRRs and capacitor C2 gap capacitance to the series coupled SRR.



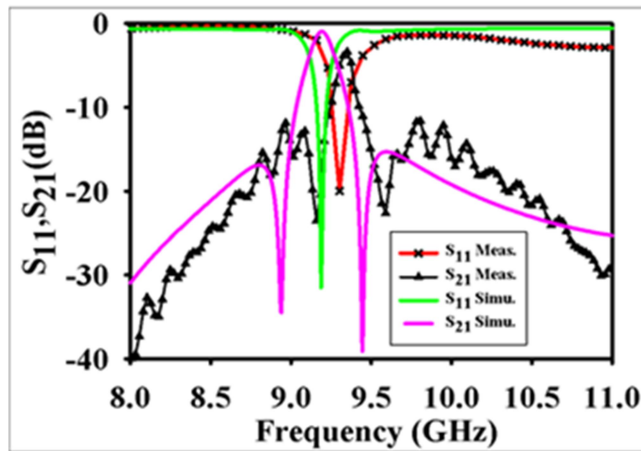
**Fig. 4.32. LC equivalent circuit model**

The proposed structure is fabricated on Rogers RT/Duroid 5880 ( $\epsilon_r = 2.2$ ,  $h = 0.79$  mm,  $\tan\delta = 0.0002$ ) substrate with the standard PCB process. Photograph of the fabricated structure is shown in Fig.4.33 (a). The fabricated structure is measured in Rohde & Schwarz ZVB-20 vector network analyzer. The measured S-parameters in comparison with simulated ones are shown in Fig. 4.33 (b). The measured transmission zeros show a small shift from simulated value ( 8.93 GHz and 9.44 GHz) to 9.16 GHz and 9.56 GHz with the centre frequency simulated (9.19 GHz) is shifted to 9.30 GHz in the measured result.

### 4.2.4 Fabrication and Measurement



(a)



(b)

Fig. 4.33. (a) Photograph of Fabricated Filter (b) Insertion and Return Loss Characteristics

### 4.3 HMSIW bandpass filter with SRR and CSRRs

The filter discussed in section 4.3 is an extension of the one discussed in section 4.2 with some additional techniques used for size reduction. The CSRR which is the dual of SRR embedded in this filter reduces the structure size effectively. The electric field orientation in the  $TE_{1,0}$  mode of HMSIW excites the CSRRs at its resonant frequency and two transmission zeros at both the ends of the passband are formed.

#### 4.3.1 Geometry

The proposed filter makes use of the CSRRs embedded in the HMSIW structure for the stopband performance. This technique gives size reduction as well as better coupling. The edge coupled SRRs featured in the filter discussed in section 4.2 is replaced by the embedded CSRRs in this filter structure as shown in Fig. 4.34. The filter is fabricated on Rogers RT 5880. The total size of the structure is  $30 \times 13 \text{ mm}^2$ . The filter parameters and the optimized SRR dimensions are shown in Table 4.5 and Table 4.6.

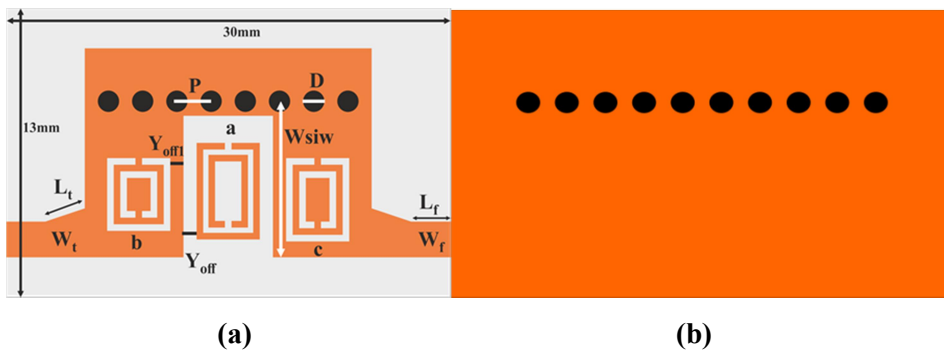


**Fig. 4.34. Filter Layout (a) Top View (b) Bottom View**

**Table 4.5. Filter Parameters**

Filter Parameters (mm)								
Lf	Lt	Wf	Wt	Wsiw	Yoff	D	P	Yoff1
5	5	2.7	3.7	11	0.6	0.8	1.2	0.5

**Table 4.6. SRR Dimensions**

SRR/CSRR Dimensions (mm)					
SRR Name	W1	S	G	La, Lb, Lc	Wa, Wb, Wc
CSRR (a)	0.5	0.5	0.5	7.3	4.6
CSRR (b)	0.5	0.5	0.5	5.5	4.8
CSRR (c)	0.5	0.5	0.5	6.3	4.8

### 4.3.2 Design Evolution

The design evolution and simulation results are described in Fig. 4.35 to Fig. 4.38. The HMSIW with a cut off frequency of 4 GHz is designed and simulated as shown in Fig. 4.35. The HMSIW with a cut in the propagation path is shown in Fig. 4.36 (a) and the simulated result is in Fig. 4.36 (b). SRR is inserted in the cut to pass a particular frequency band as shown in Fig.4.37 (a) and simulation result is in Fig. 4.37 (b). The two CSRRs are embedded into the structure to create two transmission zeros on either side of the pass band for better stopband performance as shown in Fig. 4.38 (a) and Fig. 4.38 (b).

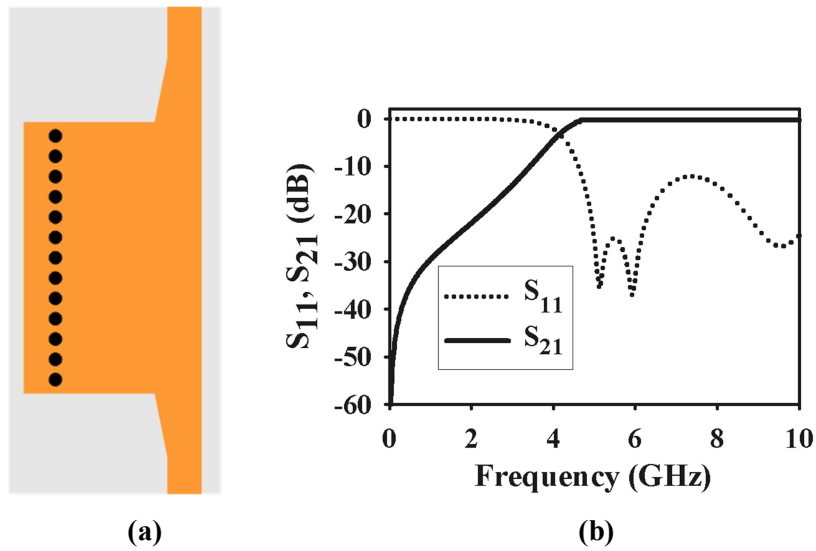


Fig. 4.35. (a) HSIW (4 GHz cutoff frequency) (b) S-Parameters

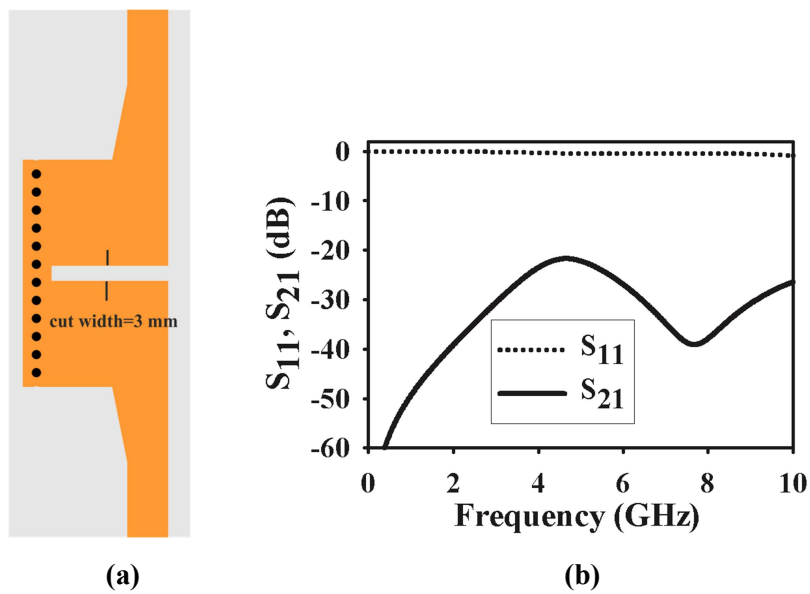


Fig. 4.36. (a) HSIW with a well-defined Discontinuity (b) S-Parameters

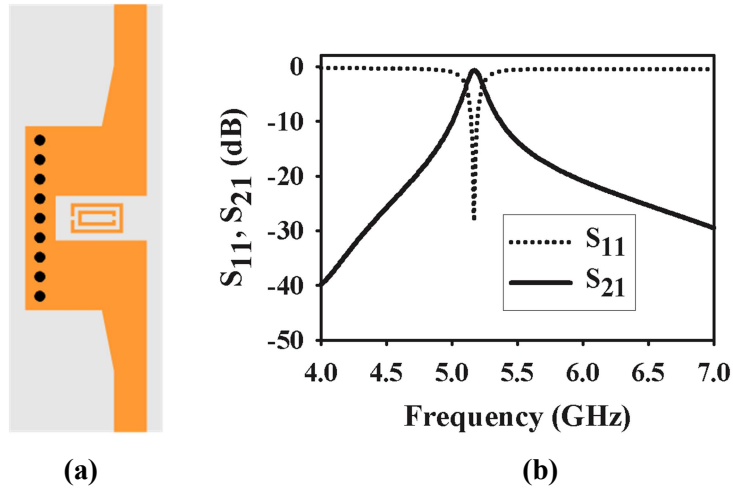


Fig. 4.37. (a) HMSIW with SRR at center (b) S-Parameters

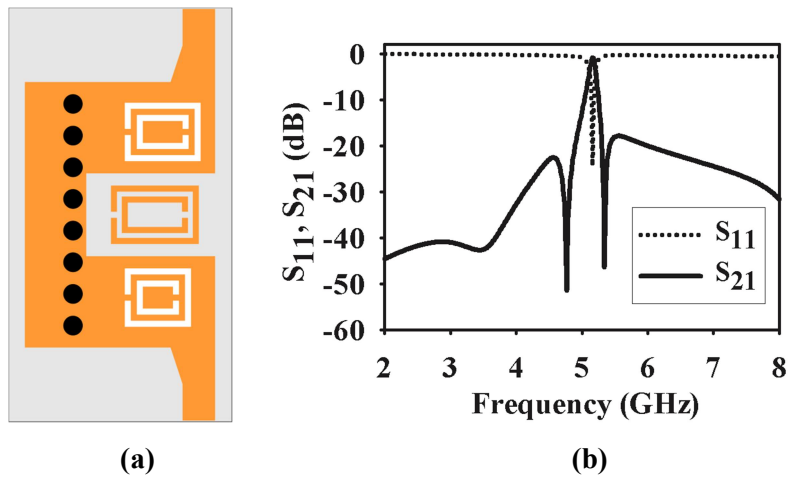
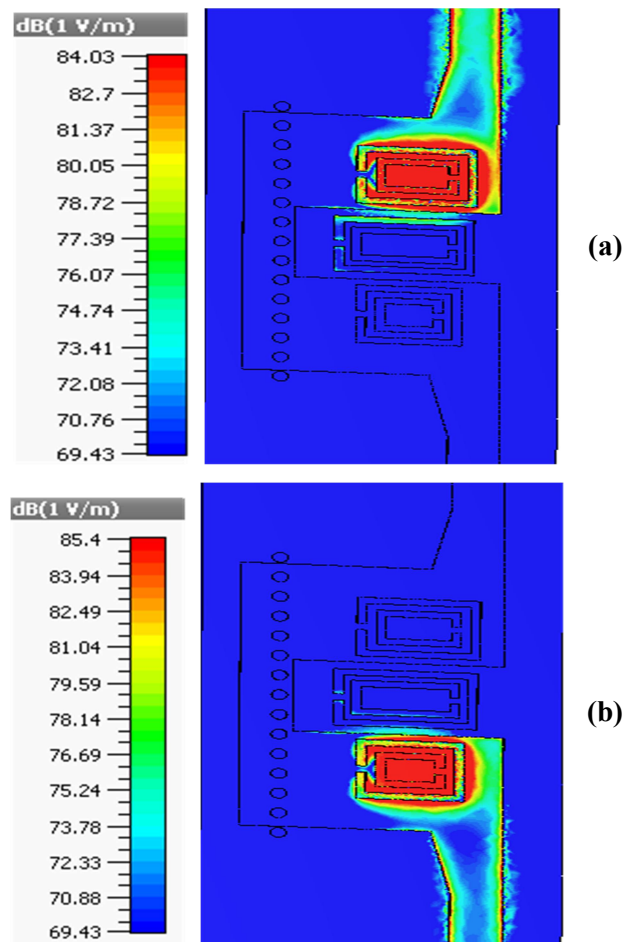


Fig. 4.38. (a) Filter Structure (b) S-Parameters

### 4.3.3 Simulation and Analysis

The CSRR is excited by the presence of axial electric field as shown in Fig.4.39. The left transmission zero is at 4.76 GHz due to the excitation of the larger CSRR. The transmission zero in the right side of the pass band is at a frequency of 5.33 GHz, due to the small CSRR in the

structure. The excitation of SRR and the surface current distribution is shown in Fig. 4.40. The parametric analysis of  $Y_{\text{off}}$  and  $X_{\text{off}}$  is also shown in Fig. 4.41. From the  $S_{21}$  plot of  $Y_{\text{off}}$  it is evident that the stopband attenuation increases as the parameter value decreases. No significant change is observed in  $S_{11}$  plot of  $Y_{\text{off}}$ . The  $S_{11}$  plot of  $X_{\text{off}}$  shows a downward frequency shift with the increase of the parameter value whereas no much change in the observed  $S_{21}$  values.



**Fig. 4.39. Electric Field Distributions (a) 4.76 GHz (b) at 5.33 GHz**

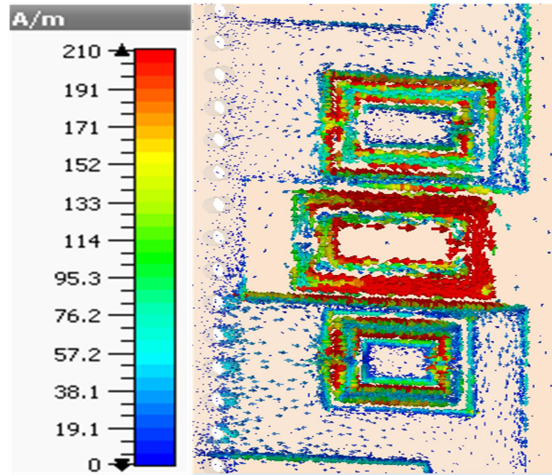


Fig. 4.40. Surface Current Distribution at 5.15 GHz

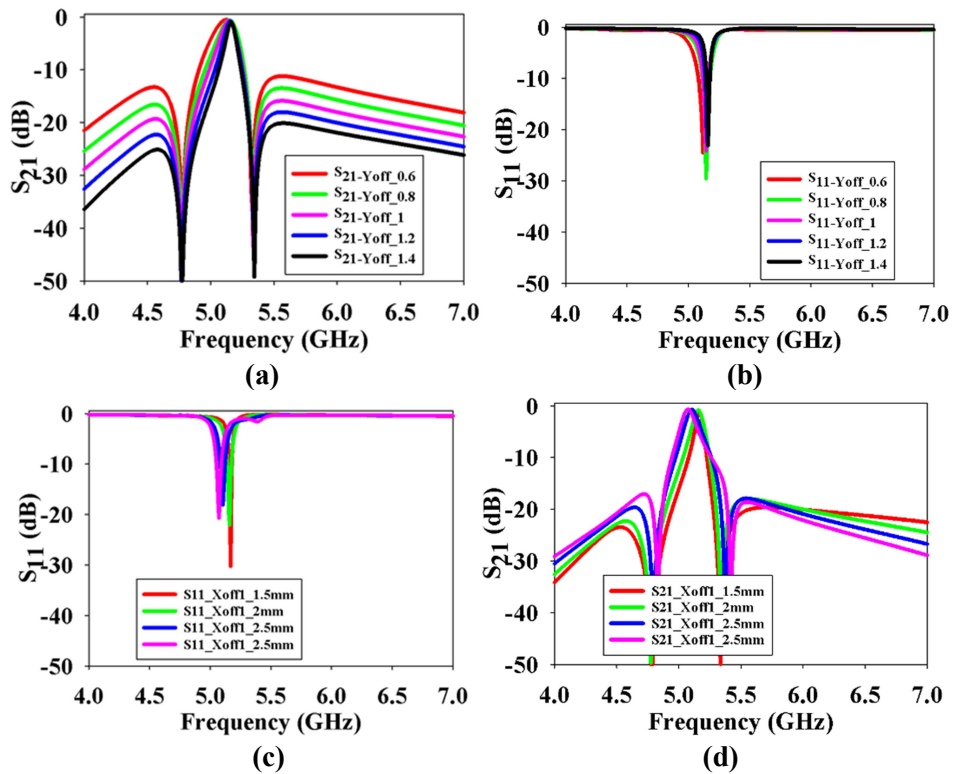
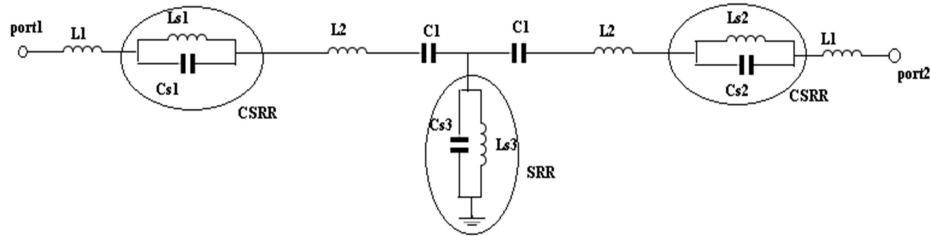


Fig. 4.41. Parametric Simulations (a)  $S_{11}$ - $Y_{off}$  (b)  $S_{21}$ - $Y_{off}$  (c)  $S_{11}$ -  $X_{off}$  and (d)  $S_{21}$ - $X_{off}$



### 4.3.3.1 Lumped element model

The proposed filter is analyzed by using its equivalent circuit shown in Fig. 4.42. The LC circuits  $Ls1$ ,  $Cs1$  and  $Ls2$ ,  $Cs2$  represent CSRRs. The  $Ls3$ , and  $Cs3$  represents SRR in the filter structure. Inductor  $L1$  represents the microstrip to SIW transition portion. Capacitor  $C1$  represent the gap capacitance between the SRR and the cutting. The inductor  $L2$  indicates the SIW portion before and after center SRR.



**Fig. 4.42. LC equivalent circuit model**

The resonant frequencies of the SRR and CSRRs are given by

$$f_a = \frac{1}{2\pi\sqrt{Ls3Cs3}}$$

$$f_b = \frac{1}{2\pi\sqrt{Ls1Cs1}}$$

$$f_c = \frac{1}{2\pi\sqrt{Ls2Cs2}}$$

#### 4.3.4 Measurement results

The structure is fabrication is done on Rogers RT/Duroid 5880 ( $\epsilon_r=2.2$ ,  $h=0.79$  mm,  $\tan\delta=0.0002$ ) substate using the standard PCB process. The photograph of the fabricated filter and the filter characteristics are shown in Fig. 4.43 (a). The simulated and measured insertion and return loss characteristics comparison is given in Fig. 4.43 (b). The measurements are taken using Rohde&Schwarz ZVB-20 vector network analyzer. The measured S-parameters show a little shift from the simulated ones. The simulated transmission zeros are at 4.76 GHz and 5.34 GHz, while the measured ones are shifted to 4.66 GHz and 5.23 GHz respectively keeping the center frequency same at 5.15 GHz. A comparison table showing designed filter compared with already reported filters in terms of fractional bandwidth, insertion loss and compactness is given in table 4.7.

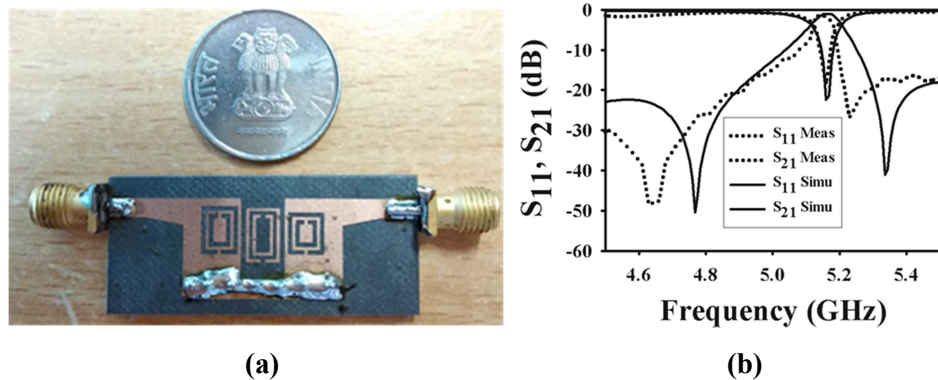


Fig. 4.43. (a) Photograph of Fabricated Filter (b) Insertion and Return Loss Characteristics

**Table 4.7. Comparison of the Designed filter with Reported Filters**

Ref.	Frequency (GHz)	3 dB FBW (%)	Mid band IL (dB)	Size $\lambda_g \times \lambda_g$	Type
[3]	14.87	1.5	3.9	$4.6 \times 4.6$	SIW
[1]	8.25	1.1	3.3	$4.0 \times 4.0$	SIW
[2]	5.00	7.6	1.8	$0.5 \times 0.2$	HMSIW
[4]	9	5.5	2.1	$3.22 \times 3.22$	SIW
This work	5.15	1.1	1.4	$0.4 \times 0.2$	HMSIW

#### 4.4 Summary of the chapter

The designs proposed in this chapter introduces narrowband filters with better insertion and return loss characteristics with the conventional resonator structures. The designs are simple which make use of SRR/CSRR only for the passband/ stopband creation. The stopband performances are also appreciable.

#### References

- [1] A. A Khan and M. K. Mandal, "Narrowband Substrate Integrated Waveguide Bandpass Filter With High Selectivity", *IEEE Microwave and Wireless Components Letters*, vol. 28, no. 5, pp. 416-418, May. 2018.
- [2] Q. L. Zhang, B. Z. Wang, D. S. Zhao and K. Wu, "A Compact Half-Mode Substrate Integrated Waveguide Bandpass Filter With Wide Out-of-Band Rejection", *IEEE Microwave and Wireless Components Letters*, vol. 26, no. 7, pp. 501-503, July. 2016.

- [3] R. Li, X. Tang and F. Xiao, “ Design of Substrate Integrated Waveguide Transversal Filter With High Selectivity”, *IEEE Microwave and Wireless Components Letters*, vol. 20, no. 6, pp. 328-330, June 2010.
- [4] P. Zhang and M. Li, “Cascaded trisection substrate-integrated waveguide filter with high selectivity”, *Electronics Letters*, vol. 50, no. 23, pp. 1717-1719, Nov. 2014.

.....❧.....

# Chapter 5

## SIW AND HMSIW COMPACT BANDPASS FILTERS

### Contents

- 5.1 SIW bandpass filter with cross slot and CSRRs
- 5.2 SIW and HMSIW bandpass filter with embedded vertical loops
- 5.3 HMSIW bandstop filter with coupled vertical loops
- 5.4 Summary of the chapter

*Simulation and experimental studies on compact filters with moderately wide bandwidth are described in this chapter. The structure is made compact by using resonators embedded in the transmission line structure without any coupling resonators. Filters with cross slots, CSRR and vertical loops are designed and experimentally verified. Parametric analysis has been carried out to investigate the filter characteristics on both SIW and HMSIW structures.*

## 5.1 SIW bandpass filter with cross slot and CSRRs

This section presents a bandpass filter on SIW with a cross slot etched on the top and CSRRs on the bottom surface. Circular CSRRs of different diameters are used to achieve the transmission zeros at different frequencies.

The total structure size is reduced due to the bottom loading of the CSRRs. The characteristics of CSRR is given in chapter 1 and its application in filters is discussed in chapter 3. For experimental verification, the filter is fabricated on the Rogers RT 5880 substrate ( $\epsilon_r=2.2$ ,  $h= 0.79$  mm) with  $25 \times 20$  mm<sup>2</sup> overall dimension.

### 5.1.1 Geometry

The proposed filter consists of SIW section with cross shaped slots embedded in it. This is fed by microstrip feed line on both sides with a tapering transition from microstrip to SIW. The ground plane of the structure consists of two CSRRs with resonant frequencies that act as the two transmission zeros of the filter. The filter layout (top and bottom) with relevant parameters marked is shown in Fig. 5.1. The filter parameters as well as the CSRR dimensions are given in Tables 5.1 and 5.2 respectively.

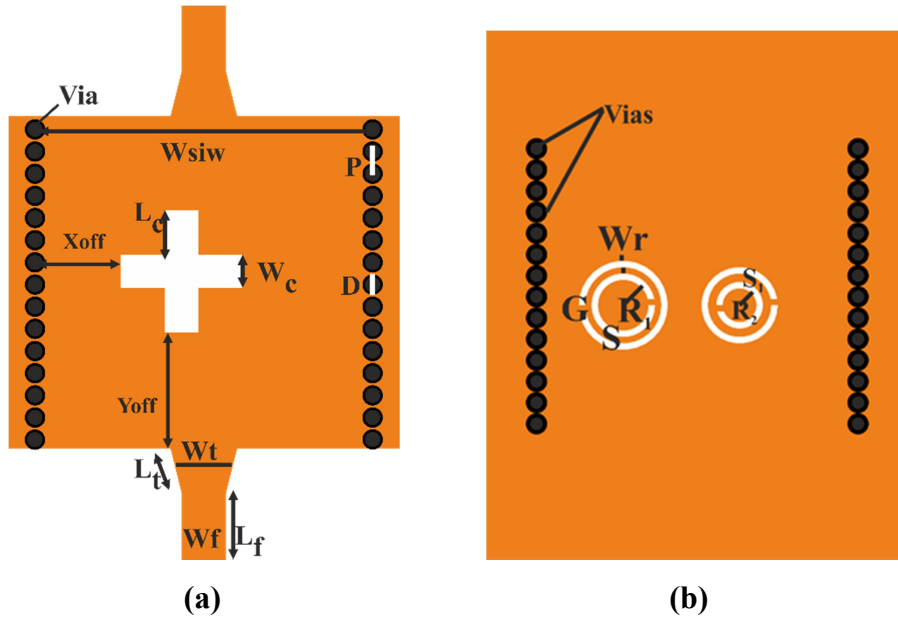


Fig. 5.1. Filter Layout (a) Top View (b) Bottom View

Table 5.1. Filter Parameters

Filter Parameters (mm)															
$L_r$	$L_t$	$W_t$	$W_r$	$W_{siw}$	$L_c$	$W_c$	$D$	$P$	$X_{off}$	$Y_{off}$	Large CSRR- $X_{off}$	Large CSRR- $Y_{off}$	Small CSRR- $X_{off}$	Small CSRR- $Y_{off}$	
3	2	3	2	16	2	1.5	0.8	1	-1	0.5	-3.5	5	2	5	

Table 5.2. CSRR Dimensions

CSRR Dimensions (mm)					
$W_r$	$G$	$S$	$S_1$	$R_1$	$R_2$
0.3	0.3	0.3	0.4	1.2	0.8

### 5.1.2 Design Evolution

SIW with a cut off frequency of 6 GHz with simulated S-Parameters is shown in Fig. 5.2. The SIW with cross slot on its top as well as the simulated response is given in Fig. 5.3. From the S-parameters it is clear that the structure can produce a wide passband. When the ground plane is provided with two embedded CSRRs, the passband is truncated between 7.3 GHz and 9.6 GHz corresponding to the resonant frequencies of the two CSRRs as shown in Fig. 5.4.

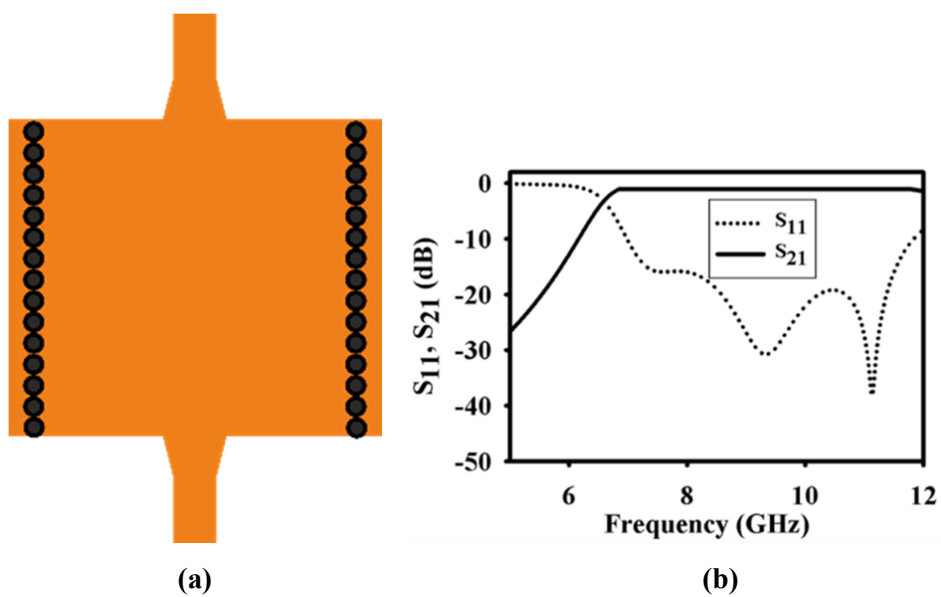


Fig. 5.2. (a) SIW (6 GHz cutoff frequency) (b) S-Parameters



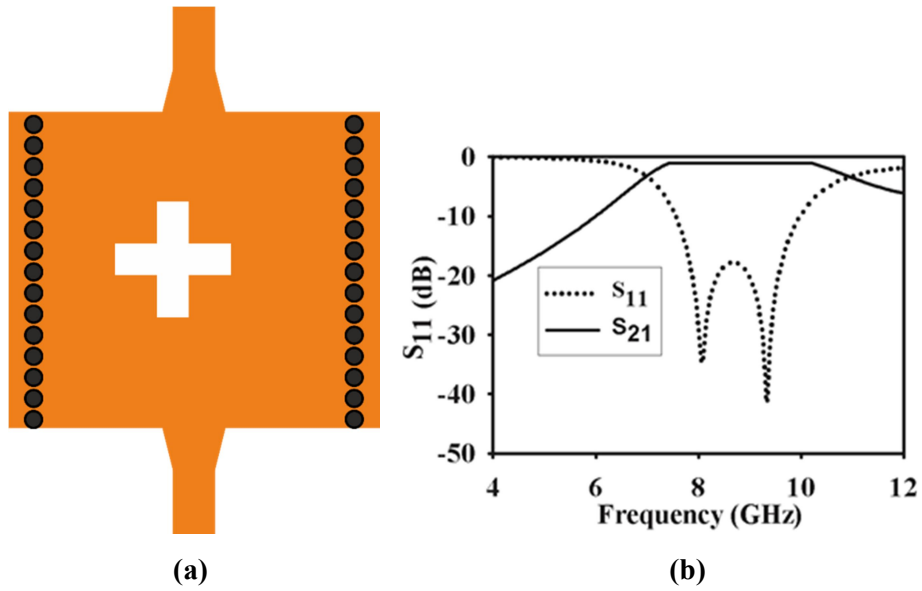


Fig. 5.3. (a) SIW with Cross slot (b) S-Parameters

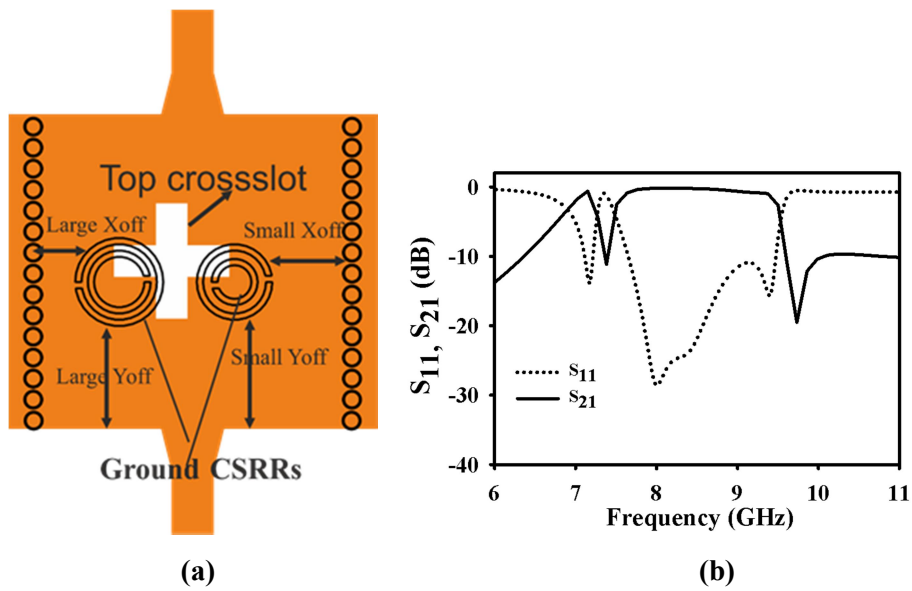
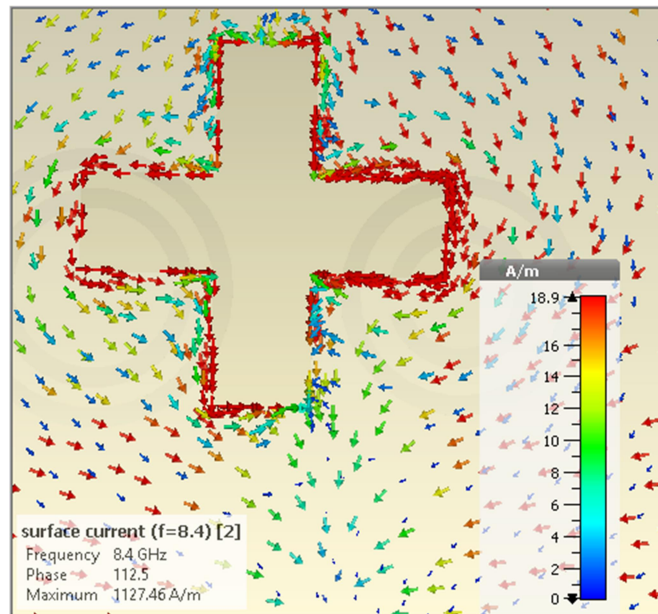


Fig. 5.4. (a) Filter Structure (b) S-Parameters

### 5.1.3 Simulation and Analysis

A detailed analysis of the electric field plots, surface current distribution and parametric analysis of relevant filter parameters are discussed below. The excitation of the cross slot and its surface current distribution due to the excitation is shown in Fig. 5.5. The CSRRs are excited by the presence of axial electric field present in the SIW structure [1], is shown in Fig. 5.6.



**Fig. 5.5. Surface Current Distribution (around the cross slot at the passband center frequency - 8.4 GHz)**

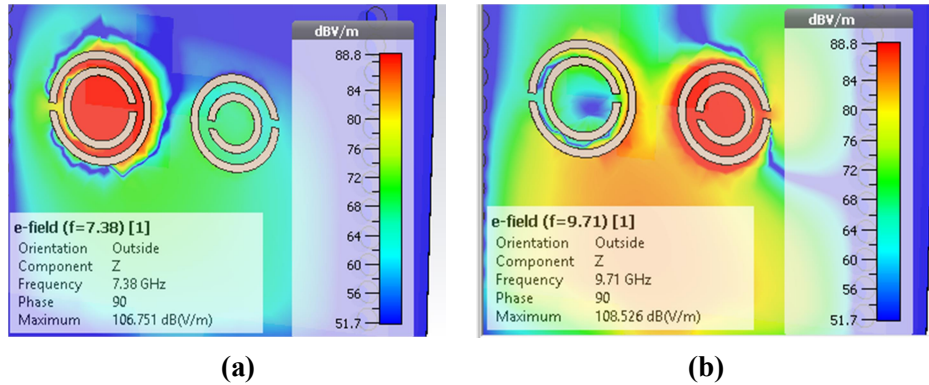


**Fig. 5.6. Electric Field Distribution at SRR Resonant Frequency (a) at 7.38 GHz (b) at 9.71 GHz**

The parametric simulations of the cross slot structure in the filter is carried out in detail. The length ( $L_c$ ) and width ( $W_c$ ) parametric simulations are shown in Fig. 5.7 (a) - (d). The higher frequency attenuation level, the insertion loss characteristics and the return loss are affected by this variation. The width ( $W_c$ ) variation affects the higher band attenuation level. The attenuation increases with increase in the parameter. The position of the cross slot in the SIW is denoted by the parameters  $X_{\text{off}}$  and  $Y_{\text{off}}$ . The passband characteristics and return loss depends on the position of the cross slot. It is evident from the parametric analysis given in Fig. 5.7 (e), (f). The  $Y_{\text{off}}$  parameter has an effect on the return loss of the filter as well a little impact on the higher frequency attenuation characteristics. This is shown in Fig. 5.7 (g), (h).

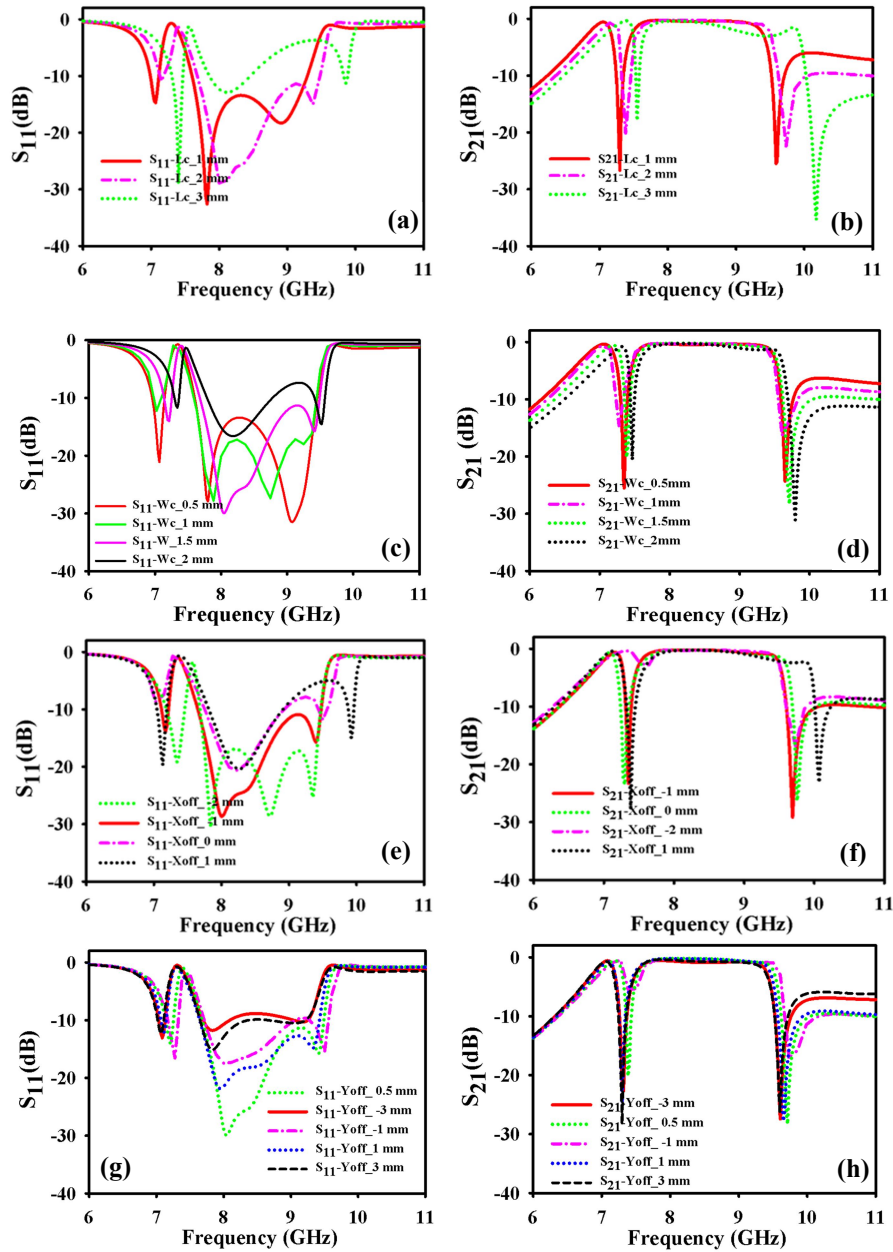


**Fig. 5.7.** Parametric Simulations of (a) Cross slot length (Lc)-  $S_{11}$  (b) Cross slot length (Lc)-  $S_{21}$  (c) Cross slot width (Wc)-  $S_{11}$  (d) Cross slot width (Wc)-  $S_{21}$  (e) Cross slot  $X_{off}$ -  $S_{11}$  (f) Cross slot  $X_{off}$ -  $S_{21}$  (g) Cross slot  $Y_{off}$ -  $S_{11}$  (h) Cross slot  $Y_{off}$ -  $S_{21}$

The CSRR position parameter on the ground plane is varied and analyzed in Fig. 5.8.

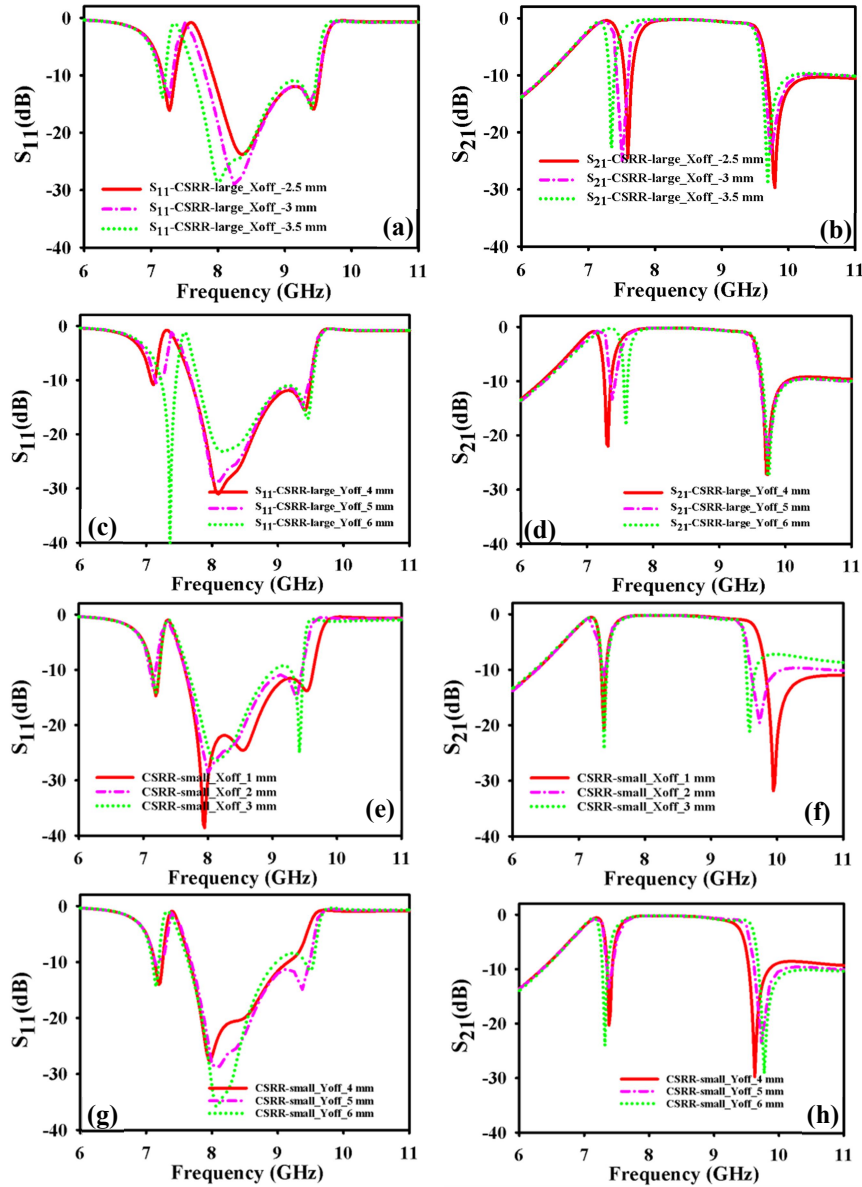


**Fig. 5.8.** Parametric Simulations of (a) CSRR-Large- $X_{\text{off}}S_{11}$  (b) CSRR-Large- $X_{\text{off}}S_{21}$  (c) CSRR-Large- $Y_{\text{off}}S_{11}$  (d) CSRR-Large- $Y_{\text{off}}S_{21}$  (e) CSRR-Small- $X_{\text{off}}S_{11}$  (f) CSRR-Small- $X_{\text{off}}S_{21}$  (g) CSRR-Small- $Y_{\text{off}}S_{11}$  (h) CSRR-Small- $Y_{\text{off}}S_{21}$

The parametric analysis of  $X_{\text{off}}$  and  $Y_{\text{off}}$  of large CSRR is shown in Fig. 5.8 (a) - (d). The lower cut off frequency of the bandpass filter is shifting downwards and upwards with increase in  $X_{\text{off}}$  and  $Y_{\text{off}}$  respectively. The offset parametric studies of the small CSRR is given in Fig. 5.8 (e)-(h). The higher frequency transmission zero is shifting downwards and upwards with the increase in  $X_{\text{off}}$  and  $Y_{\text{off}}$  respectively.

#### 5.1.4 Fabrication and Measurement

The photograph of the fabricated filter is shown in Fig. 5.9. The simulated and measured S-parameters of the structure is shown in Fig. 5.10 (a). The 3 dB bandwidth starting from 7.4 GHz to 9.4 GHz with transmission zeros of left and right of passband at 7.3 GHz and 9.6 GHz respectively can be observed from the insertion and return loss characteristics. A fractional bandwidth of 23.8% is obtained with proposed filter. The group delay characteristics is shown in Fig. 10 (b). A flat group delay can be observed in both simulated and measured responses.

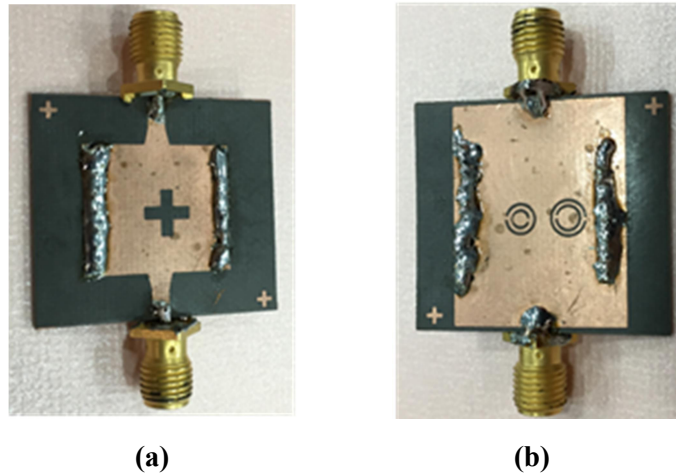


Fig. 5.9. Photograph of Fabricated Filter (a) Top (b) Bottom

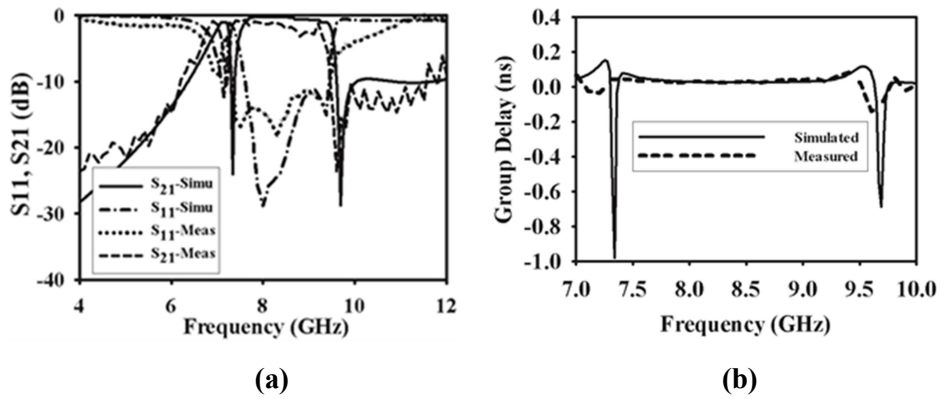


Fig. 5.10. (a) Insertion and Return Loss Characteristics (b) Group Delay Characteristics

## 5.2 SIW and HMSIW bandpass filter with embedded vertical loops

Vertical loop loaded SIW bandpass filter is presented in this section. By arranging the vertical loops of different lengths, the generation of a passband is ignited by the excitation of the loops by the SIW electric field component. A moderately wide bandpass filter is presented in this work. The passband is located in the Ku band with an overall filter dimension of  $33 \times 13 \text{ mm}^2$  and with a reasonable attenuation in the stopband. The vertical loops are visualized by a double sided structure utilising the SIW top and bottom planes.

The vertical loop embedded HMSIW filter is also designed and tested to enhance the compactness of the filter. A wide passband located at the X-band is realized with an overall dimension of  $30 \times 12 \text{ mm}^2$ . Standard photolithographic process is used for both the structure fabrications. The filter fabrications are done on the Rogers RT 5880 substrate ( $\epsilon_r=2.2$ ,  $h=0.79\text{mm}$ ).



## 5.2.1 Geometry

### 5.2.1.1 Geometry of SIW Filter

The microstrip line fed tapered feeding is introduced to the filter topology. The SIW section consisting of three vertical loops which engages the top and bottom planes of the SIW is shown in Fig. 5.11 (a) and (b). The top and bottom positions (in terms of  $X_{\text{off}}$  and  $Y_{\text{off}}$ ) are identical for the loop. The enlarged view of the vertical loop is shown in Fig. 5.11 (c). The filter and loop parameters are given in Tables 5.3 and 5.4 respectively.

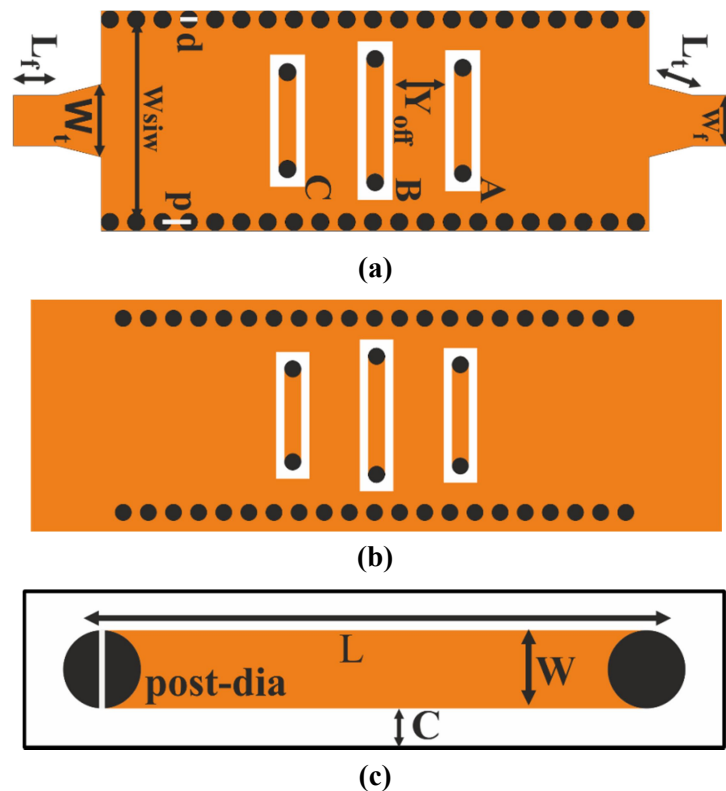


Fig. 5.11. (a) SIW Bandpass Filter with Vertical Loops (top)  
 (b) SIW Bandpass Filter with Vertical Loops (bottom)  
 (c) Enlarged View of Vertical Loop

**Table 5.3. Filter Parameters**

<b>Filter Parameters (mm)</b>							
<b>Lt</b>	<b>Wt</b>	<b>Lf</b>	<b>Wf</b>	<b>Wsiw</b>	<b>p</b>	<b>d</b>	<b>Yoff</b>
3	3.3	3	2.3	10	1.2	0.8	2.4

**Table 5.4. Loop Parameters**

	<b>A</b>		<b>B</b>		<b>C</b>
L	5.6	L	6.4	L	5.2
W	0.8	W	0.8	W	0.8
C	0.4	C	0.4	C	0.4
Post-dia	0.8	Post -dia	0.8	Post- dia	0.8

### 5.2.1.2 Geometry of HMSIW Filter

A fifty percentage size reduction can be obtained by transforming the SIW filter into HMSIW one. The geometry of HMSIW vertical loop filter top and bottom at X-band is shown in Fig. 5.12 (a) and (b). The enlarged view of the loop is shown in Fig. 5.12 (c). Both the filter parameters and the loop parameters are given in Tables 5.5 and 5.6 respectively.

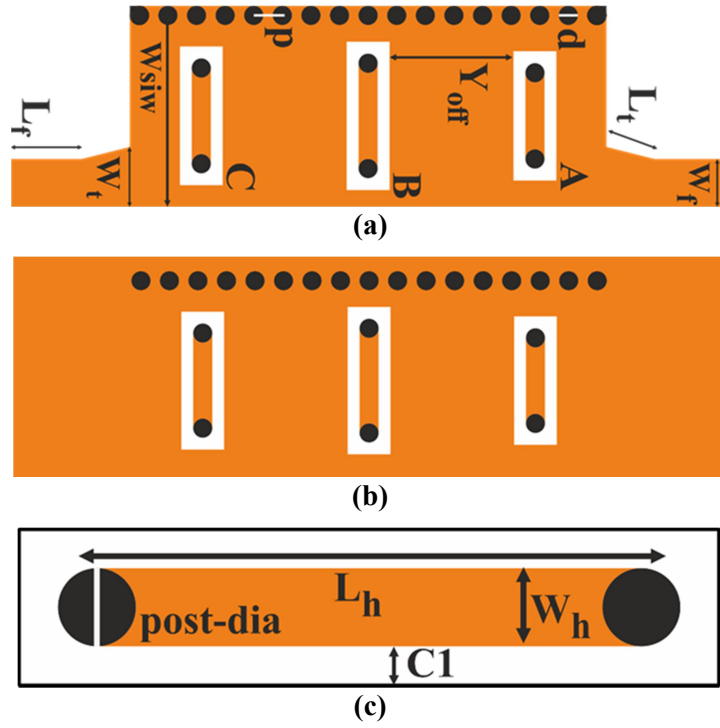


Fig. 5.12. (a) HSIW Bandpass Filter with Vertical Loops (top)  
 (b) HSIW Bandpass Filter with Vertical Loops (bottom)  
 (c) Enlarged View of Vertical Loop

Table 5.5. Filter Parameters

Filter Parameters (mm)							
Lt	Wt	Lf	Wf	Wsiw	p	d	Yoff
3	3	3	2	8.4	1.2	0.8	5.2

Table 5.6. Loop Parameters

	A		B		C
L <sub>h</sub>	4.4	L <sub>h</sub>	5.2	L <sub>h</sub>	4.8
W <sub>h</sub>	0.8	W <sub>h</sub>	0.8	W <sub>h</sub>	0.8
C1	0.5	C1	0.5	C1	0.5
Post-dia	0.8	Post -dia	0.8	Post- dia	0.8

## 5.2.2 Design Evolution

### 5.2.2.1 SIW Filter

The vertical loop filter is designed by placing a closed loop occupied by the top and bottom plane of the SIW. The loop structure is possible by the introduction of vias on both sides of the metal strip surrounded by a metal free region. The loop orientation in Fig. 5.13 (a) gives a narrow stopband as shown in Fig. 5.13 (b). But proceeding for a bandpass filter, this orientation makes the total structure large, due to the number of loops involved and the separation between them. An alternative loop orientation on the SIW gives a wide bandpass result is shown in Fig. 5.14. By properly optimizing the length, width, separation and gaps of the loops a moderate band bandpass filters is designed as shown in Fig. 5.15.

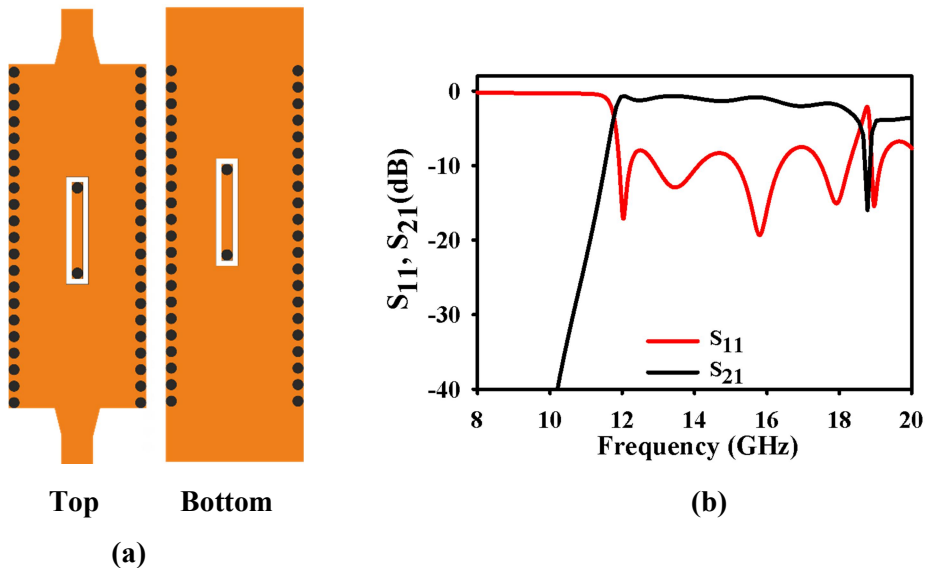


Fig. 5.13. (a) Loop Orientation 1 (b) S-Parameters

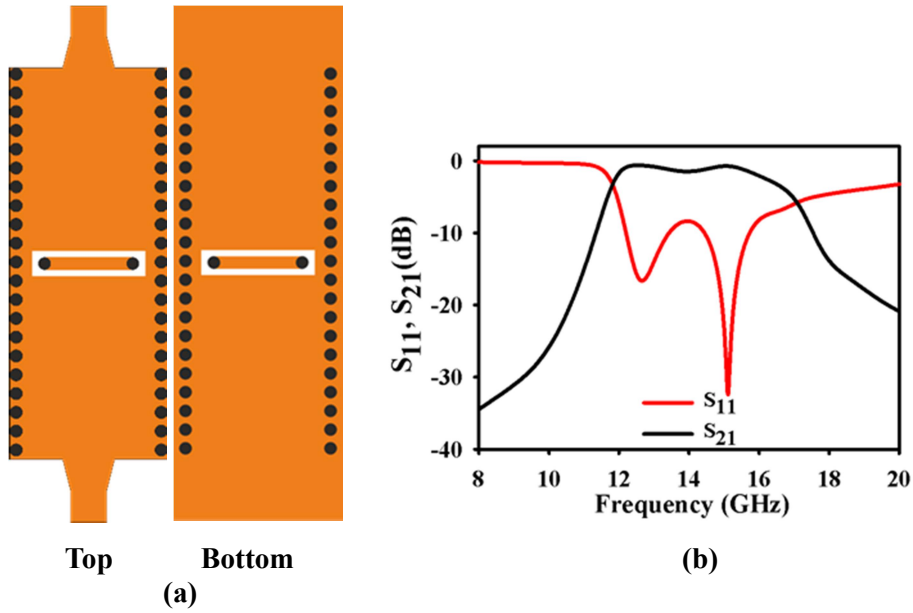


Fig. 5.14. (a) Loop Orientation 2(b) S-Parameters

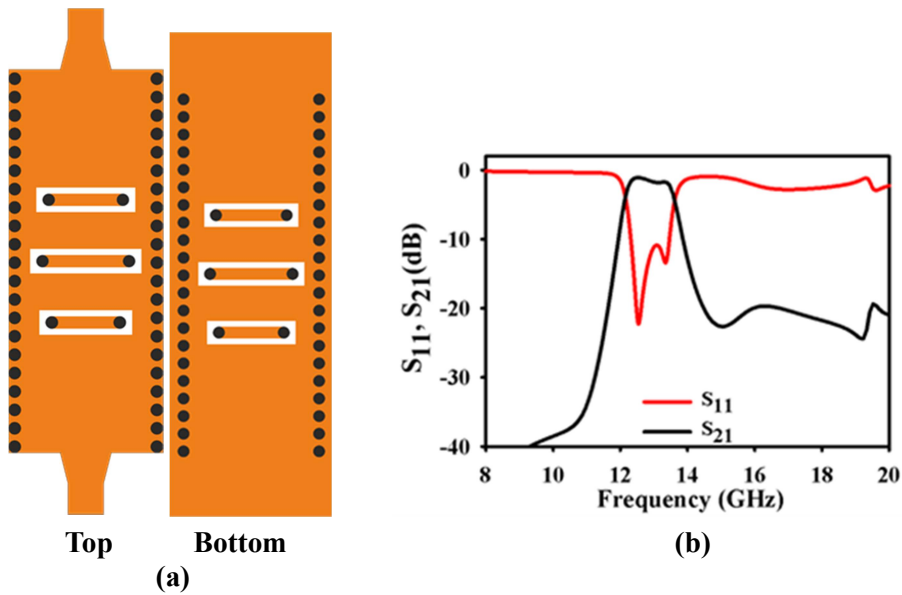


Fig. 5.15. (a) Filter Structure (b) S-Parameters

### 5.2.2.2 HMSIW Filter Design

The SIW vertical loop filter discussed above can be made compact by the introduction of HMSIW loop filter as shown in Fig. 5.16. The transition from moderate bandwidth to wide bandwidth [2] is detailed using this structure. A wide bandwidth with a flat passband can be realized by this method.

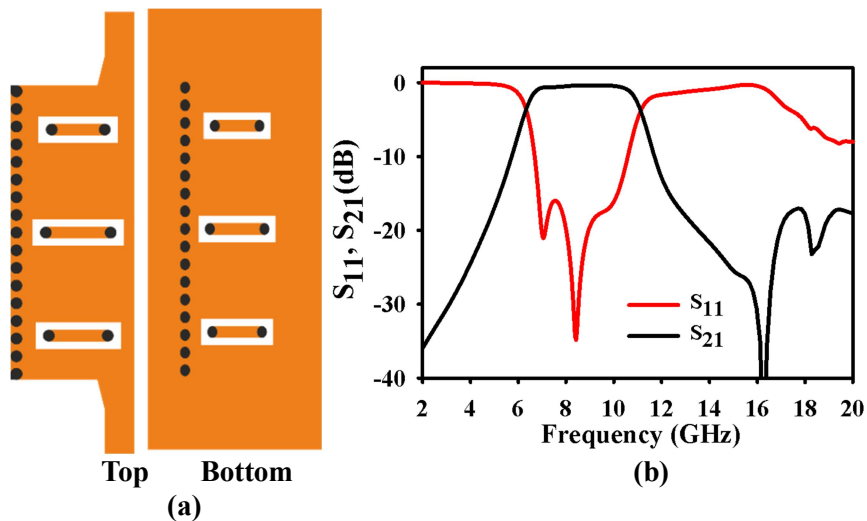
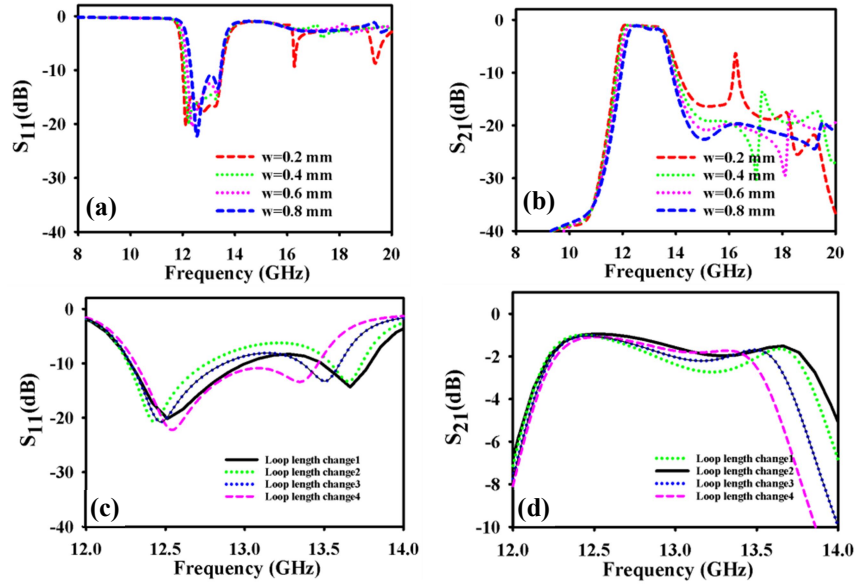


Fig. 5.16. (a) Filter Structure (b) S-Parameters

## 5.2.3 Simulation and Analysis

### 5.2.3.1 SIW Filter

The parametric studies of the SIW filter structure is shown in Fig. 5.17. The loop width ( $W$ ) changes affect the upper frequency attenuation level. It increases with the increase in the loop width as shown in 5.17 (a) and (b). Three loops with different lengths are placed for the desired filter response.



(Loop length change1:l1=6, l2=5.4, l3=5; Loop length change2: l1=6, l2=5.6, l3=5.2; Loop length change3:l1=6.2, l2=5.6, l3=5.2; Loop length change 4:l1=6.4, l2=5.6, l3=5.2)

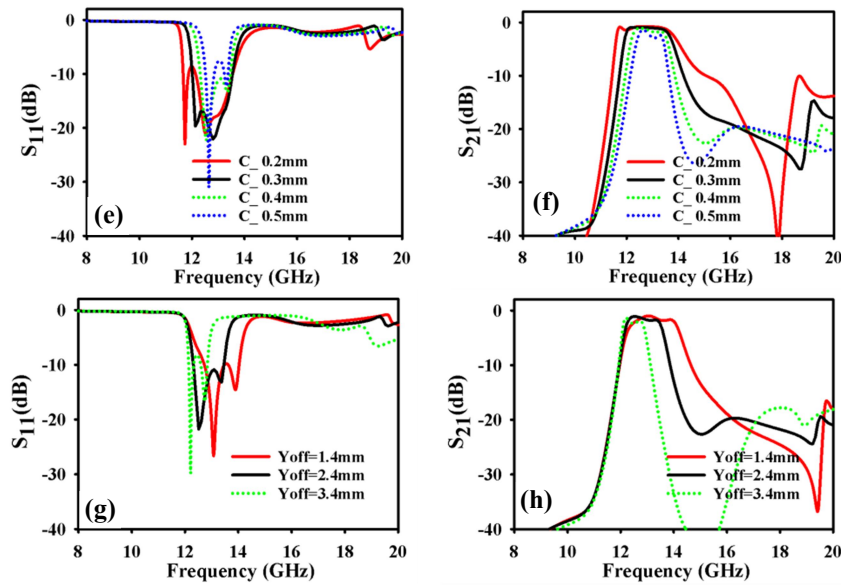
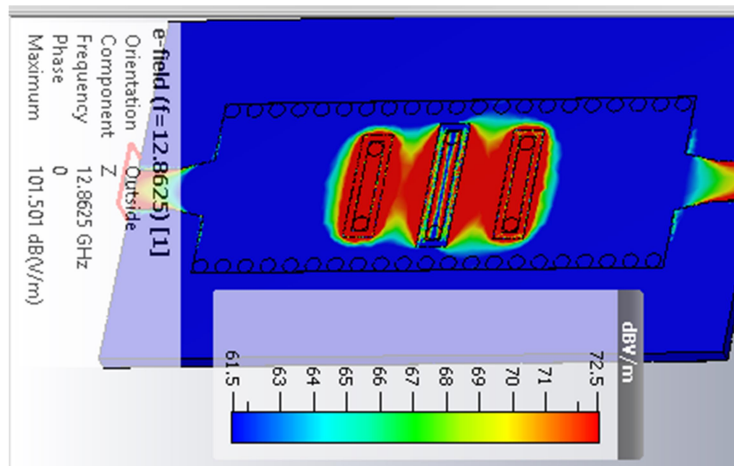


Fig. 5.17. Parametric Simulations of (a) Loop width (W) – S<sub>11</sub> (b) Loop width (W) – S<sub>21</sub>(c) Loop length changes (l1, l2, l3) –S<sub>11</sub> (d) Loop length changes (l1, l2, l3) –S<sub>21</sub> (e) Gap change (c)-S<sub>11</sub> (f) Gap change (c)-S<sub>21</sub> (g) Yoff- S<sub>11</sub> (h) Yoff- S<sub>21</sub>

The passband flatness varies with the changes in the loop lengths (l1, l2, l3) as shown in Fig. 5.17 (c) and (d). The gap between the metallic strip and the non-metallic portion of the loop (C) variations shifts the upper frequency cut off of the filter. It shifts to higher frequency range with the increase in the gap as shown in Fig. 5.17 (e) and (f). The passband bandwidth can be increased with the increase in the distance between the loops ( $Y_{off}$ ) as shown in Fig. 5.17 (g) and (h). The loop excitations are shown in Fig. 5.18 at the center frequency of the passband (12.86 GHz).

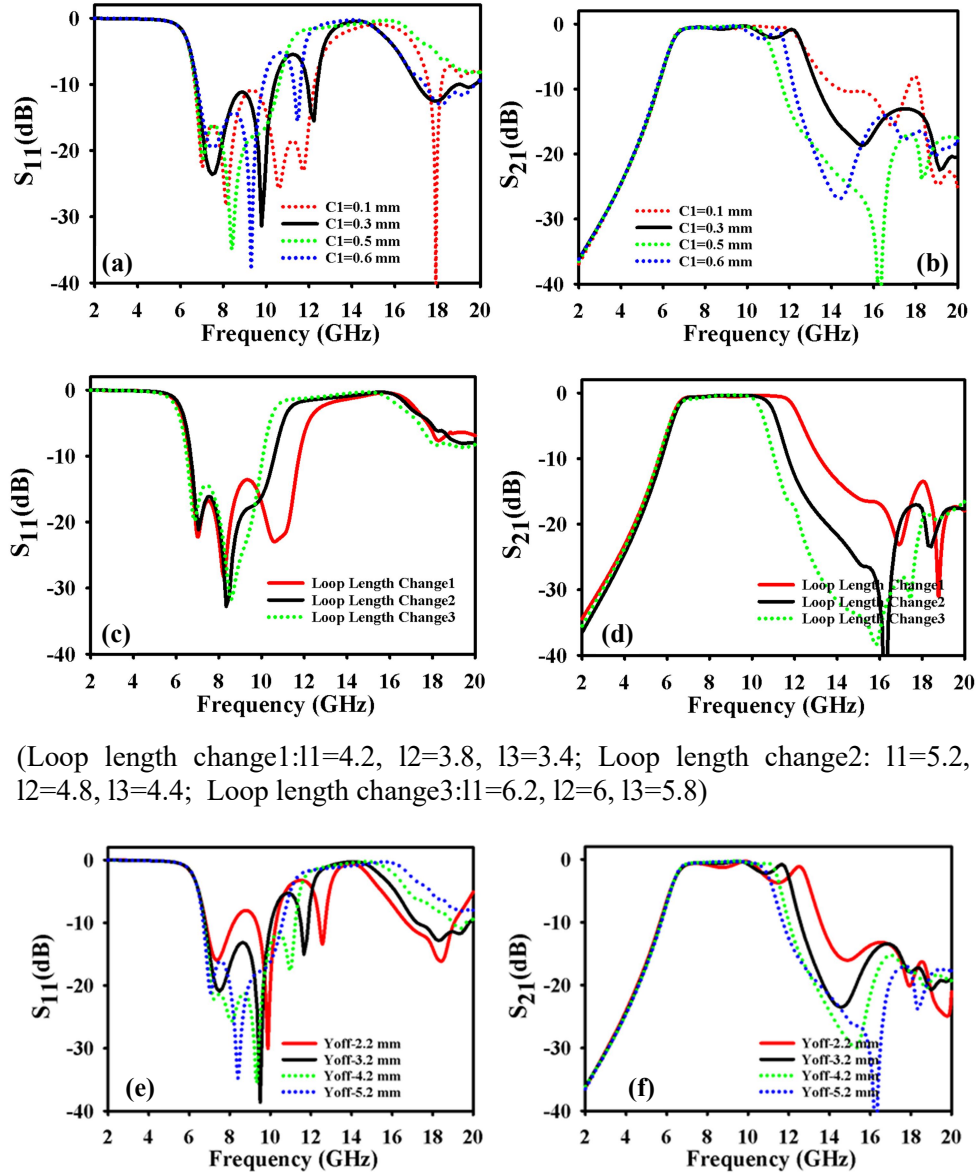


**Fig. 5.18. Electric Field Distribution of the Vertical Loops at 12.86 GHz (passband center frequency)**

### 5.2.3.2 HMSIW Filter

The vertical loop loaded HMSIW filter parametrically studied is shown in Fig. 5.19. The gap between the metal strip and the nonmetallic portion of the loop (C1) variation changes the upper cutoff frequency and bandwidth with corresponding changes in the return loss of the filter as shown in Fig. 5.19 (a) and (b).





(Loop length change1:l1=4.2, l2=3.8, l3=3.4; Loop length change2: l1=5.2, l2=4.8, l3=4.4; Loop length change3:l1=6.2, l2=6, l3=5.8)

**Fig. 5.19.** Parametric Simulations of (a) Gap change (C1)- $S_{11}$ (b) Gap change (C1)- $S_{21}$  (c) Loop length changes (l1, l2, l3) - $S_{11}$  (d) Loop length changes (l1, l2, l3) - $S_{21}$  (e) Yoff-  $S_{11}$  (h) Yoff-  $S_{21}$

The parametric analysis of the loop lengths is given in Fig. 5.19 (c) and (d). The upper cut off frequency of the passband as well as the passband

bandwidth increases with the decrease in length of the loops with corresponding changes in return loss characteristics. The variations in  $Y_{off}$  and the corresponding S- parameters are shown in Fig. 5.19 (e) and (f). This parameter contributes to the flatness of the passband and higher cut off frequency. The electric field distribution of the HMSIW loop filter at 8.7 GHz (passband center frequency) shown in Fig. 5.20, depicts the field plot for individual loops.

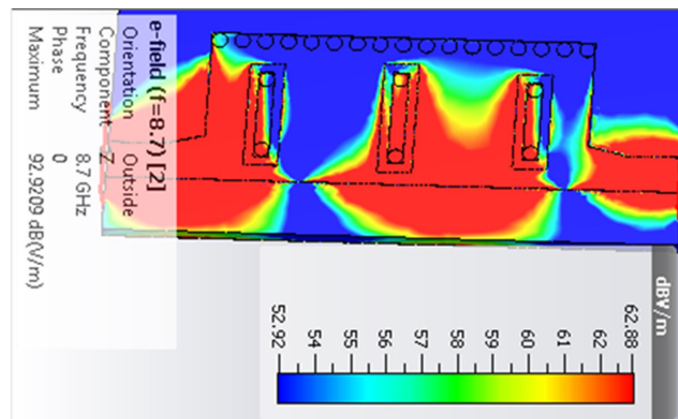


**Fig. 5.20. Electric Field Distribution of the Vertical Loops at 8.7 GHz (passband center frequency)**

## 5.2.4 Fabrication and Measurement

### 5.2.4.1 SIW Filter

The SIW filter fabrication and measurement is detailed in this section. The photograph of the fabricated structure is shown in Fig. 5.21. A comparison of the simulated as well as the measured s-parameters are given in Fig. 5.22 (a). The simulated 3 dB bandwidth ranges from 12.19 GHz to 13.54 GHz, with a bandwidth of 1.35 GHz and center frequency of 12.865 GHz.

The measured passband exhibits a shift and ranges from 12.42 GHz-13.48 GHz. The filter has attained a reasonably good attenuation band after this range. The fractional bandwidth of the proposed filter is 8% which comes under the moderately wide bandwidth filter category. The measured and the simulated group delays are compared and is shown in Fig. 5.22 (b). The simulation shows a relatively flat group delay compared to the measured one. The measurement results show a slight deviation from the simulation results in the passband flatness and upper and lower cut offs, which may be due to the fabrication tolerances and soldering effects.

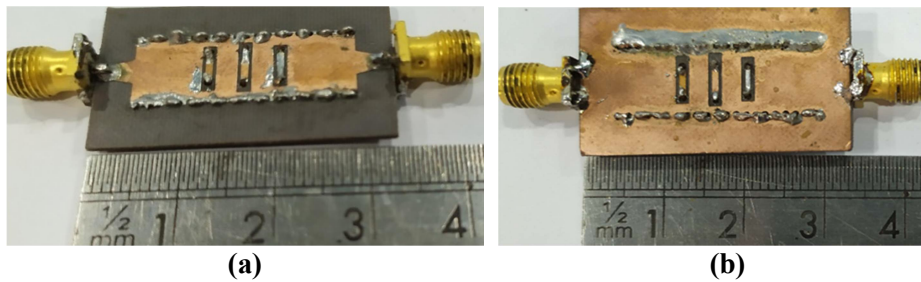


Fig. 5.21. SIW Bandpass Filter with Vertical Loops (a) Top (b) Bottom

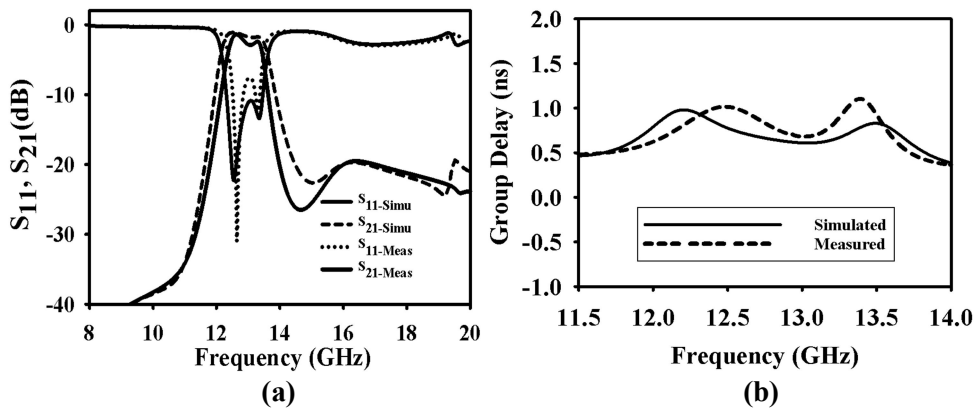


Fig. 5.22. (a) Insertion and Return Loss Characteristics (b) Group Delay Characteristics

### 5.2.4.2 HMSIW Filter

The size reduction of the SIW loop filter leads to the design of an HMSIW filter with embedded vertical loops utilizing top and bottom surface of the HMSIW. The photograph of the fabricated filter structure is shown in Fig. 5.23. The insertion and return loss characteristics of the simulated and the measured structures are shown in Fig. 5.24 (a). The simulated filter exhibits a passband of 4.6 GHz from 6.39 GHz to 11.02 GHz with a percentage bandwidth of 53%. The measured results shows a widening of the passband upto 11.75 GHz with a percentage bandwidth of 59.8% along with an undesirable distortion in the passband as shown in the characteristics curve. The group delay shown in Fig. 5.24 (b) plots the distortion in the measured insertion loss.

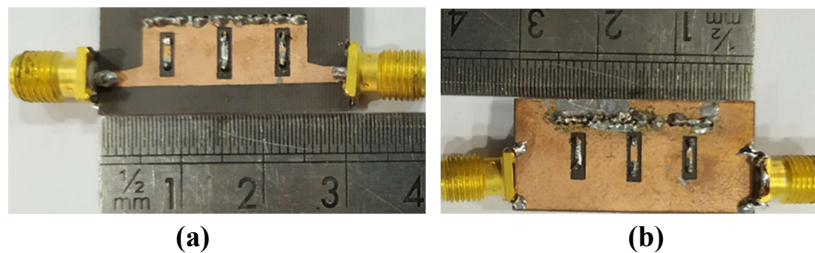


Fig. 5.23. HMSIW Bandpass Filter with Vertical Loops (a) Top (b) Bottom

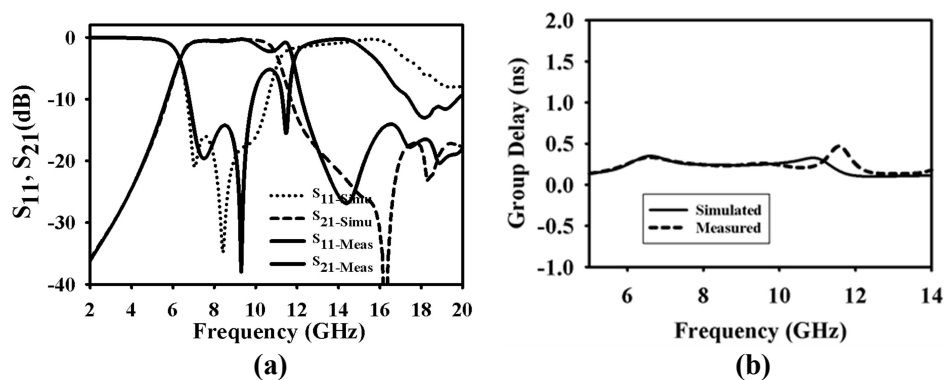


Fig. 5.24. (a) Insertion and Return Loss Characteristics (b) Group Delay Characteristics

### **5.3 HMSIW bandstop filter with coupled vertical loops**

The vertical loop with slit is a new approach to the conventional resonator structures [3] in connection with SIW. In order to limit the loop size [4], conductor strip separated by a nonconductor region with vias on either side is placed vertically in the top and bottom surface of the HMSIW. The bandpass filter design topologies of the embedded vertical loops are studied in the previous section.

The bandstop filter using HMSIW coupled vertical loop is studied in this section. The filter is fabricated on Rogers RT 5880 laminate ( $\epsilon_r=2.2$ ,  $h= 0.79$  mm) with  $33\times 13$  mm<sup>2</sup> overall dimension. A narrow stopband is realized in the proposed structure. The structure is fabricated using standard photolithography process.

#### **5.3.1 Geometry**

The HMSIW loop filter is fed using microstrip line with a tapering for impedance transformation. The HMSIW section is edge coupled to vertical loop with slit. The top and bottom structure topology is shown in Fig. 5.24 (a) and (b) respectively. The geometry of the slitted loop is shown in Fig. 5.24 (c). The filter parameters and the loop parameters are shown in Tables 5.7 and 5.8 respectively.

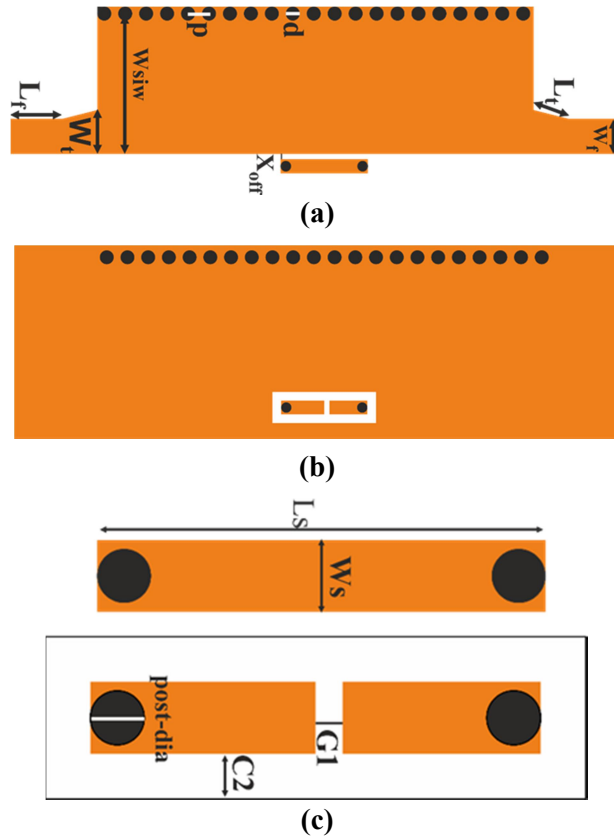


Fig. 5.24. (a) HSIW Bandstop Filter with Vertical Loop with slit (top) (b) HSIW Bandstop Filter with Vertical Loop with slit (bottom) (c) Enlarged View of Vertical Loop with slit

Table 5.7. Filter Parameters

Filter Parameters (mm)							
Lt	Wt	Lf	Wf	Wsiw	p	d	Xoff
2	3	3	2	8.4	1.2	0.8	0.2

**Table 5.8. Loop Parameters**

Loop Parameters (mm)				
Ls	Ws	C2	G1	Post dia
5	0.8	0.5	0.3	0.8

### 5.3.2 Design Evolution

The HMSIW coupled with vertical loops are designed and simulated. A loop without slit is placed near the magnetic wall of HMSIW and no remarkable excitation is found as shown in Fig. 5.25. A slit introduced at the ground portion of the loop affects the loop excitation and a narrow stopband is observed as shown in Fig. 5.26. The stopband bandwidth can be increased by increasing the number of loops involved in the design as given in Fig. 5.27.

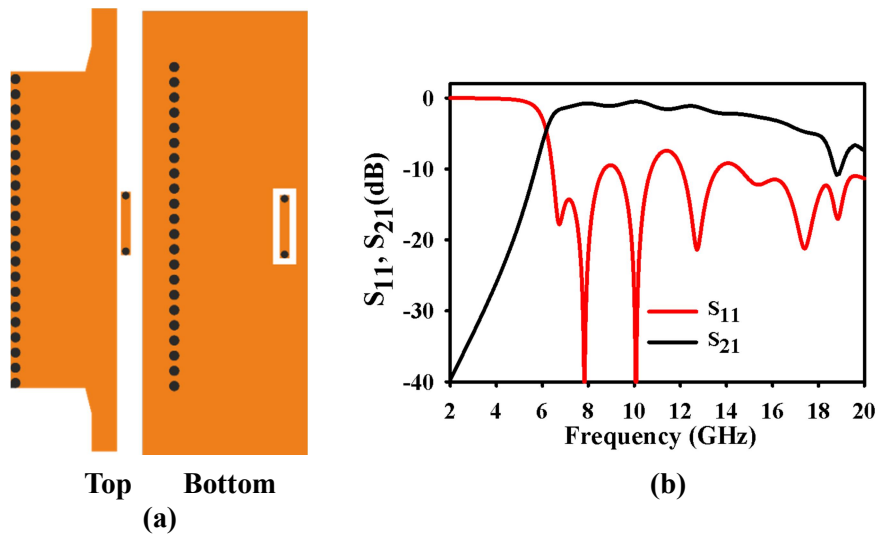


**Fig. 5.25. (a) Loop Orientation (b) S-Parameters**

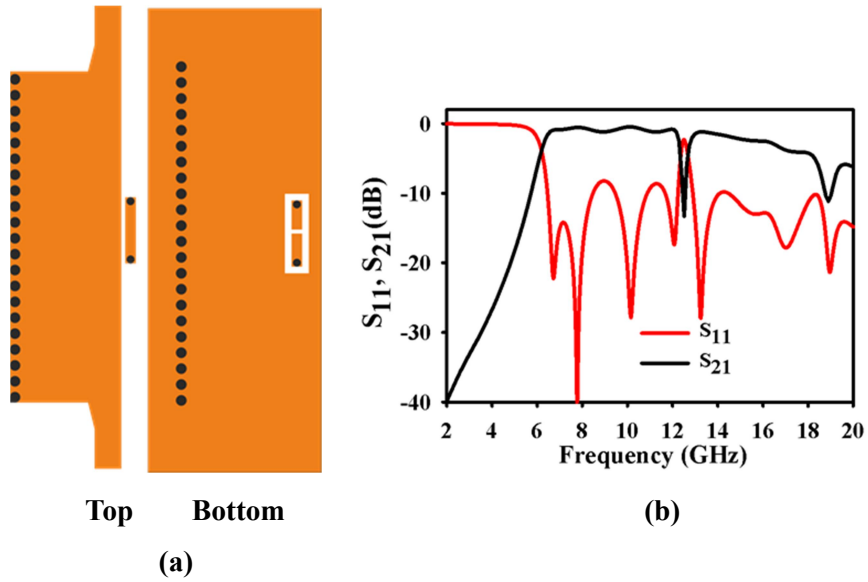


Fig. 5.26. (a) Loop with slit at the bottom plane (b) S-Parameters

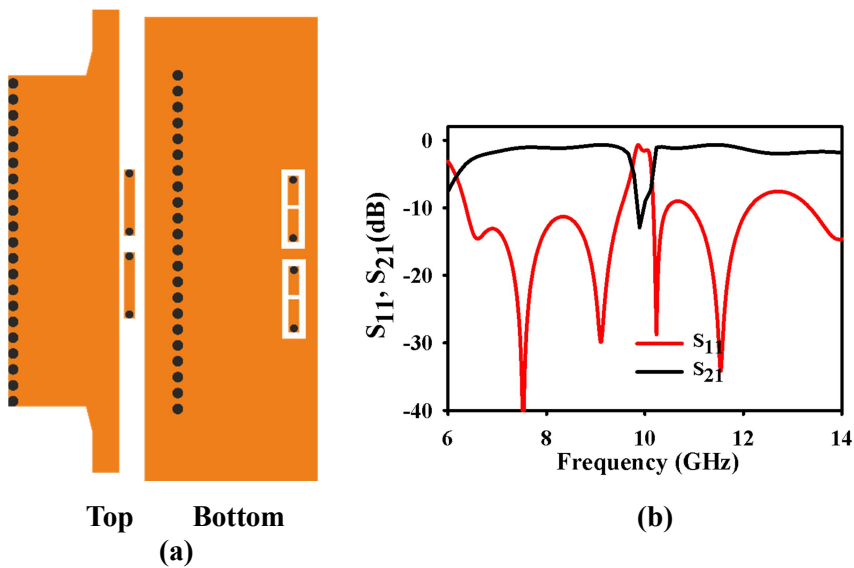


Fig. 5.27. (a) HMSIW with two loops (b) S-Parameters



### 5.3.3 Simulation and Analysis

The frequency dependence of various loop parameters are studied in this section. The loop parameters such as loop width ( $W_s$ ), gap ( $C_2$ ) and slit separation ( $G_1$ ) shifts the frequency to higher range with the increase in the parameter as shown in Fig. 5.28 (c), (d), (e), (f), (i) and (j) respectively. An increase in parameters like loop length ( $L_s$ ) and  $X_{\text{off}}$  shifts the frequency to the lower range as given Fig. 5.28 (a), (b), (g) and (h).

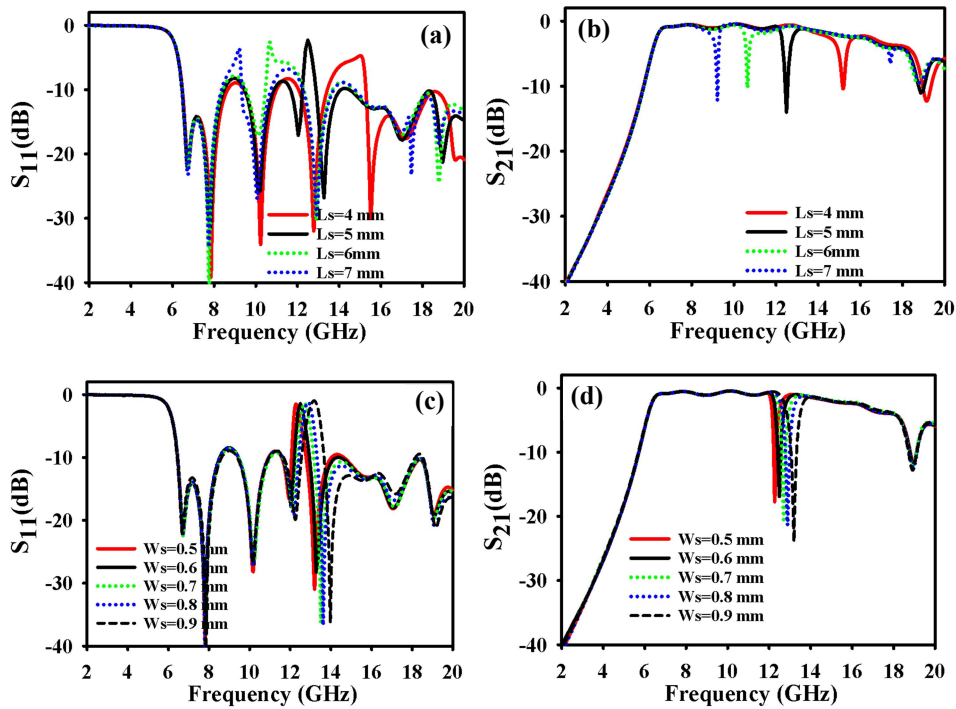


Fig. 5.28. Parametric Simulations of (a) Loop Length ( $L_s$ ) -  $S_{11}$  (b) Loop Length ( $L_s$ ) -  $S_{21}$  (c) Loop width ( $W_s$ ) -  $S_{11}$  (d) Loop width ( $W_s$ ) -  $S_{21}$

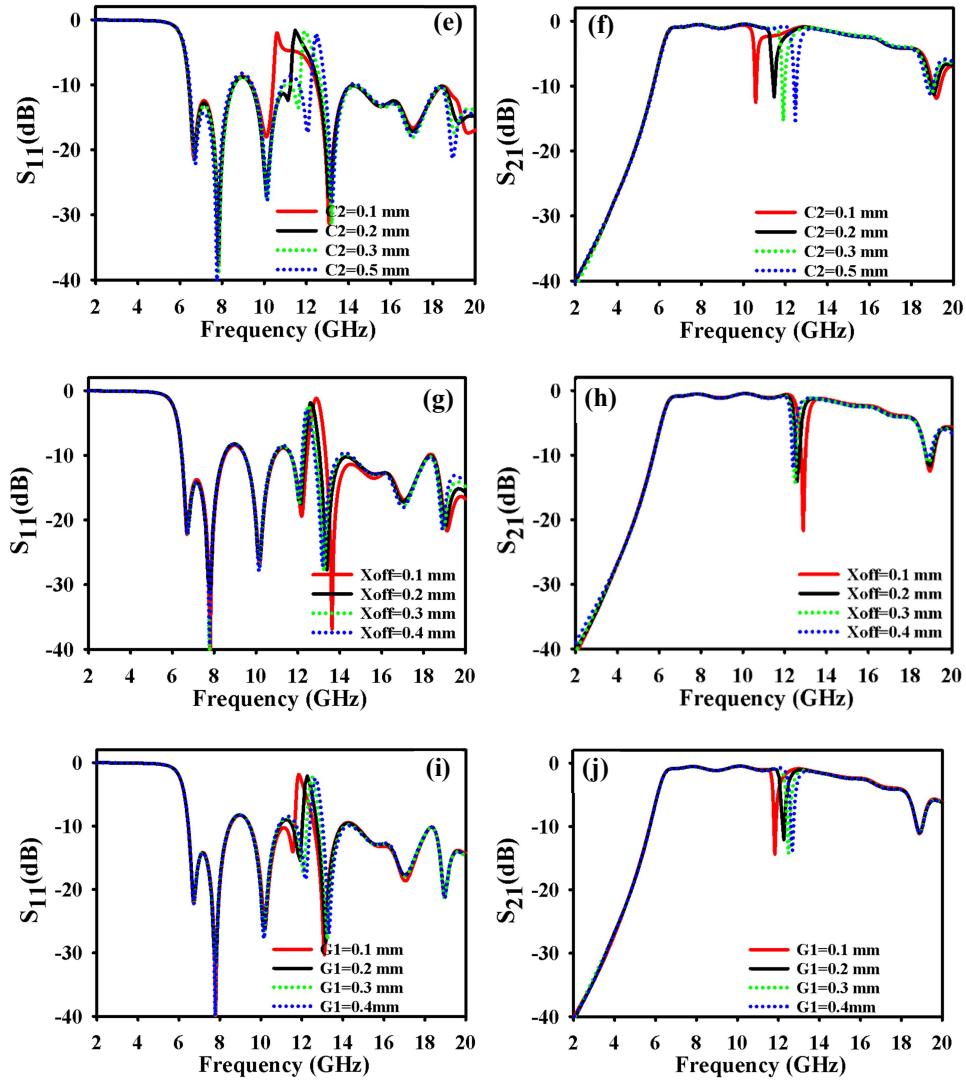


Fig. 5.28. Parametric Simulations of (e) Gap(C2)- $S_{11}$  (f) Gap(C2)- $S_{21}$  (g) Xoff-  $S_{11}$  (h) Xoff-  $S_{21}$  (i) Slit Width (G1)- $S_{11}$  (j) Slit Width (G1)- $S_{21}$

### 5.3.4 Fabrication and Measurement

The Fig. 5.29 shows the photograph of the fabricated filter with the SMA connectors. Standard photolithography is used for the fabrication process and the S parameter measurements are taken using Rohde & Schwarz ZVB20 vector network analyzer. The measured result in comparison with the simulated results are shown in Fig. 5.30. A small frequency shift is observed in the measurement result, which may be caused due to the fabrication inaccuracies of the tiny featured loop in the filter structure.

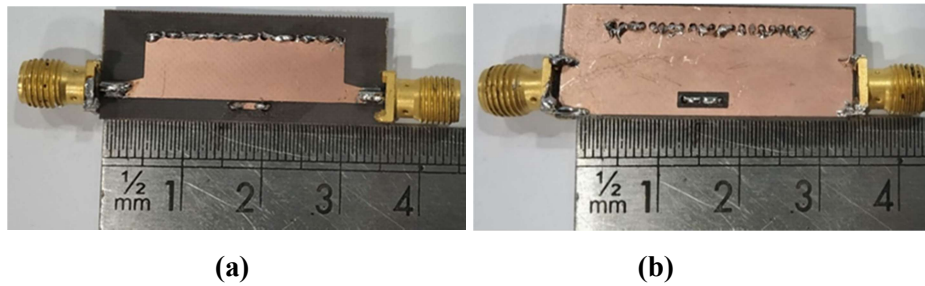


Fig. 5.29. Photograph of Fabricated Filter (a) Top (b) Bottom

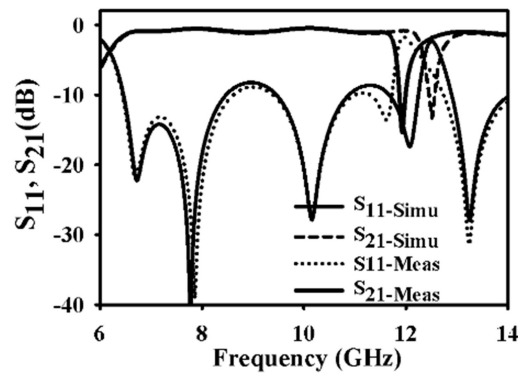


Fig. 5.30. Insertion and Return Loss Characteristics

## 5.4 Summary of the chapter

The proposed designs describe new techniques for the generation of wide bandpass filters. A new method for the embedding of loop structure is introduced in the chapter. Bandpass filters and bandstop filter is realized using the newly proposed loop structure. Embedded loops are used for the generation of bandpass filters while the coupled loops are used for the bandstop filter. All the double sided structures are fabricated using the standard photolithography process.

## References

- [1] Juan Domingo Baena, Jordi Bonache, Ferran Martin, Ricardo Marques Sillero, Francisco Falcone, Txema Lopetegi, Miguel A. G. Laso, Joan Garcia-Garcia, Ignacio Gil, Maria Flores Portillo, and Mario Sorolla, "Equivalent-Circuit Models for Split-Ring Resonators and Complementary Split-Ring Resonators Coupled to Planer Transmission Lines," *IEEE Trans. Microwave Theory and Techniques*, Vol.53, No.4, April 2005.
- [2] Liwen Huang, Hao Cha, "Compact Ridge Half-Mode Substrate Integrated Waveguide Bandpass Filter," *IEEE Microwave and Wireless Components Letters*, Vol. 25, No. 4, April 2015.
- [3] X.-C. Zhang, Z.-Y. Yu, and J. Xu, "Novel Band-Pass Substrate Integrated Waveguide (SIW) Filter based on Complementary Split Ring Resonators (CSRRS)," *Progress In Electromagnetics Research, PIER* 72, 39-46, 2007
- [4] Juan Hinojosa, Marcello Rossi, Adrian Saura-Rodenas, Alejandro Alvarez-Melcon, and Felix Lorenzo Martinez-Viviente, "Compact Bandstop Half-Mode Substrate Integrated Waveguide Filter Based on a Broadside-Coupled Open Split-Ring Resonator," *IEEE Trans. Microwave Theory and Techniques*, Vol. 66, No. 6, June 2018.

.....✂.....

# Chapter 6

## CONCLUSIONS

### Contents

- 6.1 *Thesis highlights*
- 6.2 *HMSIW narrow bandstop and bandpass filters*
- 6.3 *SIW and HMSIW compact bandpass filters*
- 6.4 *Suggestions for future work*

---

*The conclusions drawn from the simulation and experimental investigations carried out on SIW and HMSIW along with SRR, CSRR and vertical loops for the development of bandpass and bandstop filters are presented in this chapter. A few suggestions for further investigations on this topic are also provided.*

---

## 6.1 Thesis highlights

This chapter presents the summary of the investigations carried out and the conclusions on the results obtained therein. The essence of this thesis is incorporated in chapter 4 and 5. The HMSIW bandpass and bandstop filters are studied in chapter 4. A simple HMSIW-SRR combination to achieve a narrow bandstop is implemented. It is demonstrated that by introducing SRR in the HMSIW discontinuity, we can create a passband. The edge coupled SRRs are used in this filter for transmission zero generation. A compact version of the previously mentioned bandpass filter is realized later in the chapter. Narrow bandpass filters with better insertion loss and stopband characteristics are attained in this study. Edge coupled SRRs are replaced by CSRRs to achieve compactness in the design. Cross slot wideband bandpass filter and SIW, HMSIW vertical loop filters are investigated in chapter 5. A flat passband characteristics is obtained with moderately wide percentage bandwidth by the cross slot approach. A different approach in placing the loop resonators are discussed later in this chapter. Vertically loaded loops in the SIW give rise to a passband with good stopband bandwidth. A compact version of the previously mentioned one as HMSIW filter and a bandstop filter using vertical loops are also detailed in the chapter.

## 6.2 HMSIW narrow bandstop and bandpass filters

The characteristics of HMSIW coupled SRR is studied which led to the realization of the narrow bandstop filter, which is discussed in

section 4.1. Different SRR slit orientations are studied with relevant surface current distributions. The bandwidth of the bandstop filter can be increased by introducing more number of SRRs.

The bandpass filter with transmission zeros on either side of the passband and well defined attenuation is discussed in section 4.2. Edge coupled as well as series coupled SRRs are utilized in the proposed structure. With a simple HMSIW-SRR arrangement, a narrow bandpass filter is proposed.

A modified and compact version of the previously discussed filter is detailed in 4.3. By introducing CSRRs instead of SRRs, the filter size reduction is achieved with a stopband attenuation level of below 20 dB. Extensive parametric analysis, field plots and surface current distributions are studied in detail for the realized filters. Equivalent circuit models developed for the bandpass filters are also discussed in the chapter. The fabricated structures along with its insertion and return loss characterises are also investigated. A comparison of the previously reported filters with the compact filter discussed in this chapter is also depicted.

### **6.3 SIW and HMSIW compact wide bandpass filters**

A moderate wideband bandpass filter with flat passband is realized using the SIW cross slot filter is discussed in 5.1. The CSRR resonant structures are utilized in this filter for the upper and lower stopband frequencies. A flat group delay is attained by the realization of the flat

passband. Compactness is also achieved by the introduction of the CSRRs.

A different approach for the realization of resonant loops for the realization of bandpass filters are proposed in section 5.2. Different types of loop orientations are studied to understand its characteristics in each situations. The best possible one to achieve a compact filter geometry by employing the loop array is implemented in the SIW vertical loop filter structure. Moderately wide bandwidth with reasonable group delay characteristics have been achieved. The stopband attenuation and characteristics are commendable in this case. To establish the aim of fifty percentage size reduction, HMSIW loop filter is also tested. This gives wide bandwidth and good group delay characteristics but compromises in stopband attenuation.

The HMSIW coupled vertical loop bandstop filter is investigated in 5.3. A slit is also introduced at the ground portion of the loop for the better interaction between the HMSIW and the vertical loop. A narrow bandstop filter is realized by the field coupling between the two structures. The comparison of the important filter parameters of the developed filters are shown in Table 6.1.



**Table 6.1. Comparison of salient features of various filters developed**

<b>Filter Names</b>	<b>Passband (GHz)</b>	<b>Operating band</b>	<b>3dB FBW %</b>	<b>Measured Insertion Loss (dB)</b>	<b>Stopband Attenuation</b>	<b>Group Delay</b>	<b>Size mmXmm</b>
HMSIW bandpass Filter (narrowband)	9.16-9.56	X	4	2.11	15	-	35×20
Compact HMSIW Bandpass filter (narrowband)	4.66-5.23	C	1.1	1.4	20	-	30×13
SIW bandpass filter with cross slot and CSRR	7.4 -9.4	X	23.8	1.5	10	<0.06	25×20
SIW bandpass filter with vertical loops	12.42-13.48	Ku	8	1.6	20	<0.6	33×13
HMSIW bandpass filter with vertical loops	6.34-11.75	X	59.8	0.5	20	<0.2	30×12

#### 6.4 Suggestions for future work

This thesis presents SIW filters in the C-band, X- band and Ku-band. The designs can be scaled and converted for use in the millimetre wave regions since the SIW filters are promising candidates in that range. The stopband and its characteristics of the HMSIW vertical loop filter can be fine-tuned to get a better response. The passband flatness of the loop filters can be improved by adopting group delay minimisation techniques. The designs are tested as stand-alone prototype filters. The issues related to actual PCB integration and shielding/packaging are to be addressed.

.....✂.....

## ||| List of Publications |||

### International journals

- [1] **P. M. Anju**, A. O. Lindo and C. K. Aanandan, "Compact Narrowband HMSIW Filter with SRR and CSRRs," International Journal of microwave and Optical Technology, Vol. 14, No. 2, March 2019.
- [2] **P. M. Anju**, A. O. Lindo and C. K. Aanandan, "Half - Mode Substrate Integrated Waveguide Bandpass Filter with Split Ring Resonators," European Journal of Advances in Engineering and Technology, Vol. 4, No.11, 2017, pp. 844-849.
- [3] **P. M. Anju**, A. O. Lindo, and C. K. Aanandan. Substrate Integrated Waveguide Bandpass Filter with Cross Slots and CSRRs. Journal of Microwave Engineering & Technologies. Vol. 5, No.2, 2018, pp. 1-4
- [4] A. O. Lindo, **P. M. Anju**, and C. K. Aanandan, "Substrate Integrated Waveguide Without Metallized Wall Posts," Progress In Electromagnetics Research Letters, Vol. 77, 2018, pp. 7-12.

### International Conferences

- [1] **P. M. Anju**, A. O. Lindo and C. K. Aanandan, X-Band Bandstop filter using Half Mode Substrate Integrated Waveguide with Split Ring Resonators, Proceeding of International Symposium on Antenna and Propagation APSYM 2016.
- [2] **P. M. Anju**, A. O. Lindo, C. K. Aanandan, D. D. Krishna and P. R. Young, "Novel Millimeter-Wave Antenna Array Using Half Mode Substrate Integrated Waveguide (HMSIW)," International Conference on Advances in Computing and Communications, Cochin, Kerala, 2012, pp. 274-277.

- [3] **P. M. Anju**, A. O. Lindo, and C. K. Aanandan, Substrate Integrated Waveguide Bandpass Filter with Cross Slots and CSRRs, Conference: Proceedings of the International Multi-Conference on Computing, Communication, Electrical & Nanotechnology (I2CN-2K18), April 2018.
- [4] A. O. Lindo, **P. M. Anju**, Gopikrishna M, Nurul Osman, Robert Leigh, Dr. Charles Free and Dr. Aanandan Chandroth, "Parallel and end coupled microstrip band pass filters at W-band," Asia Pacific Microwave Conference, Singapore, 2009, pp. 345-348.
- [5] A. O. Lindo, **P. M. Anju**, C. K. Aanandan, A. J. Farrel and P. R. Young, "Half Mode Substrate Integrated Waveguide without via," Loughborough Antennas & Propagation Conference (LAPC), Loughborough, 2013, pp. 131-134

.....✂.....

## Resume of Author

### ANJU P MATHEWS

Puthiyadam House, Vengalloor P.O

Thodupuzha– 685608, Kerala.

Phone: 8075626191, 8547585492

Email:anjupmathews@gmail.com

### TECHNICAL SKILLS

#### Skills & Expertise

- Programming Languages: MATLAB, C.
- Electromagnetic Simulation Softwares: CST, ADS
- Office Suite: MS Office- Word, Excel, PowerPoint
- Graphics: CorelDRAW X7

#### Hardware Skill

Vector Network Analyzer

### PROJECT & RESEARCH EXPERIENCE

#### UKIERI Project

Integrated smart antennas for next generation millimeter wave systems

#### INUP Project

Medium term project to characterize BST (Barium Strontium Titanate) thin film and device millimeter-wave phase shifter (around 60 GHz).

### TEACHING EXPERIENCE

Assistant Professor in Electronics, St.Joseph's College, Moolamattom - 2012- 2019

### PERSONAL ACHIEVEMENTS

#### Academic/Professional

Qualified UGC-JRF/NET on 07<sup>th</sup> October 2010

### AREAS OF INTEREST

- Substrate Integrated Waveguide (SIW)
- Microwave Filters
- Antenna

**ACADEMIC CREDENTIAL**

---

<b>Course</b>	<b>Year</b>	<b>Board/University</b>	<b>Aggregate (%)</b>	<b>Institution</b>
Ph.D	2008	Cochin University of Science and Technology (CUSAT)	pursuing	Department of Electronics, CUSAT
Masters in Electronics Science	2007	Cochin University of Science and Technology	8.74/10 (CGPA)	Department of Electronics, CUSAT
Bachelors Electronics and Computer Hardware	2005	Mahatma Gandhi University	86%	College of Applied Science, Thodupuzha, Kerala
Class XII	2002	Kerala State Board	79%	St. George HSS Muthalakodam, Kerala
Class X	2000	Kerala State Board	91%	St. Ritas HS Paynkulam, Kerala

---

**PERSONAL DETAILS**

---

Age & Date of Birth : 34 years, 20-01-1985  
Sex : Female  
Marital status : Married  
Nationality : Indian  
Languages Known : English, Malayalam, and Hindi

**REFERENCE**

---

Prof. K. Vasudevan  
Emeritus professor  
Dept. of Electronics  
CUSAT, Cochin-22

Prof. C.K. Aanandan  
Emeritus Professor  
Dept. of Electronics  
CUSAT, Cochin-22

.....✍.....